JOURNAL OF GEOPHYSICAL RESEARCH, VOL. 91, NO. A3, PAGES 3177–3224, MARCH 1, 1986

The Theta Aurora

L. A. FRANK,[1] J. D. CRAVEN,[1] D. A. GURNETT,[1] S. D. SHAWHAN,[1] D. R. WEIMER,[1,2] J. L. BURCH,[3] J. D. WINNINGHAM,[3] C. R. CHAPPELL,[4] J. H. WAITE,[4] R. A. HEELIS,[5] N. C. MAYNARD,[6,7] M. SUGIURA,[6] W. K. PETERSON,[8] AND E. G. SHELLEY[8]

The theta aurora is a remarkable configuration of auroral and polar cap luminosities for which a generally sun-aligned transpolar arc extends contiguously from the dayside to nightside sectors of the auroral oval. Four individual occurrences of theta aurora over earth's northern hemisphere are examined in detail with the global auroral imaging instrumentation on board the high-altitude, polar-orbiting spacecraft DE 1. Simultaneous measurements of fields and plasmas with this high-altitude spacecraft and its low-altitude, polar-orbiting companion, DE 2, are examined in order to establish an overview of auroral and polar cap phenomena associated with the appearance of the theta aurora. For these series of observations, two general states of the polar cap are found corresponding to (1) a bright, well-developed transpolar arc and (2) a dim or absent transpolar arc. During periods of a relatively bright transpolar arc the plasma convection in the polar cap region associated with the transpolar arc is sunward. Elsewhere over the polar cap the convection is antisunward. The convection pattern over the auroral zones and polar cap is suggestive of the existence of four cells of plasma convection. Field-aligned electron acceleration into the polar atmosphere and field-aligned current sheets are present in the transpolar arc plasmas. This electron precipitation and these current sheets are relatively absent over the rest of the polar cap region. The transpolar arc plasmas exhibit similar densities and ion compositions relative to those plasmas observed simultaneously over the poleward zone of the auroral oval. The ion compositions include hot H^+, He^{++}, and O^+ ions and thus are of both ionospheric and solar wind origins. Principal hot ions in the remainder of the polar cap region are H^+ and He^{++}, indicating access from the magnetosheath for these ions. Low-energy electrons identified with a magnetosheath source are also present in this region. The dominant thermal ions in the polar cap region are O^+ ions flowing upward from the ionosphere. These thermal ions are heated along magnetic flux tubes within the transpolar arc plasmas. Pairs of current sheets with oppositely directed current densities occur in the transpolar arc region and with magnitudes similar to those associated with the poleward zones of the auroral oval. The upward currents are carried by electrons accelerated by a field-aligned potential. Funnel-shaped auroral hiss and broadband electrostatic noise are associated with the presence of the transpolar arc plasmas. Energetic solar electrons are employed to show that the magnetic field lines threading both the transpolar arc and the poleward zone of the auroral oval are probably closed. In contrast, the accessibility of these electrons to the remainder of the polar cap indicates that these polar regions are characterized by a magnetic topology that is connected directly to field lines within the interplanetary medium. Thus the overall character of the transpolar arc region appears to be very similar to that observed over the poleward zones of the auroral oval. This latter region is currently thought to be magnetically mapped into the boundary layer of the plasma sheet in the magnetotail, namely, the boundary layer of high-speed ion beams and field-aligned currents. When the transpolar arc is dim or at its initial stages of brightening, there is a severe corresponding change in the character of luminosities, convection electric fields, fields, and plasmas over the polar cap region. The plasma convection is no longer the signature of a simple four-cell convection pattern. Plasma convection is generally turbulent or sunward in the polar cap. Remarkably, the zone of hot H^+, He^{++}, and O^+ ions, which is a unique signature of the presence of a transpolar arc, is still present for the two examples of dim or absent transpolar arc luminosities presented here. However, the ionosphere displays a complex system of polar arcs and glows over almost the entire polar cap region. Similarly, the occurrence of field-aligned electron acceleration, broadband electrostatic noise, and field-aligned currents is widespread within the polar cap region. Outside the zone of hot H^+, He^{++}, and O^+ ions associated with the position of the transpolar arc the primary hot ions are H^+ and He^{++}, a composition that is indicative of direct access of these ions from the magnetosheath. The existence of the theta aurora implies a corresponding unique magnetospheric convection pattern and magnetospheric topology. The dynamics of the magnetosphere during these periods is currently an actively contested issue. The comprehensive, correlated observations presented here are intended to provide a foundation for future theoretical and interpretive efforts.

1. INTRODUCTION

The first observations of a transpolar arc that extended contiguously from the dayside auroral oval across the polar cap to the night sector of the oval are reported by *Frank et al.* [1982]. These images are obtained with the spin-scan photometers on board the high-altitude, polar-orbiting satellite DE 1 at wavelengths for atomic oxygen (O I) 130.4, 135.6 nm. The striking resemblance of the spatial distributions of auroral luminosities to the Greek letter θ provides the motivation to denote these auroral configurations as "theta auroras." The two principal advantages of the DE 1 imaging instrumentation in identifying the existence of the theta aurora over previous observations are (1) viewing of the entire auroral oval from high polar altitudes for extended periods of time, 4–5 hours, and (2) filters at ultraviolet wavelengths that allow imaging of the aurora in the sunlit atmosphere. The theta aurora occurs during periods of northward interplanetary magnetic fields and hence during periods of relatively quiet magnetic activity. Polar cap arcs and diffuse emissions have previously been reported with optical measurements from the ground, aircraft, and lower-altitude spacecraft (cf. *Davis*

[1] Department of Physics and Astronomy, University of Iowa, Iowa City.
[2] Now at Research Center, Regis College, Weston, Massachusetts.
[3] Southwest Research Institute, San Antonio, Texas.
[4] NASA Marshall Space Flight Center, Huntsville, Alabama.
[5] University of Texas at Dallas, Richardson.
[6] NASA Goddard Space Flight Center, Greenbelt, Maryland.
[7] Now at Space Physics Division, Air Force Geophysics Laboratory, Hanscom Air Force Base, Massachusetts.
[8] Lockheed Palo Alto Research Laboratory, Palo Alto, California.

Paper number 5A8688.
0148-0227/86/005A-8688$05.00

[1960], *Akasofu* [1963], and *Lassen and Danielsen* [1978] for ground measurements; *Eather and Akasofu* [1969] for observations from aircraft; and *Anger et al.* [1973], *Akasofu* [1976], *Bunn and Shepherd* [1979], and *Ismail and Meng* [1982] for auroral imaging from satellites). Most of these observations of polar emissions are taken during periods of relative global magnetic quiescence and hence presumably during periods of northward interplanetary field. *Ismail and Meng* [1982] classify polar cap auroral arcs into three types: type 1, distinctly sun-aligned polar cap arcs; type 2, morning/evening polar cap arcs that are expanded from the auroral oval; and type 3, hook-shaped arcs connecting the polar cap arc with the oval arcs. A comparison of the DE 1 images with those from the Defense Meteorological Satellite Program (DMSP) spacecraft reported by Ismail and Meng shows that type 3 polar arcs are most likely associated with the occurrence of theta auroras. *Gussenhoven* [1982] examines over 1600 DMSP images of the polar cap and identifies four major classes of polar cap arcs. One of these classes, *P*(1), displays one or two long arcs that are contiguous with the midnight sector of the auroral oval and extend into the polar cap. Again, these polar cap auroras are most likely the nighttime segment of the transpolar arc of the theta aurora. Other examples of similar sun-aligned arcs are published by *Anger et al.* [1974], *Akasofu* [1976], and *Meng and Akasofu* [1976]. Ground observations indicating that these sun-aligned arcs can durably exist for periods of hours are reported by *Ismail et al.* [1977]. For none of these previous sightings of sun-aligned arcs are the viewing conditions sufficient to establish their complete traversal of the polar cap from the day to night sectors of the auroral oval. With DE 1 the complete extent of the transpolar arc is observed, and the temporal evolution of the theta auroras can be monitored for periods of hours.

Plasma distributions and electric fields over the polar caps also exhibit remarkable features during periods of northward interplanetary magnetic fields and corresponding low magnetic activity as indicated in the *AE* indices. *Maezawa* [1976] interprets an analysis of ground-based magnetograms in terms of sunward plasma convection over the polar caps, i.e., a dusk-to-dawn electric field, during these periods. Measurements with spacecraft are also used to show that such sunward convection can exist [*Burke et al.*, 1979, 1982]. These investigators suggest that a four-cell convection pattern exists during periods of northward interplanetary fields and is contrasted to the well-known two-cell system present during other magnetic conditions [cf. *Heppner*, 1972]. *Winningham and Heikkila* [1974] find two primary electron distributions over the polar caps. The first of these electron distributions is a "polar rain" of low-energy electron fluxes with characteristic energies of 100 to 300 eV and energy fluxes of $\sim 10^{-3}$ to 10^{-2} erg/cm^2 s sr. The second electron population is embedded in this polar rain and comprises narrow regions of more energetic ($\sim$keV) electrons. *Hardy et al.* [1982] report similar electron distributions over the polar cap and evidence of a third population of magnetosheath electrons. Electron velocity distributions are observed that are indicative of field-aligned acceleration over the polar cap [*Hardy et al.*, 1982; *Burch et al.*, 1979; *Frank et al.*, 1982]. Analyses of the Birkeland, or field-aligned, currents that couple the magnetosphere with the polar ionosphere are now available. *Lassen* [1979] shows that the patterns of such currents as inferred from polar cap arcs are correlated with the *y* component of the interplanetary magnetic field. Observations of the magnetic perturbations due to Birkeland currents over the polar caps with the Magsat satellite show that there is a well-defined current system to be identified with a two-cell polar convection pattern [*Iijima*, 1984; *Potemra et al.*, 1984; *Iijima et al.*, 1984; *Zanetti et al.*, 1983]. The relative sizes of these cells are strongly influenced by the *y* component of the interplanetary field; e.g., for a positive *y* component the dawn convection cell expands across the polar cap.

Our present purpose is to provide an overview of the remarkable spatial configuration of auroral luminosities known as the theta aurora and of the distributions of plasmas, electric fields, field-aligned currents, and plasma waves that are associated with this auroral state. Such a study is uniquely accommodated by (1) comprehensive fields-and-particle instrumentation on two spacecraft, DE 1 and DE 2, in coplanar, polar orbits and (2) simultaneous global auroral imaging from the higher-altitude spacecraft DE 1. In order to limit the length of the presentation, we shall discuss only the major findings. The reader can easily identify numerous topics of further interest that are to be pursued by the authors in later publications. Four examples of theta auroras are presented here. Two of these occurrences of theta auroras are characterized by well-defined, relatively quiescent transpolar arcs, the third by a transpolar arc with fluctuating luminosities, and the fourth by an initially complex system of polar cap emissions followed by the appearance of a truly transpolar arc. The above examples are ordered according to their observational complexity and are ordered thus in our discussion. Since there are a large number of types of measurements, e.g., low-altitude plasmas, plasma waves, and high-altitude convection electric fields, it is found to be less confusing to provide each type a separate section in the text. The reader is encouraged to carefully understand the use of the images as discussed early in section 2 in order to enjoy a similar excitement of discovery with the correlative, in situ measurements as was experienced by the authors.

2. Imaging the Theta Auroras: A Global Reference for in Situ Fields-and-Particles Measurements

The high-altitude DE 1 spacecraft obtained series of images of several theta auroral events over the northern hemisphere during the fall of 1981. This spacecraft is equipped with three imaging photometers with off-axis parabolic reflectors as the primary optical elements. Two of these imaging photometers provide global auroral images at visible wavelengths with any of 12 filters, each selected by ground command. The third photometer is capable of auroral imaging at vacuum ultraviolet wavelengths with a similar selection of one of its 12 filters. In typical operation of these instruments a 30° × 120° image is obtained every 12 min for each photometer. The images are centered in the earth nadir direction. The 120° dimension of the image is taken in the plane perpendicular to the rotation axis of the spacecraft. This rotational axis is perpendicular to the orbital plane. A detailed description of the imaging instrumentation has been given previously by *Frank et al.* [1981*a*].

Series of images for four occurrences of theta auroras are presented here along with in situ measurements of fields and particles from the two spacecraft DE 1 and DE 2. Orbital parameters for these two spacecraft are summarized in Table 1 for the periods of the four events. These theta auroras occur during periods of northward directed interplanetary magnetic fields. In order to aid the reader in easily digesting the relationship between the instantaneous positions of the two spacecraft and the temporally and spatially variable auroral luminosities we are providing three tools. The first such aid comprises the images at the times for DE 1 crossings of mag-

TABLE 1. Orbital Parameters for DE 1 and DE 2

Date, 1981	Apogee Latitude	Apogee Local Time	Apogee Altitude, km	Perigee Altitude, km
		DE 1		
October 17 (day 290)	77°N	0916	23,305	554
October 31 (day 304)	73°N	0822	23,309	549
November 8 (day 312)	70°N	0750	23,315	545
November 25 (day 329)	64°N	0640	23,319	539
		DE 2		
October 17 (day 290)	58°N	2115	935	308
October 31 (day 304)	67°N	0819	921	307
November 8 (day 312)	36°N	0748	918	305
November 25 (day 329)	25°S	0637	909	295

netic field lines in the morning and evening sectors of the auroral oval, e.g., Plates 1 and 3, respectively, and a third image at the time of interception of field lines threading the polar arc, e.g., Plate 2. A single image corresponding to the approximate center time for the DE 2 traversal of the auroral oval is also given, e.g., Plate 4. The second aid is a summary of the geographic latitudes of important auroral features as functions of universal time (UT) in the orbital planes of the two spacecraft, e.g., Figure 1. These two orbital planes are closely coplanar. The positions of the magnetic field line ingresses at an altitude of 300 km for each satellite are also shown in Figure 1. The altitude for the auroral luminosities is assumed to be 150 km for the purposes of mapping these luminosities. Finally, we tabulate the crossing times for morning and evening sectors of the auroral oval, as well as for the polar arc, in Table 2 for both spacecraft. This table is the focal point for correlating auroral features with in situ observations with the two spacecraft. Our discussion of the four events is ordered accordingly with their generally increasing complexity. The angles between the direction of the transpolar arc and the spacecraft orbital plane are given in Table 3 at the time corresponding to passage of each spacecraft through magnetic field lines threading the transpolar arc.

November 8, 1981. This theta aurora event has been reported previously by *Frank et al.* [1982] as the first sighting of this remarkable configuration of auroral luminosities. The polar arc of the theta aurora persists throughout the nearly 5 hours of polar cap viewing possible during this single orbit. This imaging sequence is taken in the emissions of O I 130.4, 135.6 nm. The DE 1 spacecraft exited magnetic field lines threading the morning sector of the auroral oval at approximately 1315 UT. An image of the auroral oval at a frame beginning earlier at 1234 UT is shown in Plate 1. In this frame the polar arc can be seen just poleward of the evening sector of the auroral oval near the earth's limb. The orbital motion of both spacecraft provides crossings of the auroral oval from approximately local morning to local evening for this and the following series of observations over the northern hemisphere. The magnetic field line ingress points at 300 km for field lines threading the DE 1 position are also shown for the period 1200–1400 UT. For each image the latitudes of the evening and morning sectors of the auroral luminosities are plotted in Figure 1 in the orbital planes of the two spacecraft. The positions of polar arc(s) are also given. The reader should then note that the orbital latitudes for the positions of the two spacecraft are shown in Figure 1. Thus, for example, the imaging results predict that the field lines threading the polar arc are traversed by DE 1 at 1546–1600 UT and by DE 2 at 1605–1607 UT. These interception times are tabulated in Table 1.

The images shown in Plates 1, 2, and 3 correspond to approximate periods for DE 1 crossings of magnetic field lines threading the morning oval, transpolar arc, and evening oval, respectively. An examination of these images finds that the polar arc varies considerably in brightness and position. The motion of the polar arc in the orbital plane as gained with 18 consecutive images is shown in Figure 1. The polar arc moves initially poleward (1315–1430 UT), then toward local evening (1430–1545 UT), and then again poleward (1545–1630 UT) as the arc is intercepted by the two spacecraft. Note the variability of luminosities for the polar arc by comparing Plates 2 and 3. On the other hand, the positions of the morning and evening sectors of the auroral oval remain relatively fixed during this time period, and luminosities are less variable.

The image corresponding to the nearest time for the polar cap crossing of DE 2 is shown in Plate 4. The magnetic field line ingress points at 300 km for the spacecraft position are superposed as a function of time on the image. Note that DE 2 traverses the auroral oval and polar cap in approximately 15 min. The beginning of the 12-min accumulation time for the image is 1601 UT. Thus a single image from each photometer is usually telemetered for the DE 2 traversals of the polar cap. A comparison of the previous frame (Plate 2) shows that the intensity of emissions within the polar arc is decreasing during the period between the interception of the magnetic flux sheet associated with the polar arc by DE 1 and the interception a

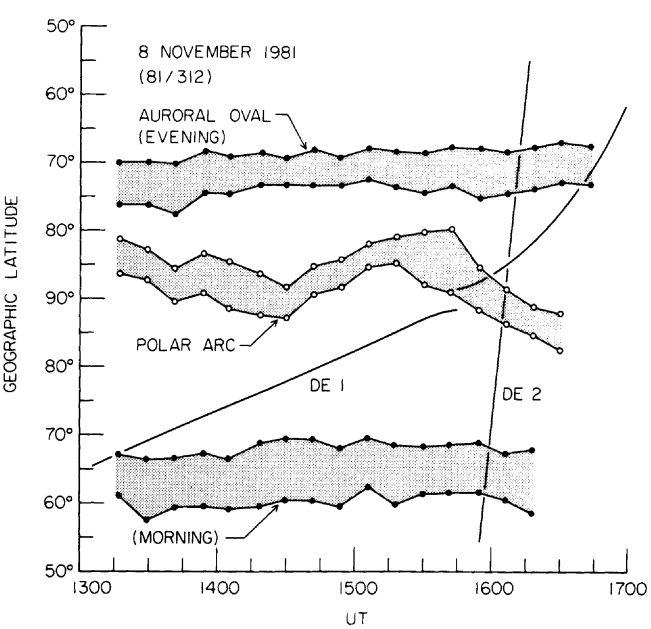

Fig. 1. Geographic latitudes for the boundaries of the morning and evening sectors of the auroral oval and of polar arcs in the orbital planes of DE 1 and DE 2 as functions of time on November 8, 1981. These positions are determined from a sequence of global images from the high-altitude spacecraft DE 1. The transpolar arc is identified with the shaded zone that is labeled polar arc.

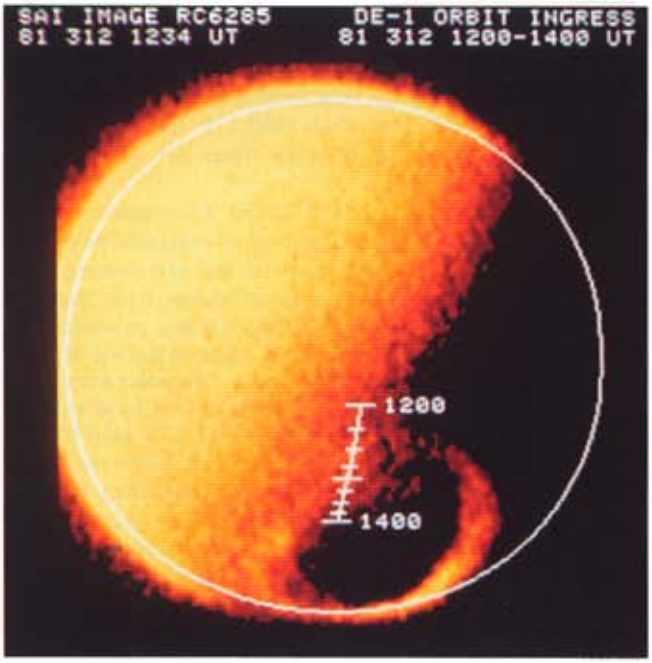

Plate 1. Image of the northern auroral zones and polar cap as seen in the atomic oxygen (O I) 130.4-, 135.6-nm emissions on November 8, 1981. The frame beginning time is 1234 UT and corresponds to the period during which the DE 1 spacecraft is positioned on magnetic field lines threading the morning sector of the auroral oval. The magnetic subsatellite positions at 300 km are also shown as a function of universal time.

Plate 3. Continuation of Plate 1 for the evening sector of the auroral oval.

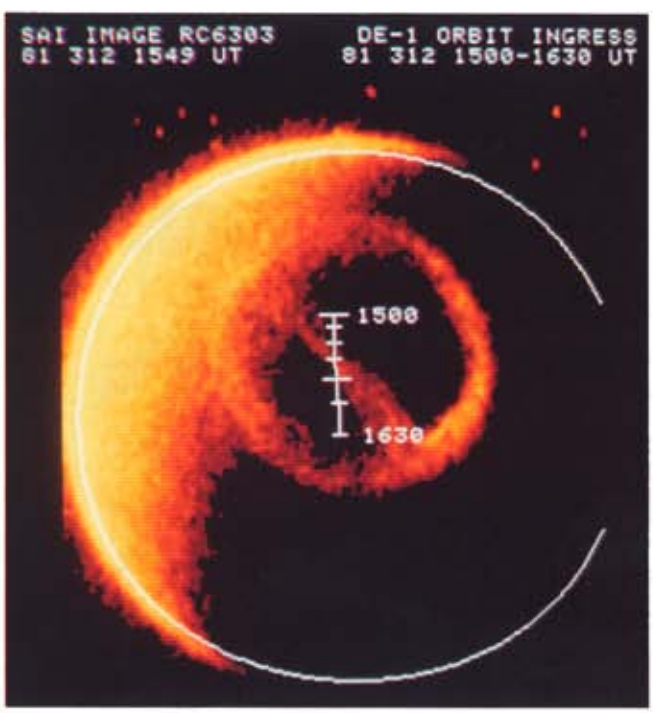

Plate 2. Continuation of Plate 1 for the transpolar arc.

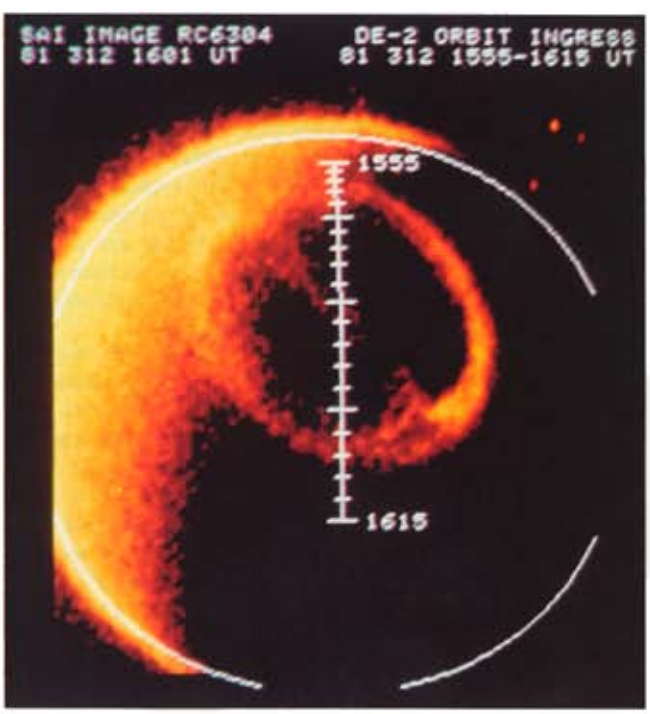

Plate 4. Continuation of Plate 1 for the crossing of the auroral zones and polar cap with the low-altitude DE 2 spacecraft on November 8, 1981. The magnetic subsatellite track is also shown.

TABLE 2. Times for Traversal of Magnetic Field Lines Associated With Auroral and Polar Cap Luminosity Features

Date, 1981	Auroral Oval, Morning Sector Enter	Auroral Oval, Morning Sector Exit	Polar Arc Enter	Polar Arc Exit	Auroral Oval, Evening Sector Enter	Auroral Oval, Evening Sector Exit
			DE 1			
October 17 (day 290)			(1) 1503*		1710	1722
			(3) 1641	1644		
October 31 (day 304)			2316	2327	2357	2359
November 8 (day 312)		1315	1546	1600	1640	1651
November 25 (day 329)		0957	1142	1146	1238	1247
			DE 2			
October 17 (day 290)			(2) 1641*			
			(3) 1644	1645	1646	1648
October 31 (day 304)			2351	2352	2357	2358
November 8 (day 312)	1557	1600	1605	1607	1611	1613
November 25 (day 329)	1127	1129	1135	1136	1140	1141

Times are in universal time.
*Too narrow to establish width.

few minutes later by DE 2 (see also Table 2). The intensities of O I 130.4, 135.6 nm are approximately 1 kR (kilorayleigh) in the spacecraft orbital planes (vertical center line of each image) for the image presented in Plate 4 [*Frank et al.*, 1982]. Intensities in the two cells between the polar arc and the morning and evening sectors of the auroral oval are above instrumental thresholds and are in the range of several hundreds of rayleighs. These lower luminosities indicate that a lower level of charged particle precipitation is also occurring within the two cells formed by the bifurcation of the polar cap by the transpolar arc.

October 31, 1981. This second series of images of a theta aurora is summarized by the images shown in Plates 5 through 8. As with the first case, the images correspond to the DE 1 crossings of field lines threading the auroral morning sector (Plate 5), the transpolar arc (Plate 6), and the evening sector (Plate 7). The image for the traversal of DE 2 over the polar cap is shown in Plate 8. The filter for these images passes both Lyman α and O I 130.4-, 135.6-nm emissions. The diffuse intensities extending beyond the earth's limb and in the vicinity of the terminator are due to the resonant scattering of solar Lyman α by the earth's exosphere. Thus the auroral oval and polar cap are somewhat obscured by these scattered intensities. The auroral oval and polar cap arcs are viewed primarily in the oxygen emissions. This filter is generally used for studies of the exosphere [*Rairden et al.*, 1983; *Frank et al.*, 1985]. Nevertheless, a well-developed theta aurora can be seen in Plates 6, 7, and 8. Simultaneous images at visible wavelengths, O I 557.7 nm, are also used to verify the position of the polar arc under the positions of the two spacecraft.

TABLE 3. Angle Between the Spacecraft Orbital Plane and Direction of the Polar Arc

Date, 1981	DE 1 UT	DE 1 Angle	DE 2 UT	DE 2 Angle
October 17	(3) 1638	20°	(2) 1638	35°
			(3) 1638	20°
October 31	2321	47°	2346	44°
November 8	1555	40°	1606	41°
November 25	1149	61°	1138	67°

The positions of the polar arc, and the morning and evening sectors of the oval, in the spacecraft orbital planes are shown in Figure 2. The positions of the morning and evening sectors of the oval remain relatively fixed during the entire series of measurements at geographic latitudes ~80° and 64°, respectively. The transpolar arc begins to form at ~2245 UT on the eveningside of the oval and proceeds to move poleward with increasing time. The high-altitude spacecraft DE 1 intercepts magnetic field lines associated with the transpolar arc during 2316–2327 UT, and later DE 2 crosses the arc at 2351–2352 UT. All crossing times are given in Table 2. In general, the luminosities of both the auroral oval and polar arc are weak during the observational period, although with a clear signature of the polar arc for both the DE 1 and DE 2 overflights.

Discrete structures within the polar arc are evident only near the late evening sector of the auroral oval. At this position, discrete auroral features on the two sides of the polar arc turn and become more aligned with the direction of the auroral oval. Inspection of Plate 8 that is taken at relatively low altitudes, ~11,000 km, finds that two narrow arcs separate near local midnight, with one arc realigning along the evening sector of the auroral oval and the other arc along the morning oval. The transpolar arc is also seen to be just resolved into two separate, approximately parallel arcs in the center of the polar cap in the last image of this series as displayed in Plate 7.

November 25, 1981. This third example of an occurrence of a theta aurora exhibits considerably more variability of the intensities of polar cap emissions. Images corresponding to intersections of magnetic field lines threading the primary luminosity features in the orbital planes are given in Plate 9 (morning sector of oval), Plate 10 (polar cap), Plate 11 (evening oval) for DE 1, and Plate 12 for the polar crossing of DE 2. The positions of the spacecraft and of these features in the spacecraft orbital planes as functions of UT are plotted in

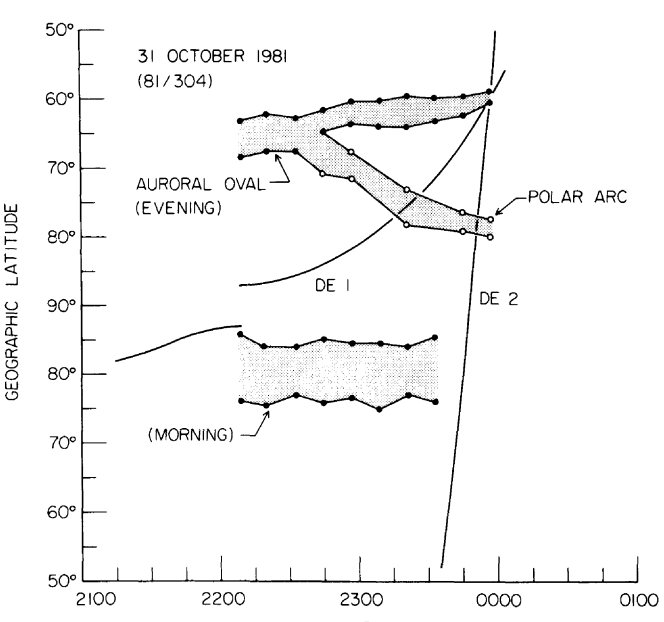

Fig. 2. Continuation of Figure 1 for October 31, 1981.

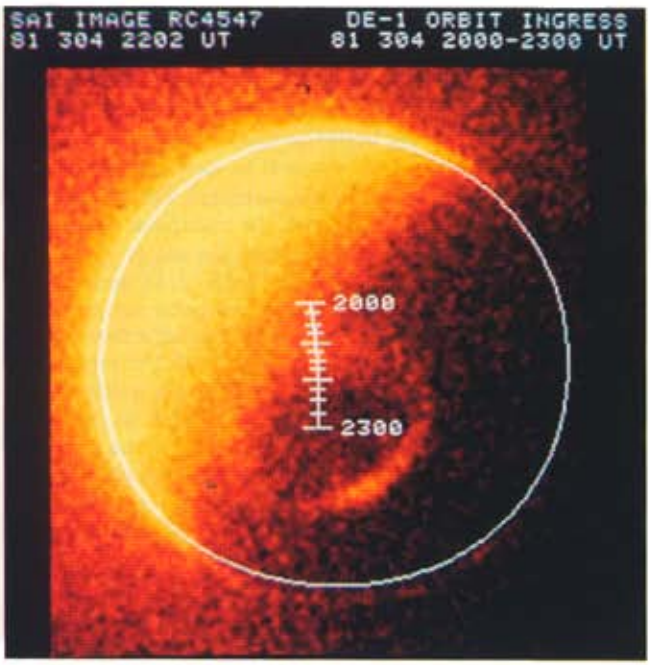

Plate 5. Continuation of Plate 1 (morning sector of oval) for October 31, 1981. This series of images is taken with a filter passband accepting Ly α as well as the O I 130.4-, 135.6-nm emissions. Thus the luminosities off earth's disk are due to the scattering of solar Ly α radiation by the exosphere. The auroral zone and polar cap features are seen primarily in the O I emissions.

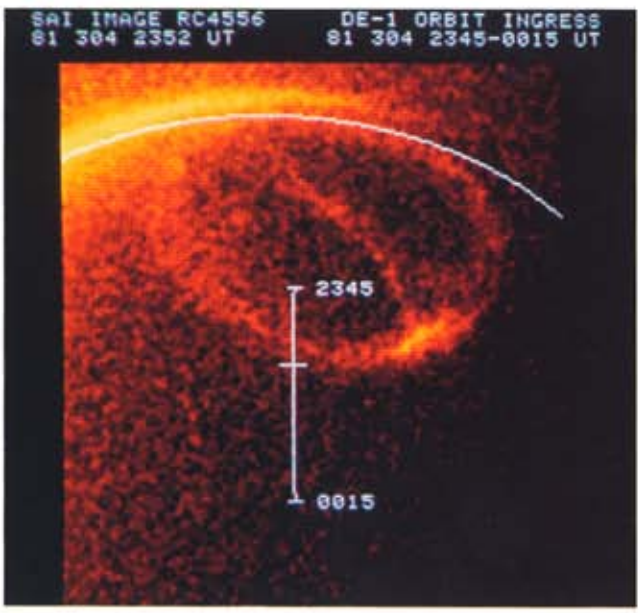

Plate 7. Continuation of Plate 5 (evening auroral oval).

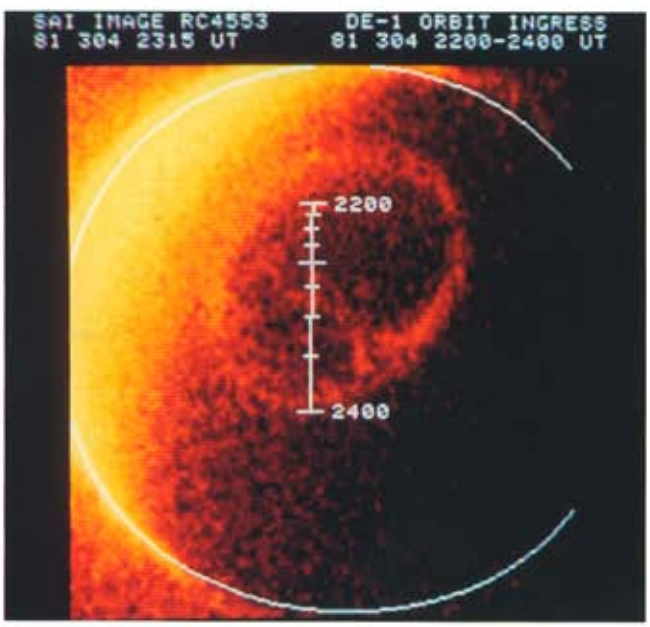

Plate 6. Continuation of Plate 5 (transpolar arc).

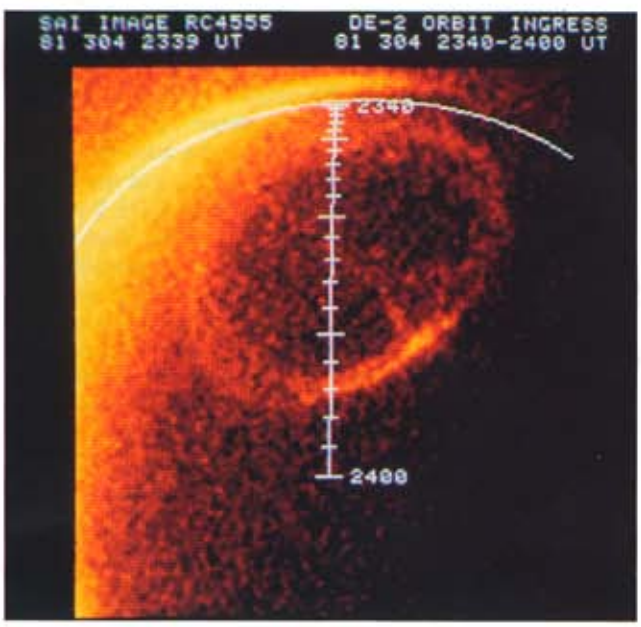

Plate 8. Continuation of Plate 5 for the low-altitude polar passage of DE 2.

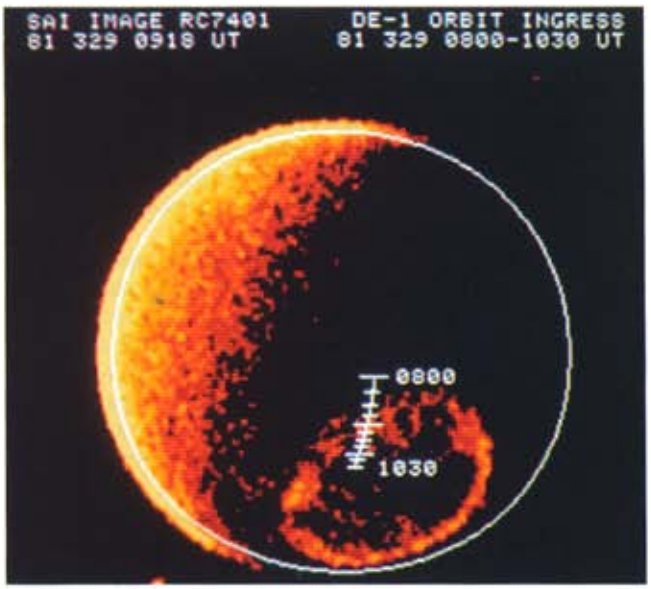

Plate 9. Continuation of Plate 1 (morning auroral oval) for November 25, 1981. This series of images is taken in the emissions of the Lyman-Birge-Hopfield (LBH) bands of N_2.

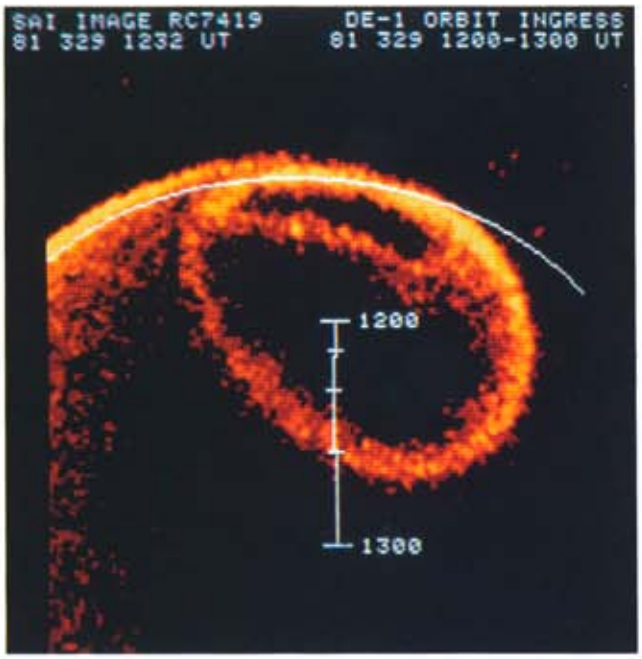

Plate 11. Continuation of Plate 9 (evening auroral oval).

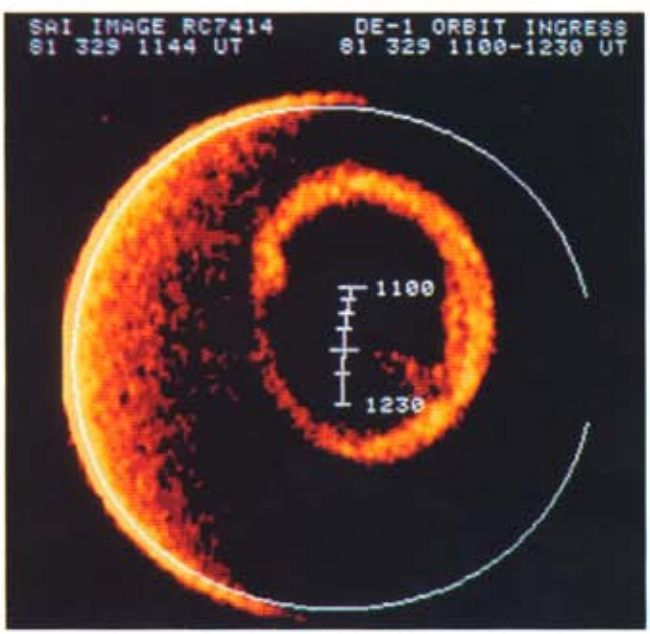

Plate 10. Continuation of Plate 9 (transpolar arc).

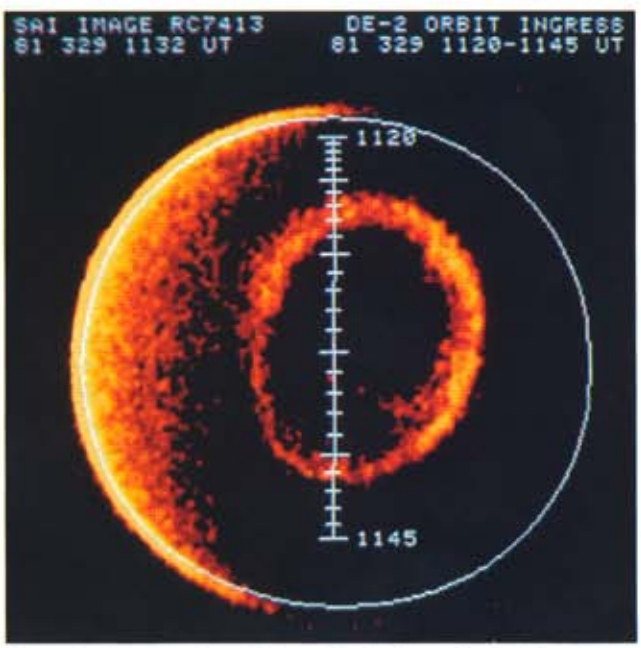

Plate 12. Continuation of Plate 9 for the low-altitude polar passage of DE 2.

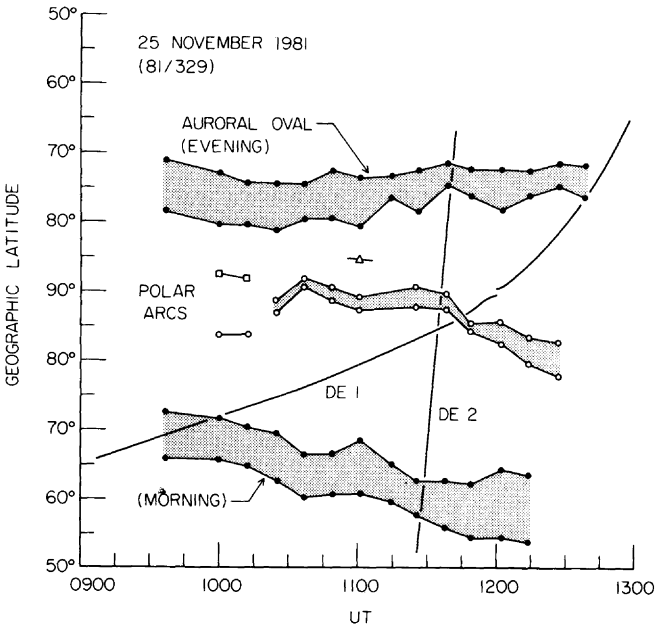

Fig. 3. Continuation of Figure 1 for November 25, 1981.

Figure 3. The crossing times are tabulated in Table 2. The two spacecraft intercept magnetic field lines threading the transpolar arc at 1142–1146 UT (DE 1) and 1135–1136 UT (DE 2), or within about 9 min of each other. The auroral and polar luminosities are viewed in the emissions in the Lyman-Birge-Hopfield band of N_2.

Early in the imaging sequence, diffuse luminosities suggestive of unresolved arcs are observed in the evening and morning regions of the polar cap (cf. Plate 9). These diffuse emissions extend toward local noon. Such diffuse emissions in the morning sector are not observed after ~0930 UT, and by ~1000 UT, two distinct arcs are observed in the evening sector (cf. Figure 3). With the onset of a small auroral substorm at ~1019 UT in the local midnight sector, only one polar arc is clearly resolved. This transpolar arc is observed to progress slowly into the center of the polar cap during the remainder of the imaging sequence. During the same time period the width of the auroral oval in the spacecraft orbital plane increases as the morning sector of the oval moves southward by ~5°.

It is important to note that the transpolar arc is very dim as both DE spacecraft traverse magnetic field lines that map into the arc (see Plates 10 and 12). After the period that DE 2 has traversed the polar cap and while DE 1 is on magnetic field lines passing through the evening sector of the polar cap, the transpolar arc brightens dramatically as shown in the image frame beginning at 1232 UT in Plate 11. The broadening of the transpolar arc as it approaches the midnight sector of the auroral oval can be clearly seen.

October 17, 1981. This sequence of images of a theta aurora is the most difficult to analyze because of the presence of multiple polar arcs, the alignment of the arcs more nearly parallel to the orbital plane (Table 3), and the cycling of two filters for each pair of consecutive images. One of these two filters passed Lyman α and O I 130.4, 135.6 nm and thus rendered the identification of weak polar arcs more difficult, if not impossible for some frames because of the background of resonantly scattered Lyman α from the exosphere. The second filter provided images of the aurora in the emissions of O I 130.4, 135.6 nm. This sequence of images provides a good example of the temporal and spatial complexity of the distributions of emissions often observed over the polar cap.

The imaging sequence begins at 1419 UT while DE 1 is positioned on magnetic field lines threading the morningside of the polar cap and poleward of the morning sector of the auroral oval. The image frame beginning at 1431 UT is shown in Plate 13. At this time there is no positive identification of a transpolar arc, although a polar arc is visible in the morning sector of the polar cap. This arc is labeled as polar arc 1 in Figure 4, which summarizes the positions of polar cap features in the spacecraft orbital planes. A second polar cap arc intersecting these coplanar orbital planes appears at ~1450 UT and is present for at least 2 hours until ~1650 UT. This polar arc moves slowly from the morning sector toward the center of the polar cap.

The first image showing the existence of a transpolar arc of a theta aurora is shown in Plate 14. This frame is taken during 1632–1644 UT. The transpolar arc is indicated as polar arc 3 in Figure 4. Examination of the ingress line for DE 1 and the orientation of the polar arc in Plate 14 shows that they are aligned within ~20°–30° of each other, i.e., the spacecraft is traversing magnetic field lines near or within the arc for this part of the polar cap crossing. The image frame for the DE 1 intercept of magnetic field lines through the late evening sector of the oval is shown in Plate 15. Again, the orbital geometry is such that the spacecraft trajectory remains close to the position of the transpolar arc. The viewing aspect and the position of the local noon sector of the auroral oval deep in the sunlit side of the terminator render difficult a critical viewing of the dayside intercept of the transpolar arc with the auroral oval.

The traversals of magnetic field lines associated with the transpolar arc are almost simultaneous for the two spacecraft, i.e., 1641–1644 UT for DE 1 and 1644–1645 UT for DE 2 (see also Table 2 and Figure 4). For this period the transpolar arc is poorly developed and dim and may be only a system of arcs that only partially traverse the polar cap. For later frames such as that shown in Plate 15 for 1657–1709 UT, the transpolar arc is well defined and relatively bright. For the frame

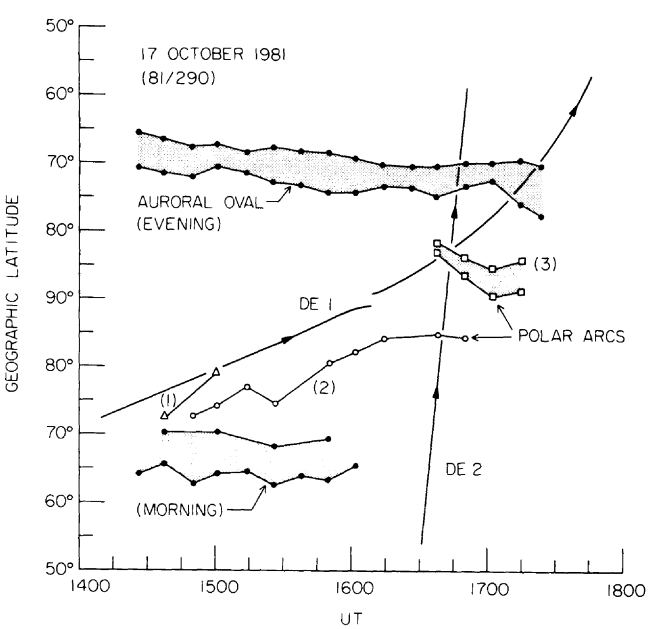

Fig. 4. Continuation of Figure 1 for October 17, 1981.

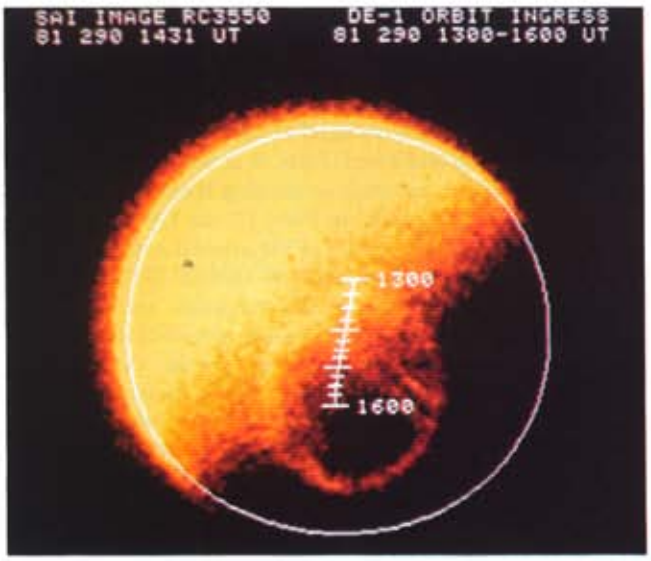

Plate 13. Continuation of Plate 1 (morning auroral oval) for October 17, 1981. This series of images is taken in the emissions of O I 130.4, 135.6 nm.

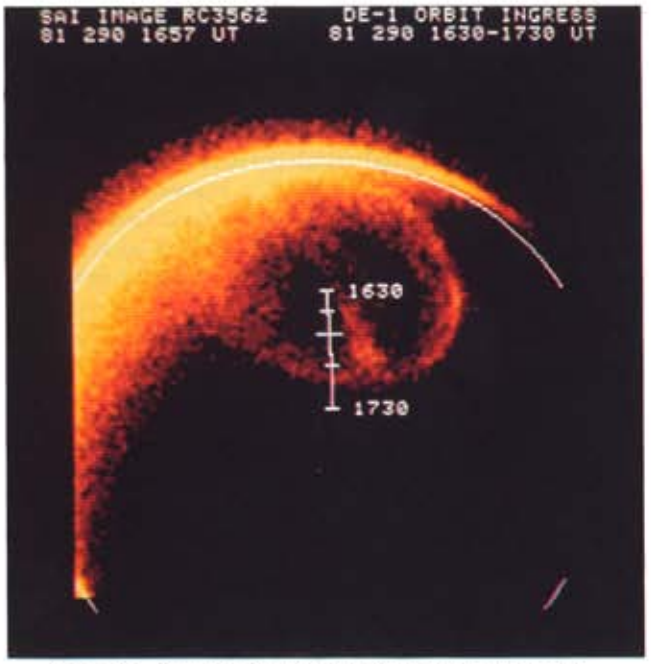

Plate 15. Continuation of Plate 13 (evening auroral oval).

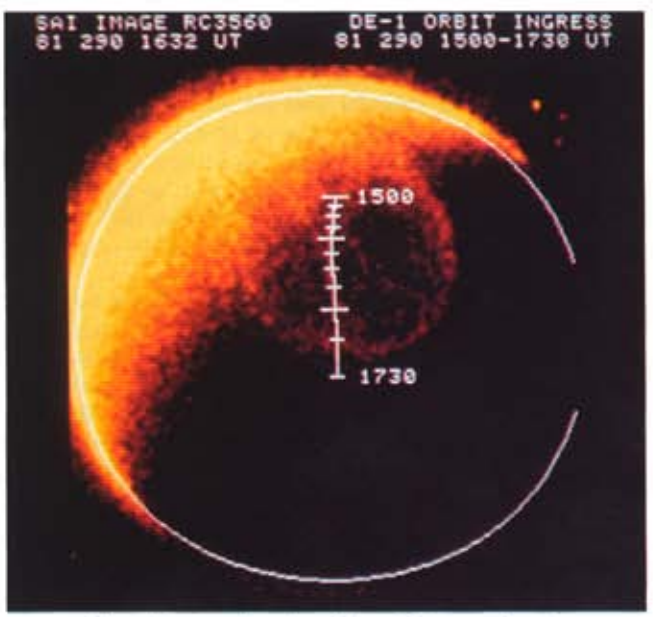

Plate 14. Continuation of Plate 13 (transpolar arc).

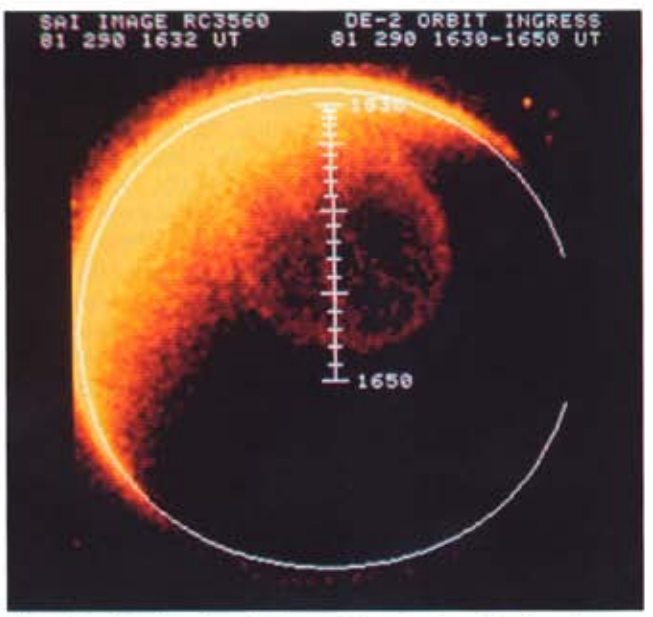

Plate 16. Continuation of Plate 13 for the low-altitude polar passage of DE 2.

spanning the interval 1632–1644 UT in Plates 14 and 16 there are measurable intensities over almost the entire evening sector of the polar cap. In particular, the DE 2 trajectory passes over these relatively unstructured emissions (see Plate 16). Thus it would be expected that plasma instrumentation on board DE 2 observed substantial precipitating plasmas for almost the entire traversal of the polar cap.

In summary for the convenience of the reader it is noted that the gross character of the four examples of theta auroras is (1) November 8, a well-developed theta aurora with motion of the transpolar arc, (2) October 31, a similar example to that for November 8, (3) November 25, a clear example of a theta aurora with great temporal variability in the intensities for the transpolar arc, and (4) October 17, a sequence for which a complex system of polar arcs and unstructured luminosity features exists for the greater part of the viewing period with a decisive appearance of the transpolar arc near the end of the imaging sequence.

3. Hot Plasmas at Low Altitudes

The low-altitude plasma instrument (LAPI) on the spacecraft DE 2 comprises an array of 15 parabolic electrostatic analyzers, each capable of measuring simultaneously the directional, differential fluxes of electrons and ions over the energy–per–unit charge range 5 V to 31 kV. A complete scan of the energy spectrum is typically telemetered once each second for each analyzer. This temporal resolution is employed for all of the examples of theta auroras presented here, with the exception of that for November 25 during which the temporal resolution is 2 s. The low-altitude spacecraft is three-axis stabilized. Thus in order to provide comprehensive pitch angle coverage the individual fields of view of the 15 analyzers are positioned to form a collective fan-shaped acceptance solid angle spanning $\sim 180°$. These analyzers are mounted on a single-axis scan platform such that the fan of acceptance angles lies parallel to the geographic meridional plane through the spacecraft position. The attitude of the DE 2 is actively controlled to maintain this orientation. The angular position of the scan platform is controlled by the output of a single-axis magnetometer such that the top of the fan, i.e., the detector at 0°, is directed along the projection of the local magnetic field onto the plane parallel to the fan angle. Thus the analyzer at 0° views charged particles incident into the atmosphere along the magnetic field line, the 90° analyzer views locally mirroring particles, etc. Further details concerning this instrumentation are given by *Winningham et al.* [1981].

November 8, 1981. Surveys of these plasma measurements are usually presented in energy-time spectrograms. Such a spectrogram is shown in Plate 17 for the polar cap crossing over the theta aurora on November 8. The upper spectrogram displays the directional, differential energy fluxes of electrons as functions of the logarithm of the energy (ordinate) and universal time (UT, abscissa). The magnitude of the flux is color coded logarithmically according to the scale on the upper right-hand side of the plate. A similar spectrogram for the measurements of positive ions is shown in the lower panel. The coordinates along the lower abscissa are invariant latitude (IL), geodetic altitude (ALT) in kilometers, and magnetic local time (MLT) in fractional hours. A parenthesis for values of invariant latitude, e.g., Plate 18, indicates estimation of this parameter at high polar latitudes via a dipole model. There are two small panels between the two major spectrograms. The lower small panel identifies the pitch angle for the plasma measurements. In this case, and for the following examples, the pitch angle is $\sim 0°$ for both electrons and ions. Thus these charged particles are precipitating into earth's atmosphere. The upper small panel summarizes the responses of two Geiger-Mueller tubes, one with field of view directed upward along the local magnetic field (precipitating) and the other viewing pitch angles of $\sim 90°$ (locally mirroring). These detectors are primarily responding to penetrating electrons with energies of >32 keV. The color code for these directional, integral intensities in units of electrons/cm^2 s sr is displayed at the lower right-hand side of Plate 17.

The precipitating electron and positive ion fluxes are summarized in Plate 17 for a traversal of the polar cap during this persistent theta auroral event. First, it is worthwhile to offer several interpretive comments concerning these spectrograms. For the time period covered in Plate 17, the DE 2 spacecraft moves over the morning sector of the auroral zone (1559:00–1602:30 UT), the polar cap (1602:30–1605:20 UT), a plasma structure to be associated with the transpolar arc of a theta aurora (1605:20–1606:40 UT), the polar cap (1606:40–1610:30 UT), and finally the evening sector of the auroral oval (1610:30–1612:00 UT). For traversals of the auroral oval, two plasma regions are generally found [cf. *Frank and Ackerson*, 1972; *Winningham et al.*, 1975]. The first region is characterized by spatially structured electron distributions and ions with typical energies of about a few keV. This region over the poleward zone of the auroral oval is encountered at 1551:00–1602:30 UT and 1610:30–1611:20 UT for the observations in Plate 17. This region is designated as the "boundary plasma sheet" by *Winningham and Heikkila* [1974] and is usually associated with the boundary layers of the plasma sheet and magnetopause. Peak electron responses as functions of energy, in the time intervals 1559:00–1602:30 UT and 1610:30–1611:20 UT, are the signatures of inverted-V precipitation events [cf. *Frank and Ackerson*, 1972; *Winningham et al.*, 1975]. The second type of plasma zone observed over the auroral oval is seen at 1611:20–1612:00 UT in Plate 17. Relatively unstructured spatial distributions of electrons and ions occur at these lower latitudes over the auroral oval, and the ion energies are often in the range of 10 keV or more. This region is generally associated with the plasma sheet proper and with the ring current. It is designated as the "central plasma sheet" by *Winningham et al.* [1975]. This region would also be seen in the spectrogram for the morning crossing of the oval for the period preceding 1559 UT.

Several types of electron distributions are seen over the polar cap, 1602:30–1610:30 UT in Plate 17. Ionospheric photoelectrons at energies 5 to 10 eV are present across the polar cap and decrease with increasing time. This decrease is due to the motion of the spacecraft toward and into the nightside of the terminator (see Plate 4). A second electron population can be identified in the general energy range of 100 eV. These energy fluxes are low and are without notable spatial structure. These electrons are identified as field-aligned low-energy electrons in the solar wind, or "strahl," that propagate directly into the magnetosphere on open magnetic field lines [*Fairfield and Scudder*, 1985]. This phenomenon is known as "polar rain" [*Winningham and Heikkila*, 1974]. The third electron population, and the most obvious in Plate 17, is that associated with the spikes of fluxes, e.g., at 1606:30 and 1607:40 UT. This population is called "polar showers" by *Winningham and Heikkila* [1974].

Inspection of the image frame in Plate 4 for the DE 2 crossing of the polar cap, the position of the trajectory relative to auroral features in Figure 1, and predicted magnetic field crossing times in Table 2 shows that the electron precipitation

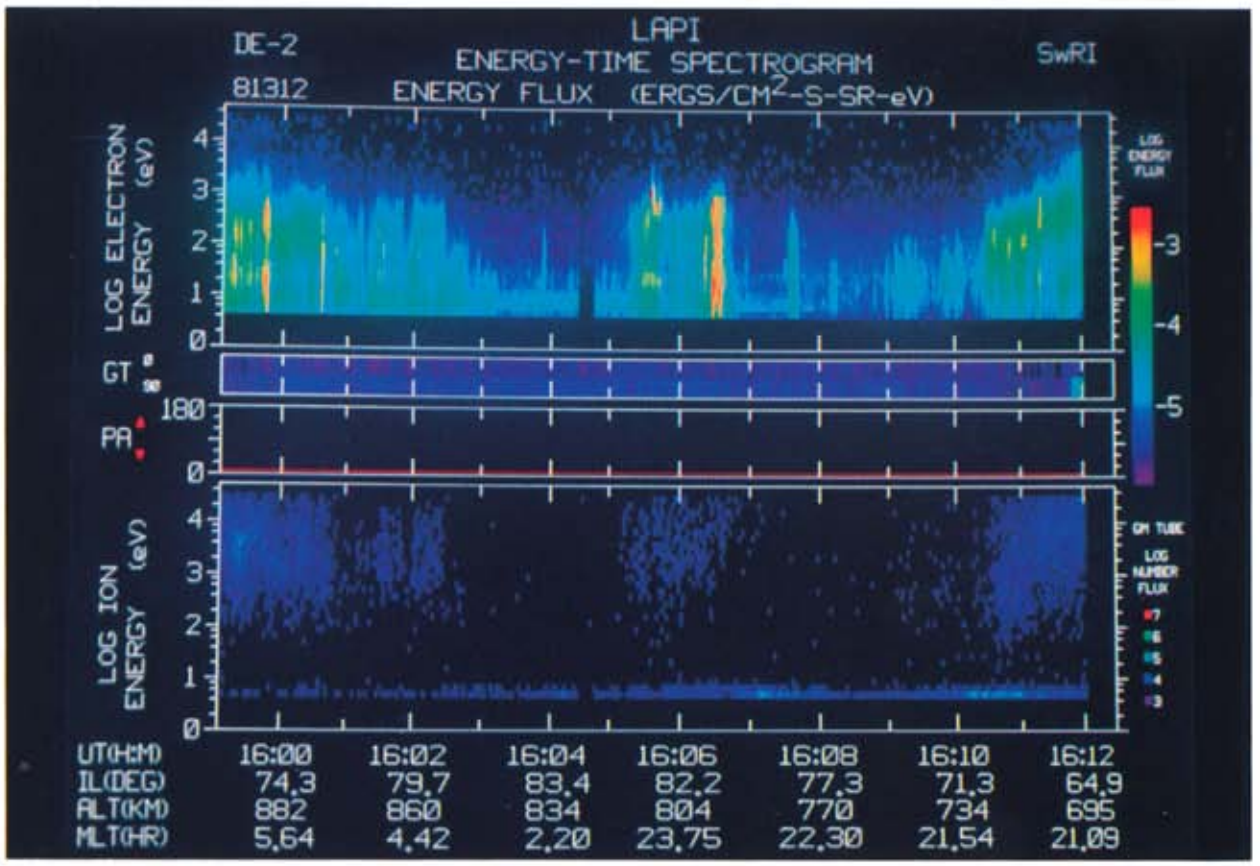

Plate 17. Energy-time spectrograms for electrons (upper panel) and positive ions (lower panel) for the low-altitude traversal of auroral and polar cap plasmas with DE 2 on November 8, 1981. The pitch angle for these charged particles is 0°, i.e., precipitating into the atmosphere. Transpolar arc plasmas are observed at 1605:20–1606:40 UT.

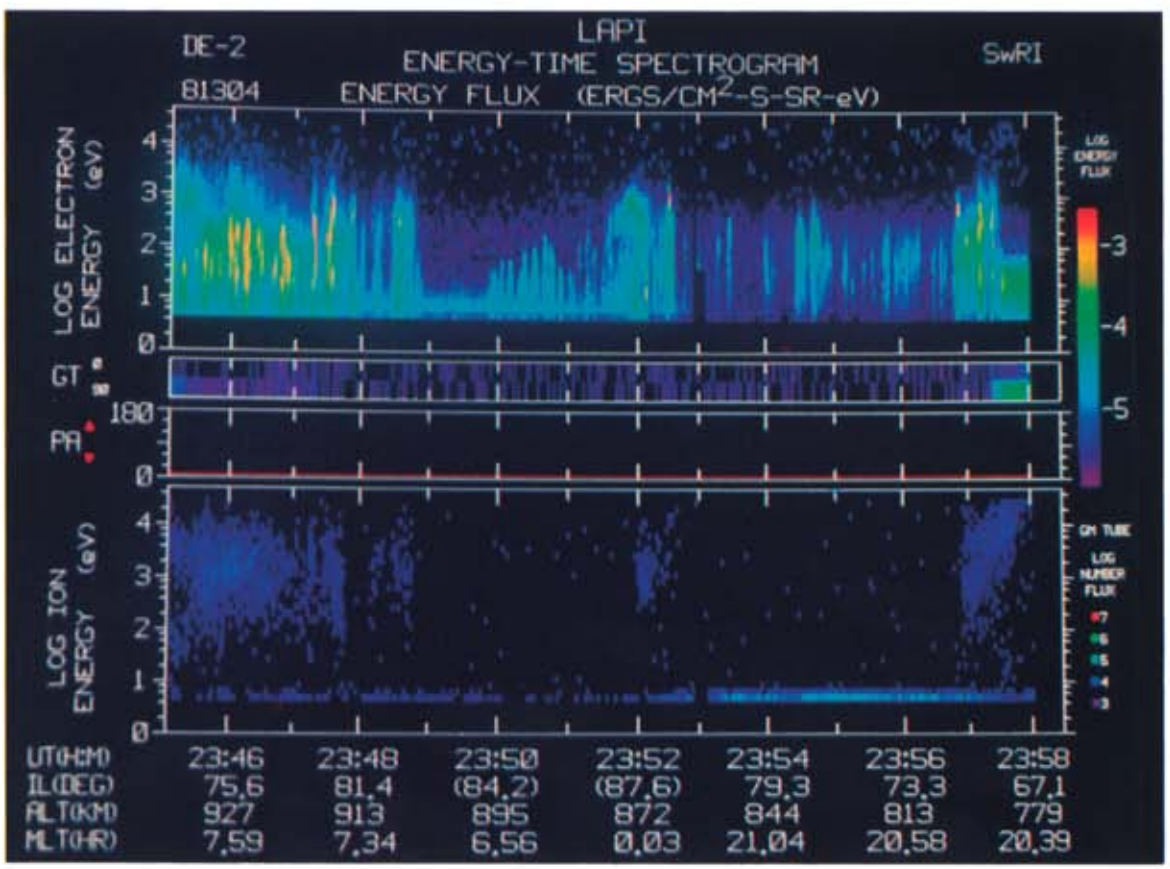

Plate 18. Continuation of Plate 17 for October 31, 1981. Transpolar arc plasmas are observed at 2351:30–2352:30 UT.

zone encountered during 1605:20–1606:40 UT is associated with the transpolar arc of the theta aurora. An inverted-V event occurs on the morning boundary of this zone at 1605:40 UT, and an intense feature is seen on the eveningside at 1606:20 UT. Thus the transpolar arc should comprise two bright arcs, as is shown earlier by *Frank et al.* [1982] for these series of measurements. The principal difference in the plasma distributions within these precipitation zones, other than energy fluxes, relative to similar spatial structures over the polar cap is the presence of ions in the energy range of several keV. No such ion fluxes are present, for example, in the feature at 1607:40 UT. In fact, the ion and electron energy spectra in the plasmas associated with the transpolar arc are qualitatively similar to those typically found in the boundary plasma sheet, i.e., the poleward regions of the auroral oval.

With regard to the spatially narrow features such as the electron features at 1607:40 UT in Plate 17, we note that the resolution of the imaging photometers is ~ 40 km and 80 km at altitudes 1.5 R_E and 3.0 R_E, respectively. The width of the narrow electron precipitation zone aforementioned is ~ 40 km. At higher altitudes the presence of numerous such features would appear as a dim luminosity over the polar cap. These weak emissions have previously been reported by *Frank et al.* [1982] for this theta aurora.

October 31, 1981. This series of plasma measurements is similar to that above for November 8. Examination of the image corresponding to this polar cap traversal by DE 2 as shown in Plate 8 finds that the electron precipitation zone at 2351:30–2352:30 UT is located over the transpolar arc of a theta aurora. The intercept times as determined nearly simultaneously with imaging are identified in Table 2. The boundary plasma sheet is encountered at 2345:00–2348:45 UT (morning sector of oval) and 2356:50–2357:30 UT (evening sector). Again, the plasmas over the transpolar arc are qualitatively similar to those found in the boundary layer plasmas in the poleward region of the auroral oval. The presence of ion fluxes with energies of about several keV is also conspicuous over the transpolar arc in contrast to other polar cap precipitation regions, e.g., at 2354:30 UT. Note that the presence of the theta aurora cannot be deduced solely from the in situ plasma observations in Plates 17 and 18. Without the global images of the polar cap the plasmas associated with the transpolar arc might be interpreted as a dramatic extension of the boundary plasma sheet region into the polar cap.

November 25, 1981. The intensities of emissions from the transpolar arc varied greatly as a function of time for this example of theta aurora (see Plates 9, 10, and 11). During the series of plasma measurements with DE 2 most of the transpolar arc is very dim as shown in Plate 12. The plasma measurements are displayed in Plate 19. The time of crossing of the magnetic field lines threading the transpolar arc with DE 2 is identified from the images as 1135–1136 UT (Table 2). Indeed, examination of Plate 19 finds that a plasma feature similar to that for the above two cases is encountered at 1135:00–1136:30 UT. The boundary plasma sheet is seen in the morning sector at 1129:00–1131:00 UT. The anticipated relative absence of plasmas is observed at 1131:00–1135:00 UT in the morning sector of the polar cap. However, there is no corresponding feature found in the traversal of the evening polar cap between the plasmas of the transpolar arc and the auroral zone. The imaging results predict that the crossing of the evening sector of the oval occurs at 1140–1141 UT (Table 2). This prediction is in agreement with the magnitudes of the precipitating electron fluxes shown in Plate 19 at these times. Thus the minimum of ion and electron fluxes is expected at 1136:30–1140:00 UT. On the contrary, a general presence of ion and electron fluxes is detected during this interval. Although the electron energy influx is low in magnitude and carried by low-energy electrons, $E \lesssim 100$ eV, relative to those associated with the position of the transpolar arc, the intensities and energies of the positive ions are very similar. Thus during a period of substantial dimming of the transpolar arc a large area of the polar cap exhibits an influx of ions similar to that found above the high-latitude regions of the auroral oval.

October 17, 1981. The series of images for this theta auroral event displays a complex system of polar arcs and polar cap emissions during most of the observational period (Plates 13, 14, and 16) and a clear development of a transpolar arc after the polar overflight of DE 2 (Plate 15). The image corresponding to the DE 2 polar traversal is shown in Plate 16. This imaging result predicts that substantial precipitating plasmas are to be detected across the entire polar cap. Crossing times for a major polar arc (2) and the transpolar arc (weakly developed stage) are given in Table 2. The trajectory of DE 2 relative to major auroral luminosity features is displayed in Figure 4. Indeed, the electron spectrogram in Plate 20 demonstrates that significant electron precipitation occurs during most of the DE 2 traversal of the polar cap. The transpolar arc is just beginning to brighten at the time that DE 2 intersects the corresponding magnetic field lines at 1644–1645 UT (Table 2). The associated plasma feature is identified in the electron and ion spectrograms at 1644:30–1645:40 UT in Plate 20. During this time period the ion intensities are relatively high. Another lesser polar arc is encountered by DE 2 at 1641:10 UT; it is characterized by considerably lesser ion intensities. This arc is also discernible in the images (see Table 2). During the interval between the encounter with this arc and the transpolar arc, i.e., 1641:10 and 1644:30 UT, no ion intensities above background rates due to a solar proton and electron event are found. On the other hand, substantial ion intensities are observed between the transpolar arc and the poleward edge of the evening sector of the oval, i.e., 1645:40 to $\sim$1647:00 UT. Note that the spacecraft is moving along a path at small angles relative to the transpolar arc (Table 3). Thus at the onset of brightening and development of this transpolar arc a complex spatial distribution of precipitating electron and ion intensities is found over the polar cap, and a plasma feature associated with the transpolar arc is identified.

It is of considerable interest to note the spatial distributions of solar electrons with $E > 32$ keV incident upon earth's polar atmosphere. The responses of the Geiger-Mueller tubes to these electrons are given in the narrow color-coded bar just below the electron spectrogram in Plate 20. Over the morningside of the polar cap during the interval 1637:50 to 1644:00 UT the electron intensities are relatively high and without structure, indicating a direct access of solar electrons to this geomagnetic region. Over the evening sector of the polar cap at 1645:40 to 1647:00 UT, solar electron intensities appear lesser than those over the morning sector. However, the trajectory of DE 2 passes near the transpolar arc without penetrating deeply into the evening sector (cf. Plate 16). On the other hand, intensities in the morning boundary plasma sheet at 1635:00 to 1636:40 UT and at 1637:00 to 1637:50 UT and in the transpolar arc region at 1644:40 to $\sim$1646:00 UT are considerably less. Electron intensities in the evening sector of the boundary plasma sheet at 1647:00 to 1647:30 UT are intermediate in relation to those in the morning sector of the polar cap and transpolar arc regions identified above. These

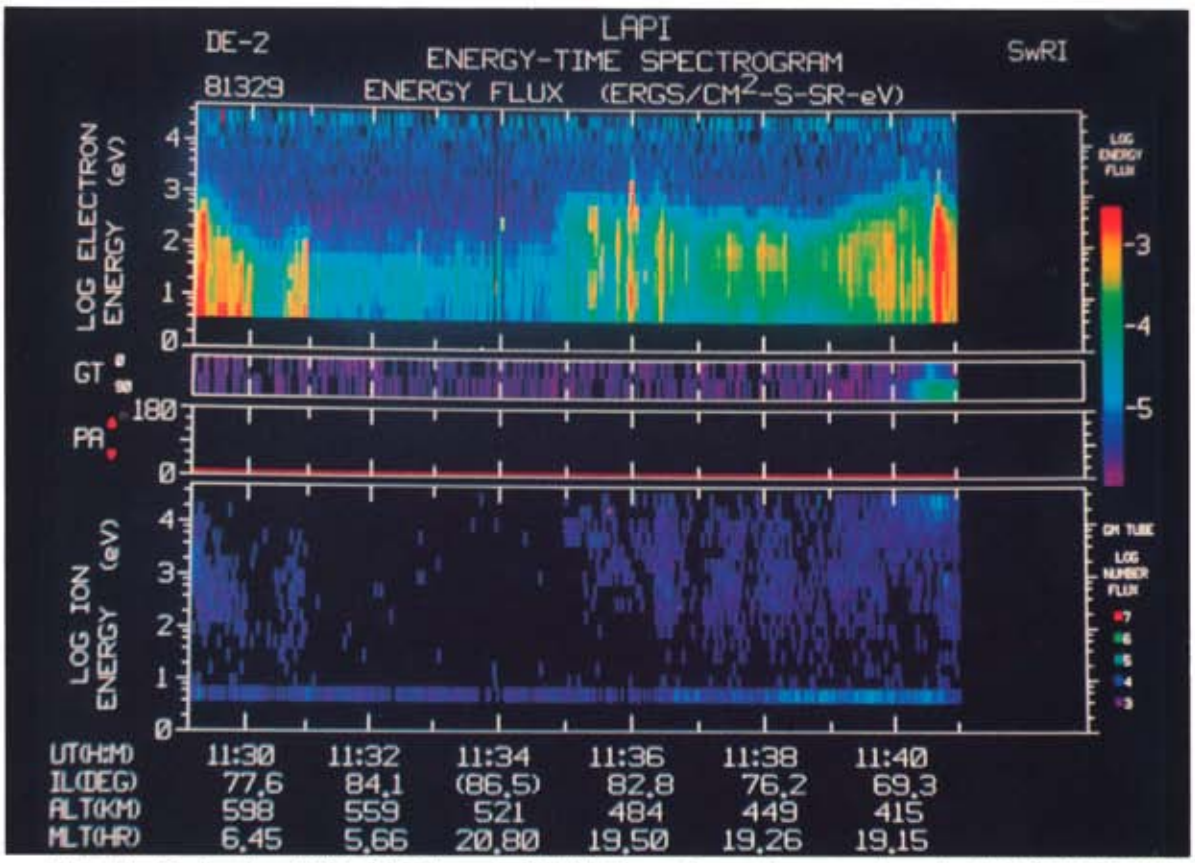

Plate 19. Continuation of Plate 17 for November 25, 1981. Transpolar arc plasmas are observed at 1135:00–1136:30 UT.

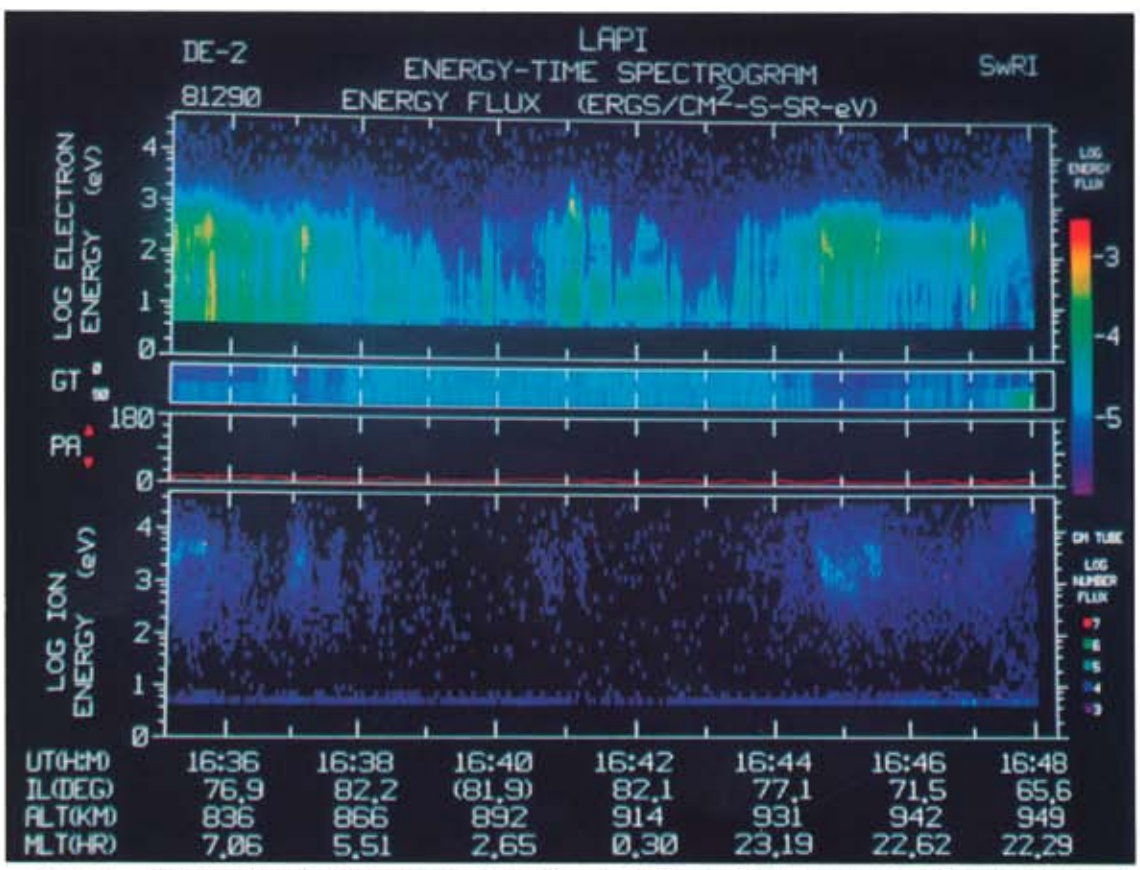

Plate 20. Continuation of Plate 17 for October 17, 1981. Transpolar arc plasmas are observed at 1644:30–1645:40 UT.

electron intensities may be attributable to the auroral acceleration mechanism, rather than a solar source. This behavior of solar electron access to earth's polar cap is indicative of a relatively complex spatial connection of geomagnetic field lines to those of the interplanetary medium. Such solar electron events will probably be important future diagnostics in resolving the issue of magnetic topology during theta auroral events.

4. Hot Plasmas at High Altitudes

The individual electrostatic analyzers that comprise the high-altitude plasma instrument (HAPI) on the DE 1 spacecraft are similar to those for the plasma instrumentation on DE 2 as discussed in the previous section. Five of these analyzers, each capable of simultaneously measuring the directional, differential intensities of positive ions and electrons over the energy-per-unit charge range 5 V to 32 kV, are mounted on the spinning DE 1 spacecraft. Since the spacecraft is spinning, the directions of the fields of view of the analyzers are positioned such that the opportunities to view in the direction of the local magnetic field are optimized and such that a reasonable survey of the three-dimensional velocity distributions of plasmas is realized. The spin axis is directed normal to the orbital plane, and the fields of view of the analyzers are directed at 45°, 78°, 90°, 102°, and 135° to this axis. The spin period is 6 s. More detailed information concerning this instrumentation is given by *Burch et al.* [1981].

November 8, 1981. As with our preceding survey of hot plasmas at low altitudes, we shall examine the character of plasmas flowing along the magnetic field into earth's atmosphere and shall utilize the spectrogram as the display medium. The format of the spectrograms is identical to those described in detail in the previous section, with the exception that the panel corresponding to the Geiger-Mueller tube responses is deleted. The spectrograms for positive ions and electrons are shown in Plates 21*a* and 21*b* for the polar passage over a theta aurora on November 8. Since the time period for crossing the entire polar cap is lengthy (several hours) in relation to the temporal evolution of the transpolar arc, three images are provided for time periods centered on the spacecraft interceptions of magnetic field lines of the morning sector of the auroral oval, the transpolar arc, and the evening sector of the oval. These images are shown in Plates 1, 2, and 3, respectively. The spacecraft exited field lines associated with the morning sector of the auroral oval at 1315 UT and intercepted those for the transpolar arc at 1546–1600 UT (Table 2). Thus the spectrogram of Plate 21*a* shows the electron and ion differential energy fluxes for a portion of the region between the morning oval and the transpolar arc. As for the low-altitude plasma, no significant ion fluxes are observed. The most striking feature in the spectrograms is the large fluxes of electrons with energies $\sim$5–10 eV. These electrons are interpreted as ambient electrons and spacecraft photoelectrons that are accelerated into the field of view of the plasma analyzer by a positive spacecraft potential. The sporadic fluxes of electrons in the energy range $\sim$10–300 eV may be associated with the lower-energy polar "showers" identified at low altitudes in this sector of the polar cap (cf. Plate 17). The relatively unstructured, low fluxes of electrons at energies in the range of 100 eV are the high-altitude signature of the polar "rain," i.e., electrons of solar coronal origins.

The encounter with field lines associated with the transpolar arc is shown in the plasma spectrograms of Plate 21*b*. This encounter occurs during 1546–1600 UT (Plate 2 and Table 2). Substantial ion intensities in the energy range 1–10 keV are observed along with electron energy fluxes with maxima in the energy range 200–500 eV. The character of the electron energy spectra indicates that significant acceleration is occurring at altitudes above the spacecraft position at $\sim$18,000 km. Comparison with similar measurements at low altitudes with DE 2 in Plate 17 shows that electron acceleration is also occurring beneath the DE 1 altitudes.

The plasmas in the polar region between the transpolar arc and the evening sector of the auroral oval at 1600–1640 UT (Table 1) are seen to be similar to those noted above for the morning polar region. The exception is the disappearance of the intense fluxes of low-energy electrons at 5–10 eV, presumably due to a negative spacecraft potential.

The period for traversal of the evening sector of the auroral oval is 1640–1651 UT (Plate 3 and Table 2). In the spectrogram of Plate 21*b* the ion fluxes and spatially structured electron fluxes that are the signature of the boundary plasma sheet appear at 1638–1645 UT. At lower altitudes the electrons are notably more energetic and are associated with inverted-V regions. The higher-temperature plasmas, with relatively no small-scale spatial structures, at 1645–1650 UT are associated with the plasma sheet and ring current.

Thus the hot plasmas at the greater altitudes of DE 1 over the polar regions are similar to those found at low altitudes with DE 2. The primary exception is the lesser electron energies associated with the transpolar arc and boundary plasma sheet (poleward region of oval) at higher altitude. This feature is presumably accounted for by field-aligned acceleration of the electrons below the DE 1 altitudes. However, some electron acceleration is observed to occur also at altitudes above DE 1.

October 31, 1981. The plasma spectrograms for this high-altitude polar pass over the theta aurora are shown in Plates 22*a* and 22*b*. During the time period 2121–2148 UT the spacecraft is exiting the morning sector of the auroral oval as noted by the presence of positive ions with energies $\sim$1 keV. This invariant latitude of the poleward boundary at $\sim$81° agrees reasonably with the observations of DE 2, shown in Plate 18, that place this boundary at $\sim$82° approximately 2 hours later. The images indicate that the position of the morning sector of the auroral oval is not changing significantly during 2200–2330 UT (Figure 2). Inspection of Plate 5 finds auroral emissions along the magnetic subsatellite track, or ingress, at 300 km until $\sim$2200 UT, in agreement with the high-altitude plasma measurements of Plate 22*a*. The electron energies are $\lesssim$200 eV, and the electron spatial distributions exhibit practically no small-scale structure. On the other hand, at the lower altitudes of DE 2 (Plate 18), considerable spatial structure is found, and electron acceleration to energies approaching 1 keV is evident in several of the narrow, intense precipitation regions. Thus acceleration of the electrons is occurring below the DE 1 altitudes of $\sim$23,000 km.

During the time periods $\sim$2147–2316 UT and 2327–2356 UT the DE 1 spacecraft is located in the polar cap on the morningside and the eveningside of the transpolar arc, respectively. For most of these periods the structured electron fluxes associated with polar showers are observed, and a relatively weak flux of solar coronal electrons (polar rain) is present. Measurable ion intensities are not observed. The crossing of the evening sector of the auroral oval occurs during $\sim$2356–2400 UT (cf. Table 2).

The traversal of the magnetic field lines associated with the transpolar arc is predicted from the imaging results for 2316–

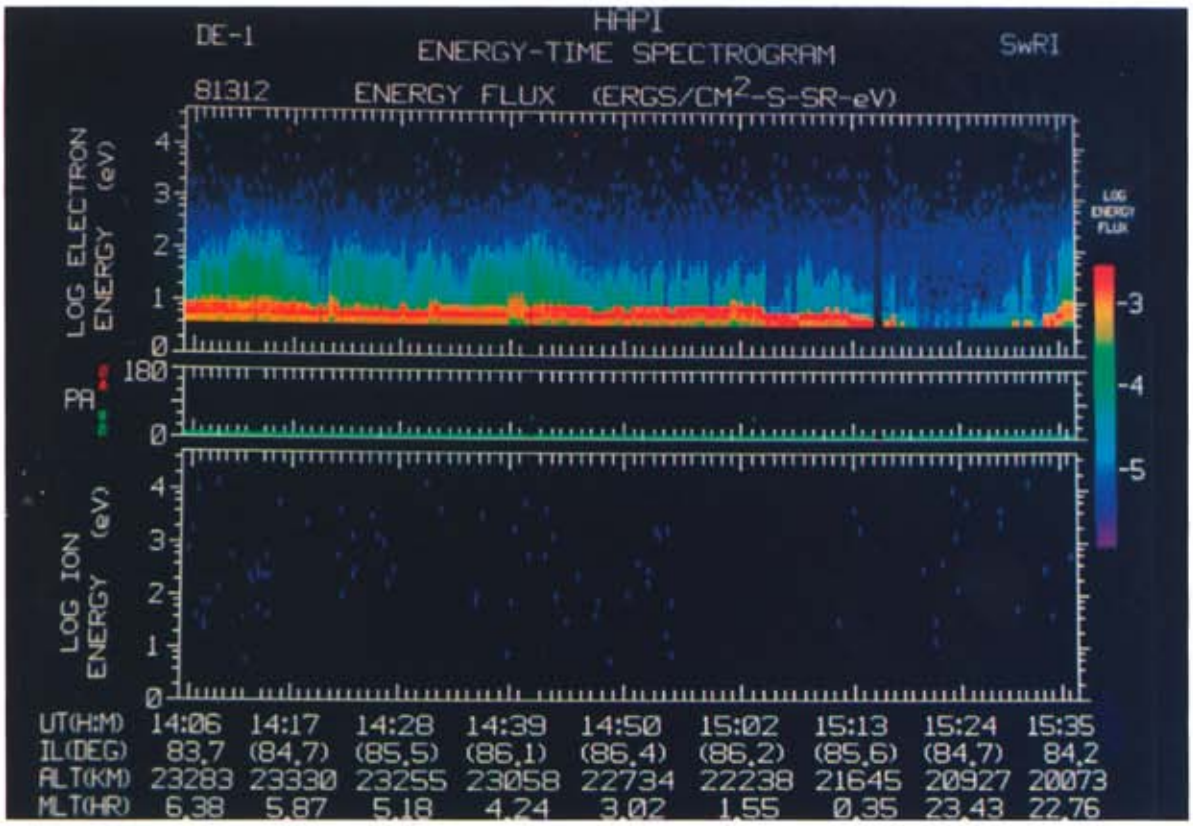

Plate 21*a*

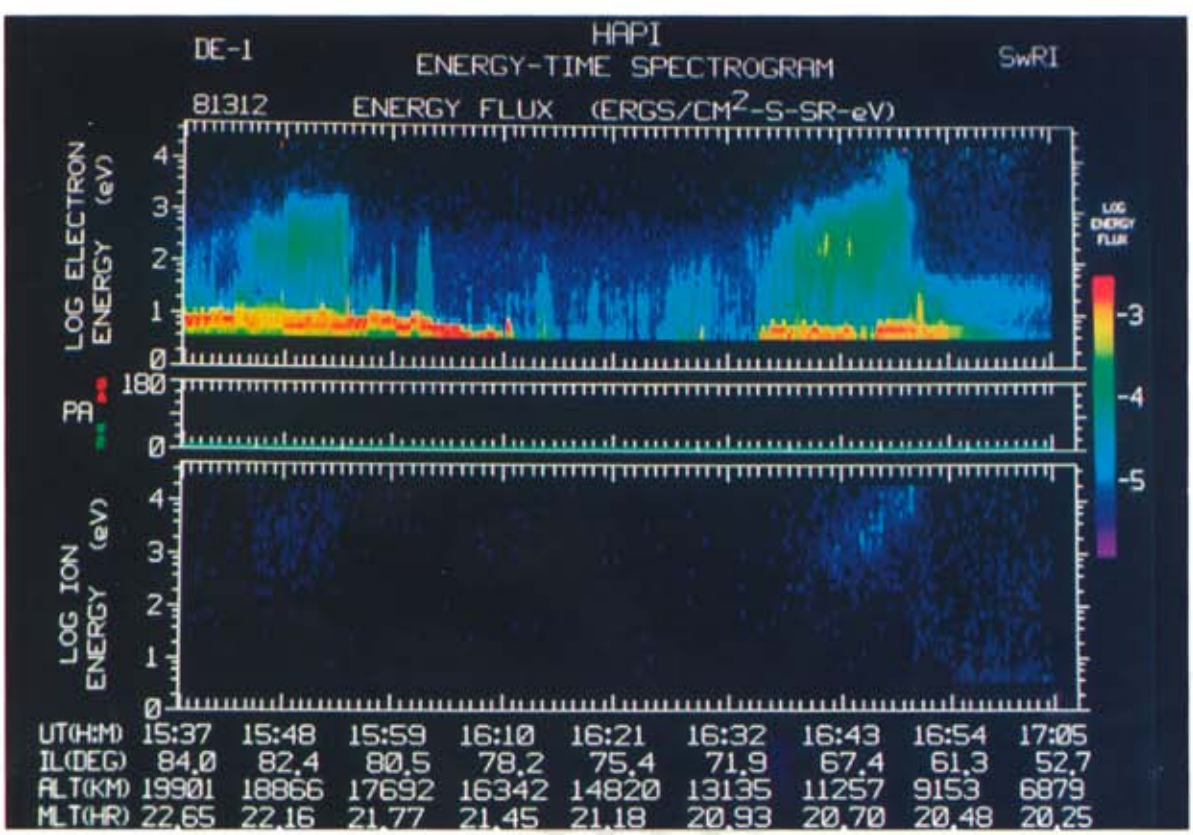

Plate 21*b*

Plate 21. Energy-time spectrograms for electrons (upper panel) and positive ions (lower panel) for the high-altitude traversal of auroral and polar cap plasmas with DE 1 on November 8, 1981. The pitch angle for these charged particles is 0°, i.e., precipitating into the atmosphere. Transpolar arc plasmas are observed at 1546–1600 UT.

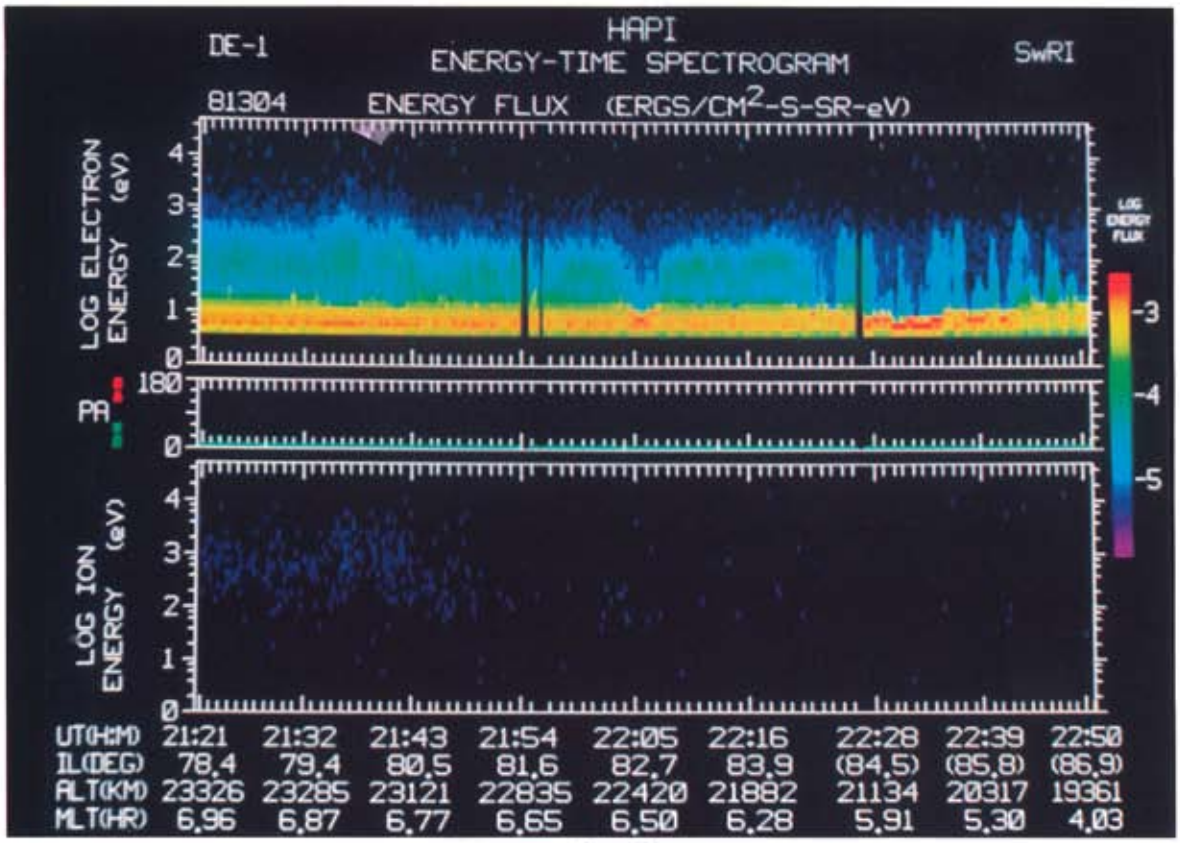

Plate 22*a*

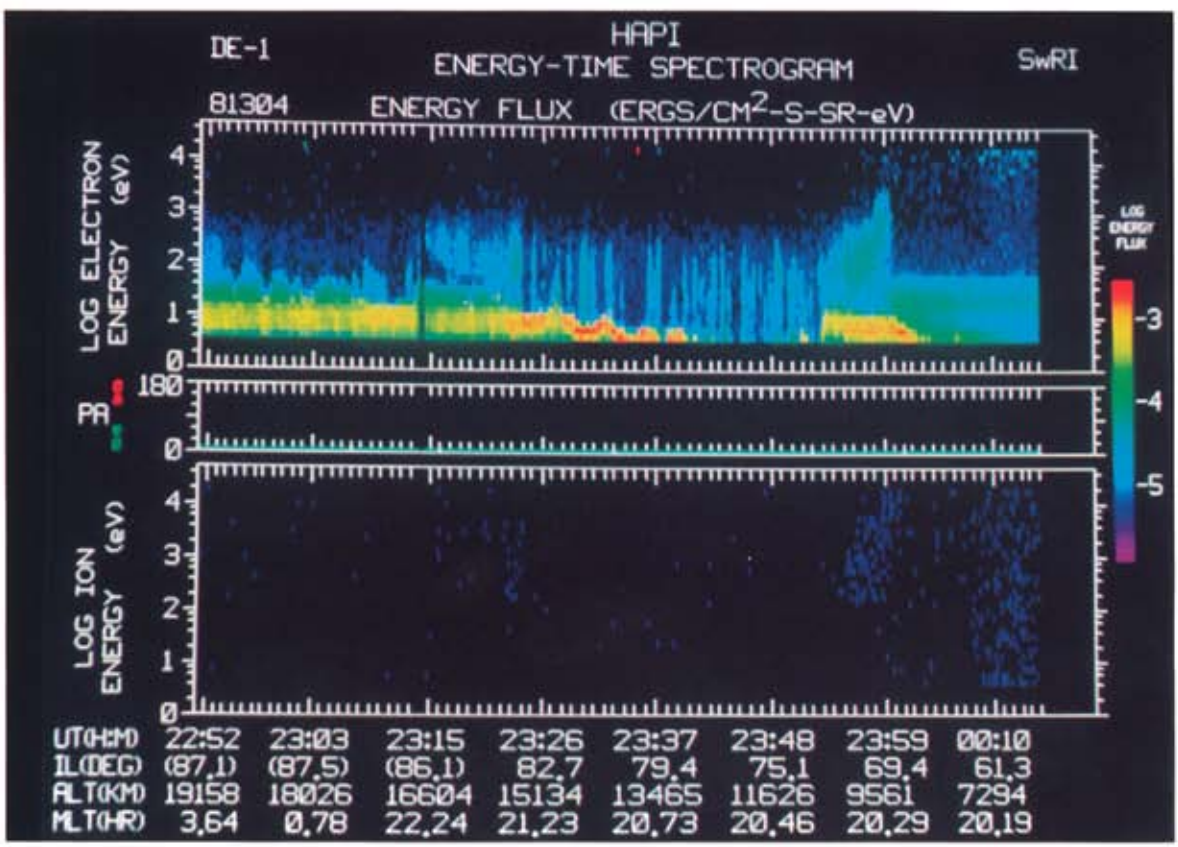

Plate 22*b*

Plate 22. Continuation of Plate 21 for October 31, 1981. Transpolar arc plasmas are observed at 2315–2327 UT.

2327 UT (Plate 6 and Table 2). Examination of the spectrogram in Plate 22*b* for this time period shows the typical presence of low fluxes of positive ions in the energy range ~1–10 keV. On the other hand, only slight heating of the electrons is noted. The transpolar arc is of similar brightness for the DE 1 and DE 2 crossings (Plates 6 and 8). The DE 2 interception of field lines threading the arc occurs ~30 min later. Significant electron acceleration reminiscent of inverted-V events is found at DE 2 altitudes. Thus the electron acceleration occurs below the DE 1 altitude of ~16,000 km.

November 25, 1981. The predicted time for the exit of DE 1 from the poleward edge of the morning sector of the auroral oval is 0957 UT (Table 2). This time is in agreement with the high-altitude plasma measurements shown in Plates 23*a* and 23*b*. The exit is indicated by the general termination of notable ion fluxes with energies ~1 keV. The polar cap is traversed at 0957–1142 UT and 1146–1238 UT (Table 2) for the morning and evening sectors, respectively. There are a multitude of narrow spatial structures of low-energy electron fluxes over most of the polar cap. Ion fluxes above the instrument threshold are generally absent. Encounter with plasmas associated with the evening sector of the auroral oval is predicted during 1238–1247 UT, a period not covered by the spectrograms in Plates 23*a* and 23*b*.

The DE 1 encounter of plasmas associated with the transpolar arc occurs during 1142–1146 UT (cf. Table 2). The electron energy is low, about several hundreds of electron volts, and the ubiquitous ion signature at 1–10 keV is present. The DE 1 and DE 2 observations of these plasmas occurred within ~10 min of each other. At these times the transpolar arc is very dim as seen in Plates 10 and 12. This dimming might be partially due to a decrease in the average energy of precipitating electrons since this series of images is taken primarily in the emissions of molecular nitrogen. Inspection of the DE 2 spectrogram in Plate 19 at 1135:00–1136:00 UT indicates acceleration of electrons to energies ~1 keV at altitudes below the DE 1 orbit.

October 17, 1981. The high-altitude plasma measurements are summarized in Plates 24*a* and 24*b*. For this series of measurements for the theta aurora that began to form at ~1640 UT (see Plates 13 through 16 and Figure 4), the imaging results are insufficient to predict accurately the period of encounter of the plasmas associated with the morning sector of the auroral oval. The termination of ion fluxes to be noted in Plate 24*a* gives the exit time from the electron precipitation in the morning sector as ~1533 UT. Examination of Figure 4 shows that an estimated time period for the exit of DE 1 from plasmas associated with the morning sector of the oval is ~1400–1415 UT. The magnetic subsatellite position for DE 1 then moves nearly parallel to a complex distribution of polar arcs poleward of the auroral oval until ~1600 UT. The crossing times for plasmas precipitating into the evening sector of the oval are found by use of the images to be 1710–1722 UT (Table 2), in general agreement with the electron spectrogram of Plate 24*b*. The polar cap is characterized by numerous electron precipitation features, e.g., at 1612 UT and 1633 UT. Again, ion fluxes in the energy range ~1–10 keV are generally not present. However, only one such precipitation event is characterized by accompanying fluxes of precipitating ions in the energy range 1–10 keV. The corresponding time period is 1641–1647 UT and is in substantial agreement with the predicted period for the presence of plasmas associated with the transpolar arc from the global images (Table 2). Electron energies are typically several hundred electron volts at the DE 1 altitudes, ~17,000 km. The crossing of the transpolar arc plasmas at low altitudes, ~940 km, with DE 2 is almost simultaneous with that of DE 1 within 1–2 min. Examination of the DE 2 spectrogram at 1644:40–1645:30 UT shows electron energies also in the range of several hundred electron volts (see Plate 20). Thus there is not a detectable acceleration of electrons between the altitudes of DE 1 and DE 2 during this time period.

The presence of positive ions in the energy range ~1–10 keV appears to uniquely characterize the plasmas of the transpolar arc of the theta aurora relative to other polar arcs. These ion intensities remain present over the polar cap when the transpolar arc dims greatly (November 25) and at the onset of the brightening of the transpolar arc before substantial electron acceleration into the atmosphere occurs (October 17).

5. Composition of Hot Plasmas at High Altitudes

The energetic ion composition spectrometer (EICS) on board the high-altitude spacecraft comprises three primary elements, a retarding potential analyzer in front of a cylindrical-plate electrostatic analyzer for energy–per–unit charge (E/Q) analyses of low- and high-energy ions, respectively, followed by a crossed field ($\mathbf{E} \times \mathbf{B}$) filter for identification of the mass per unit charge (M/Q) of the ions. For the observations presented here the ion mass spectrometer is providing both the directional, differential ion spectra for a given species over the E/Q range ~10 V to 18 kV and the identity of all major ion species to be found in earth's magnetosphere, e.g., H^+, He^+, He^{++}, and O^+. The field of view of this instrument is directed normal to the spacecraft spin axis. Since this spin axis is in turn oriented normal to the orbital plane, the instrument is often able to view the entire pitch angle distributions of the ions. The various instrument cycling modes and details of the analyzer designs have been given previously by *Shelley et al.* [1981].

November 8, 1981. As with the multidimensional measurements with the aforementioned hot plasma analyzers, it is convenient to employ similar spectrograms for the mass analyzer in order to provide a compact overview of the ion distributions at high altitudes in the northern polar regions during these theta auroral events. The ion spectrograms for the example of November 8 are shown in Plate 25. The top spectrogram shows the directional, integral intensities of protons within the energy range 1–18 keV as a function of spacecraft rotation angle 0°–360° (ordinate) and UT (abscissa). The rotation angle 0° is nearly in the direction of spacecraft motion. The units of intensity are $(cm^2\ s\ sr)^{-1}$ and are color coded according to the scale on the right-hand side of Plate 25. The minima in intensities at ~90° and 270° correspond to the source cone (ions flowing up from the ionosphere along the magnetic field) and to the loss cone (ions flowing into the ionosphere and along the local field direction), respectively. The notable minima in the source and loss cones at ~1200–1230 UT and at 1700 UT occur in plasmas associated with the morning and evening sectors of the auroral oval, respectively. For reference the DE 1 spacecraft exits plasmas associated with the morning sector at 1315 UT and enters the evening oval at 1640 UT (Table 2 and Plates 21*a* and 21*b*). The angular distributions of H^+ within the plasmas associated with the transpolar arc at 1546–1600 UT are generally isotropic with the exception of the minima at the source cone. Within the polar region between 1315 UT and 1640 UT, and

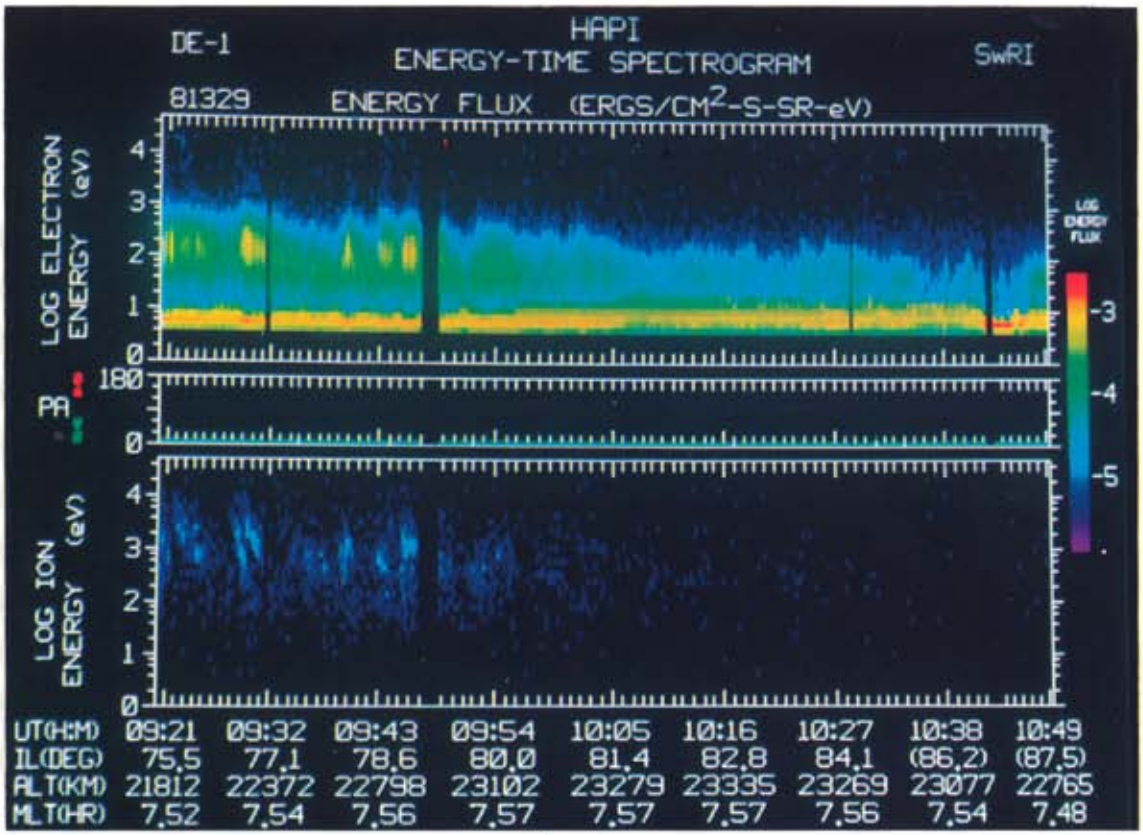

Plate 23*a*

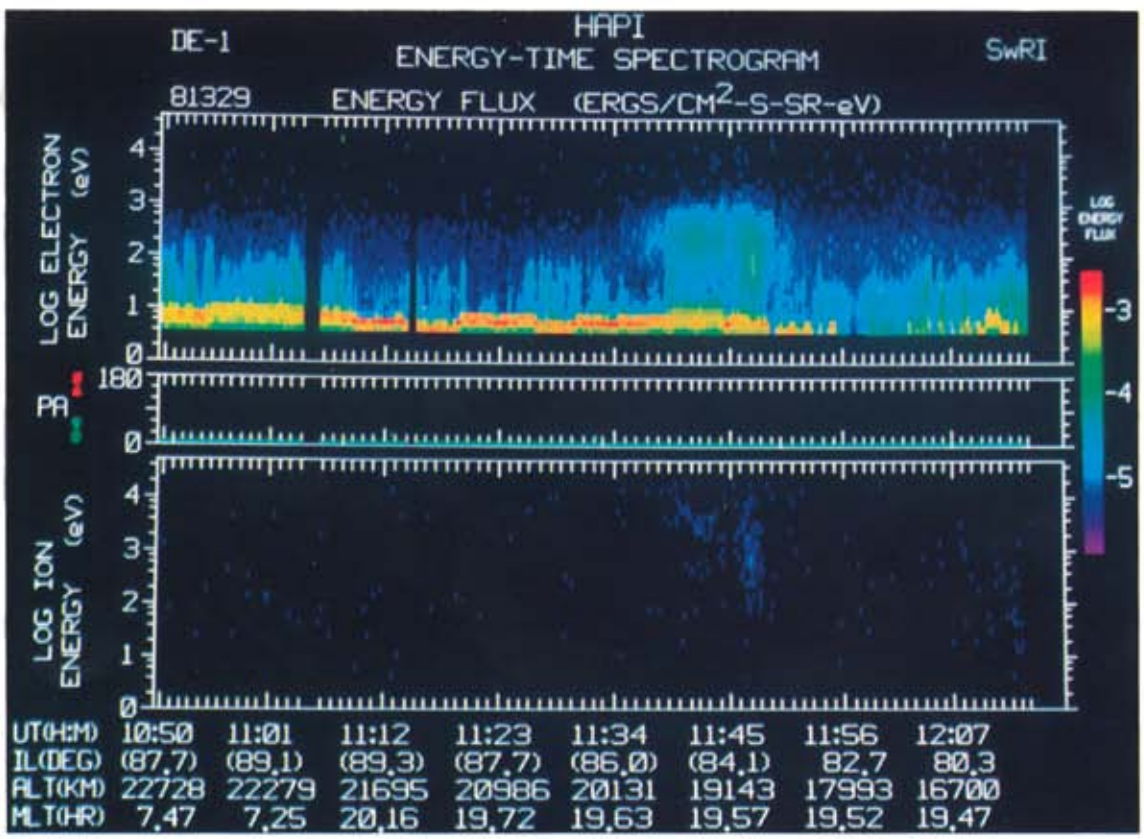

Plate 23*b*

Plate 23. Continuation of Plate 21 for November 25, 1981. Transpolar arc plasmas are observed at 1142–1146 UT.

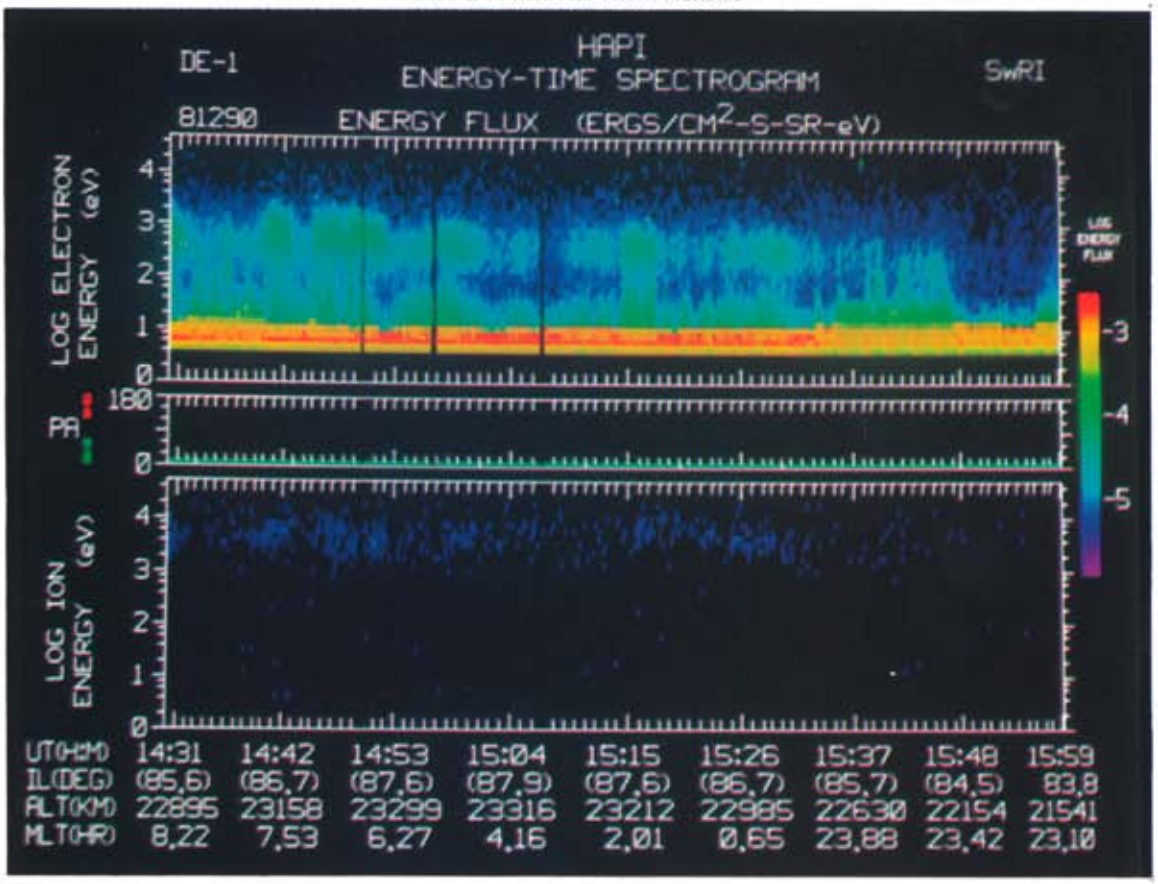

Plate 24*a*

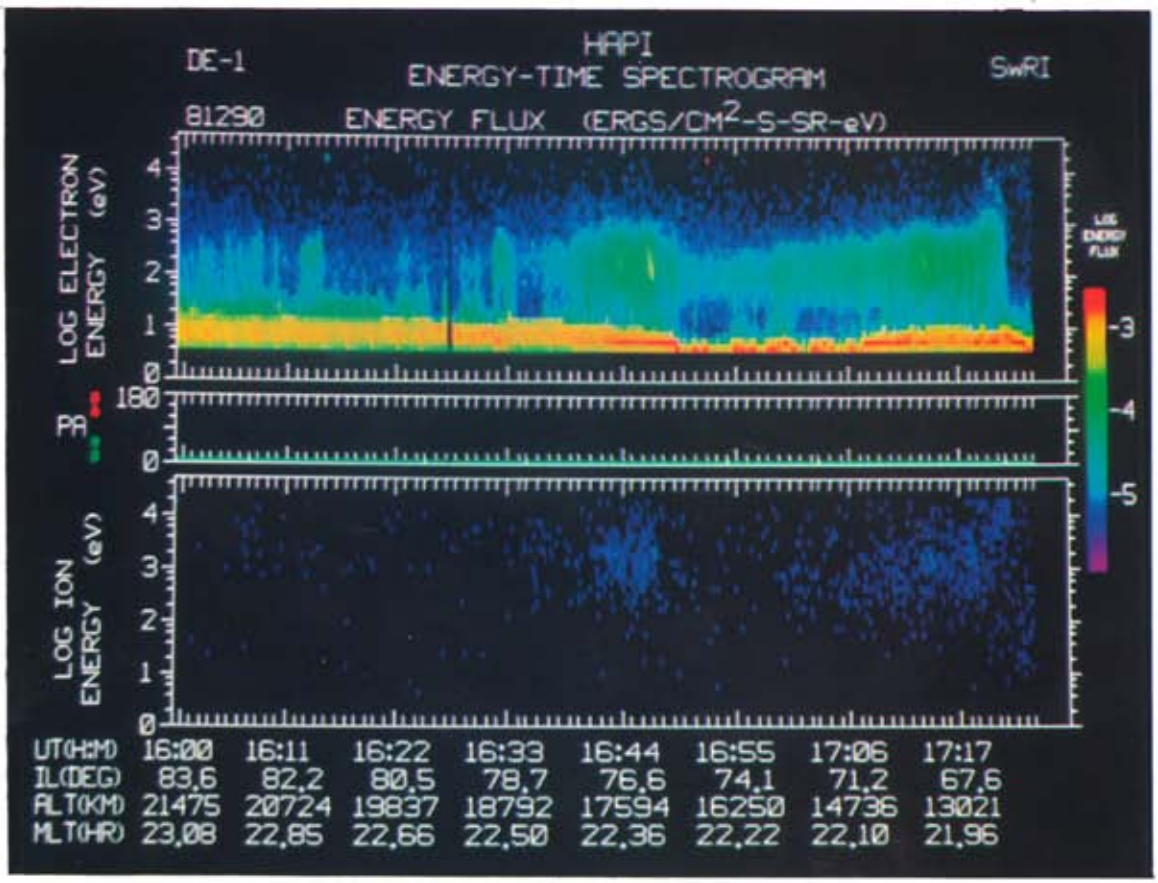

Plate 24*b*

Plate 24. Continuation of Plate 21 for October 17, 1981. Transpolar arc plasmas are observed at 1641–1647 UT.

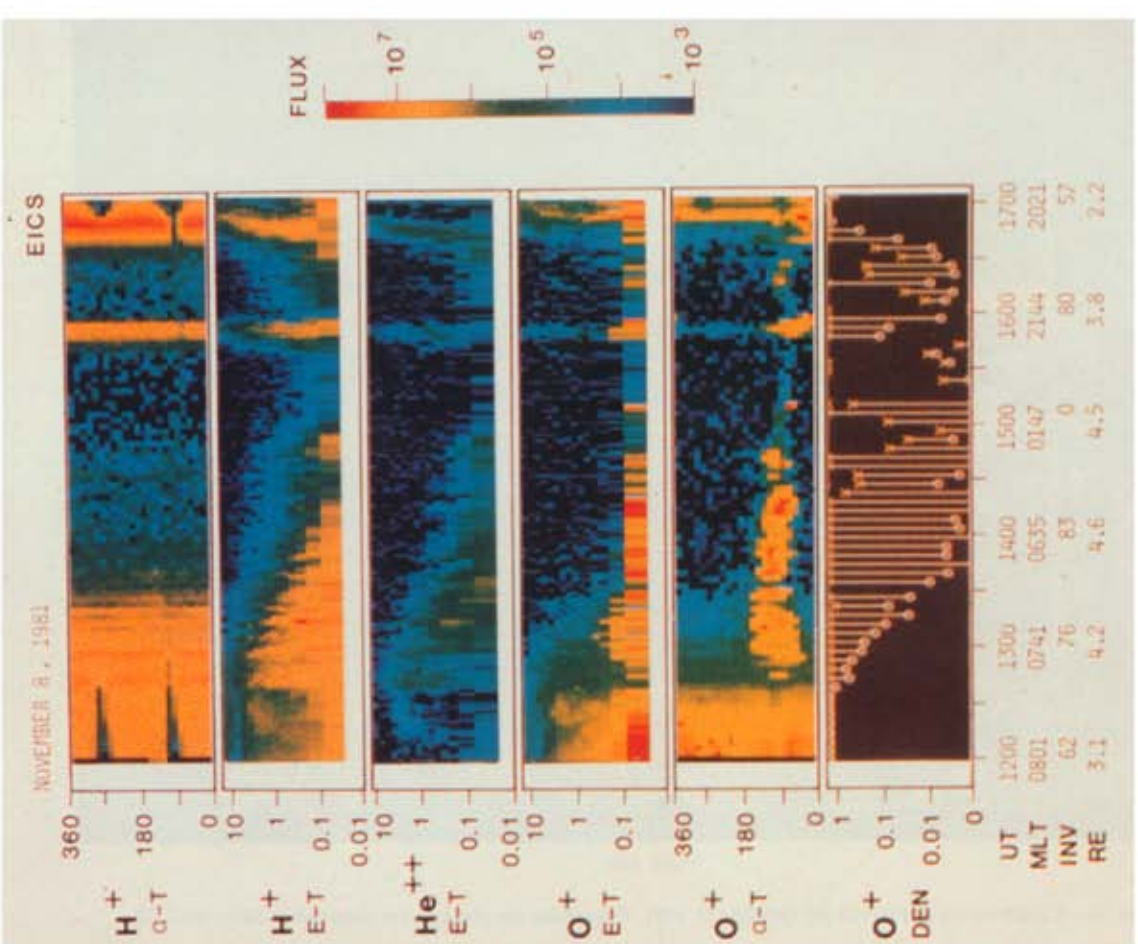

Plate 25. Angular distributions (α-t) and energy spectra (E-t) for H^+, He^{++}, and O^+ ions at high altitudes for the polar passage of DE 1 on November 8, 1981. The signature of the transpolar arc plasmas occurs at 1546–1600 UT.

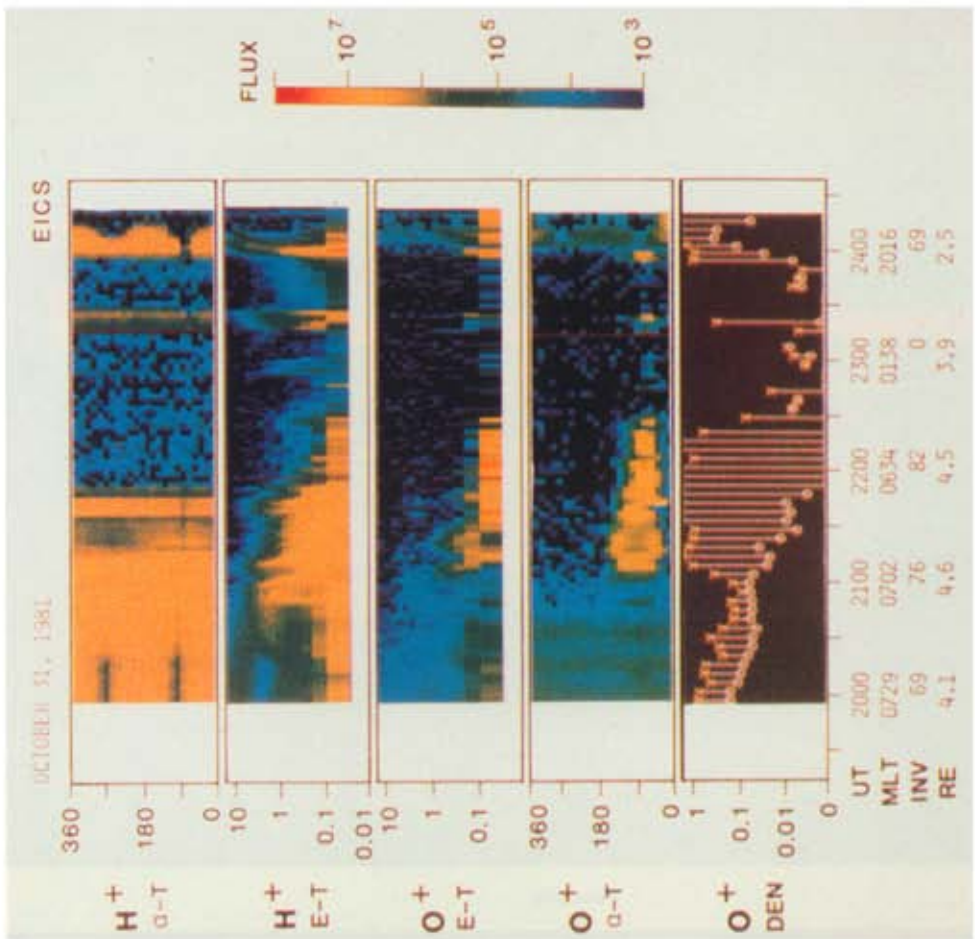

Plate 26. Continuation of Plate 25 for October 31, 1981. The signature of the transpolar arc plasmas occurs at 2315–2327 UT.

excluding the obvious signature of the transpolar arc at ~ 1550 UT, there are low, isotropic intensities of H^+ that increase as either the morning or evening sector of the auroral oval is approached. With consideration of the fact that the invariant latitudes are decreasing more rapidly toward evening with increasing UT as the spacecraft descends toward perigee, these intensity profiles are more or less symmetric in the local morning and evening sectors of the polar cap. Along the abscissa of the bottom spectrogram are given the coordinates magnetic local time (MLT), invariant latitude (INV), and geocentric radial distance (R_E) of the spacecraft position. The value of 0 for invariant latitude indicates that an accurate value for this parameter is not available for these high polar latitudes. The low H^+ intensities over the polar cap, which are not detected with the plasma instrument (section 4), are discernible in Plate 25 because of the larger geometric factor of the ion spectrometer at low energies and the longer averaging intervals employed in construction of the composition spectrograms in Plate 25.

Energy-time spectrograms are given for H^+, He^{++}, and O^+ in the second, third, and fourth panels, respectively, in Plate 25. The ordinate of each panel is the logarithm of the ion energy per unit charge, and the fluxes are color coded according to the color bar on the right-hand side of the plate. The units of these directional, differential intensities are $(cm^2\ keV\ s\ sr)^{-1}$. Intensities of H^+ and He^{++} ions are found over a substantial region of the polar cap. Singly ionized oxygen ions with energies in the range of tens of electron volts are also to be noted. These low-energy O^+ ions, which are frequently observed over the polar cap [*Shelley et al.*, 1982], are streaming upward from the ionosphere as shown by the fifth panel in Plate 25, which shows the directional, integral intensities of these ions in the energy range ~10 eV to 1 keV as a function of spacecraft rotation angle. This panel is formatted in an identical manner to the top panel of Plate 25 for H^+. The bottom panel gives the number densities in units of cm^{-3} of O^+ ions in the E/Q range 10 V to ~18 kV (crosses) and 1 kV to ~18 kV (circles). Densities greater than 2 cm^{-3} are plotted at the top of this panel.

There is a general paucity of energetic O^+ ions within the polar cap with the exception of the plasmas of the transpolar arc. This fact, coupled with the observation that there is a substantial density of He^{++} ions, leads to a general conclusion that the isotropic, polar cap plasmas observed during 1315–1546 UT and 1600–1640 UT are most likely of direct magnetosheath origins. The exception, of course, is the low-energy H^+, He^+, and O^+ ions streaming out of the ionosphere. On the other hand, substantial intensities of isotropic, energetic O^+ intensities, as well as those of H^+ and He^{++}, are observed in the plasmas of the transpolar arc at 1546–1600 UT. Low-energy ionospheric O^+ ions are also streaming along the magnetic field. The composition and energies of the transpolar arc plasmas are not dissimilar to those found at the poleward edge of the evening sector of the auroral oval at ~1640 UT. This region is also earlier referred to as the boundary plasma sheet. These general features of the ion composition within the polar cap and transpolar arc plasmas lead *Peterson and Shelley* [1984] to the conclusion that the magnetic field lines in a transpolar arc are mapped into a different magnetospheric regime than those of the polar cap. The similarities of ion composition and energies in the transpolar arc plasmas with those of the plasma sheet or its boundary layer lead several investigators to suggest that these are topologically connected regions [*Frank et al.*, 1982; *Peterson and Shelley*, 1984].

October 31, 1981. The ion compositions of plasmas for the DE 1 polar passage are shown in Plate 26 in the same format as discussed extensively in the previous example. The energy-time spectrogram for He^{++} ions is not present since the instrument is not commanded into an operational mode for their detection. Passage over the polar cap occurs during 2148–2356 UT (Table 2 and Plates 22*a* and 22*b*). The qualitative features of the ion spectra and compositions are similar to those determined for the above example on November 8 with the exception of the very low intensity of energetic O^+ ions in the transpolar arc plasmas at 2316–2327 UT (see Table 2 for this intercept time of these plasmas). However, it is of significant interest to note that the boundary plasma layer in the poleward zone of the evening auroral oval is also characterized by the comparably low fluxes of O^+ ions in the energy range ~500 eV to 18 keV. The traversal of these boundary layer plasmas in the evening oval occurs at 2356–2359 UT (Plate 22*b*). This relative paucity of energetic O^+ ions in both the plasmas associated with the transpolar arc and the plasmas associated with the boundary layer further reinforces the suggestion of the topological relationship between the extension of the transpolar arc into the magnetotail and the boundary layer of the plasma sheet.

November 25, 1981. The spectrograms shown in Plate 27 further confirm the general character of ion distributions over earth's polar cap during the presence of theta auroras. The spacecraft is positioned within the polar cap during 0957–1238 UT. Passage through the plasmas of the transpolar arc occurs at 1142–1146 UT. The polar cap is again characterized by generally isotropic intensities of H^+ and He^{++} ions, low-energy O^+ ions streaming upward from the ionosphere, and a general paucity of hot O^+ ions with the exception of the transpolar arc region. Within the arc region the higher intensities of energetic O^+ ions are present on its eveningside for this example. The presence of H^+, He^{++}, and O^+ within the plasmas of the transpolar arc attests to their solar wind and ionospheric origins [*Peterson and Shelley*, 1984].

October 17, 1981. The spacecraft is in the polar cap region during 1415–1710 UT for these series of ion measurements shown in Plate 28. As mentioned earlier, the polar cap luminosities displayed a complex arc structure during this example (see Plates 12, 14, and 15 and Figure 4). The onset of a well-defined transpolar arc occurs at ~1640 UT. The associated plasmas are present at the spacecraft position during 1641–1647 UT, roughly coincident with the appearance of a well-defined transpolar arc. The features of the polar cap plasmas are generally similar to the foregoing three examples. Inspection of Plate 28 finds that the H^+ intensities within the polar cap are substantially greater and that the typical H^+ energies are also higher than the previous three examples. The morningside of the polar cap is again generally barren of energetic O^+ ions and is contrasted with such O^+ intensities in the transpolar arc plasmas at 1641–1647 UT. However, in this example there are substantial energetic O^+ intensities in the evening sector of the polar cap during 1647–1710 UT. These O^+ densities still remain factors of $\gtrsim$10 less than maximum densities within the plasmas associated with the transpolar arc; however, the ratio of energetic ion intensities, O^+/H^+, does not differ significantly from those observed over the transpolar arc or high-latitude auroral oval in the evening sector. These peak densities of H^+ and O^+ in the transpolar arc plasmas are similar to those found in the poleward region of the evening auroral oval centered at 1711 UT and are ~0.1 to 0.5 cm^{-3}. The crossing of the transpolar arc plasmas is spatially near that for the evening oval (cf. Plate 15).

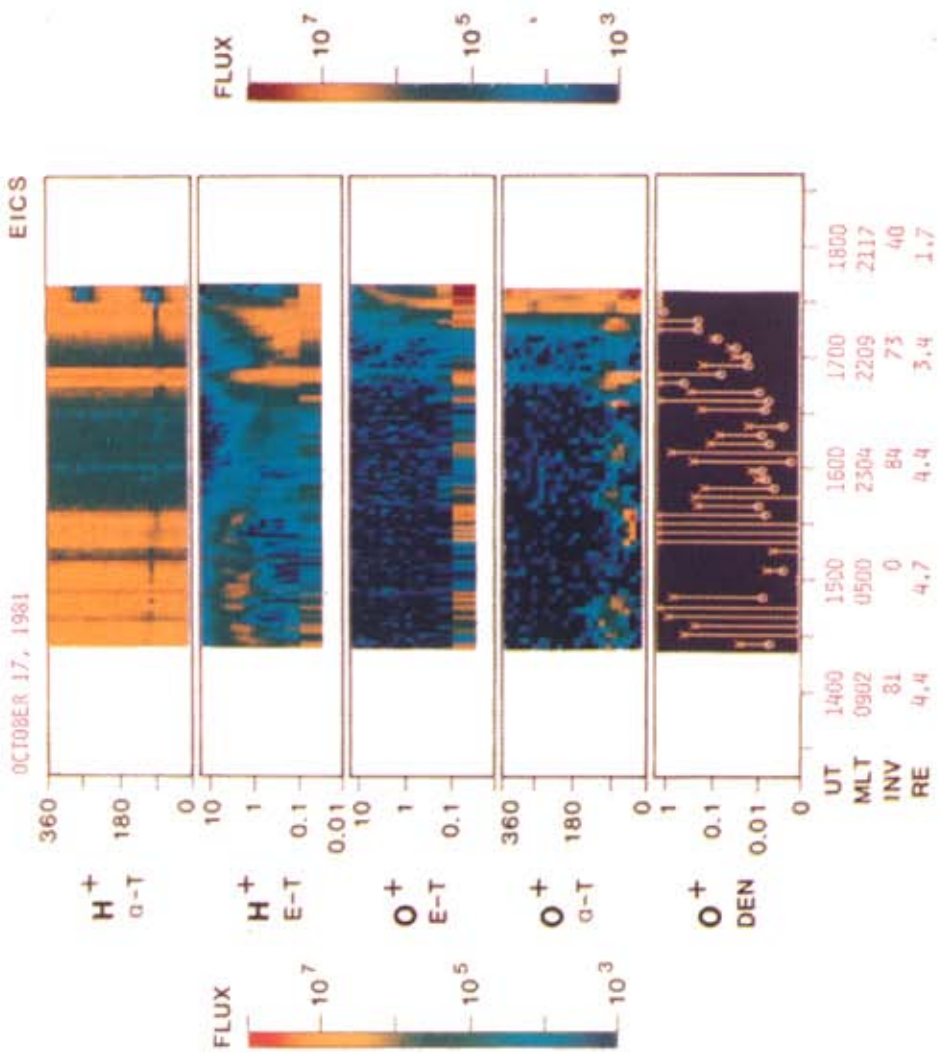

Plate 28. Continuation of Plate 25 for October 17, 1981. The operational mode of the instrument does not include measurements of He^{++} ions for this period. The signature of the transpolar arc plasmas occurs at 1641–1647 UT.

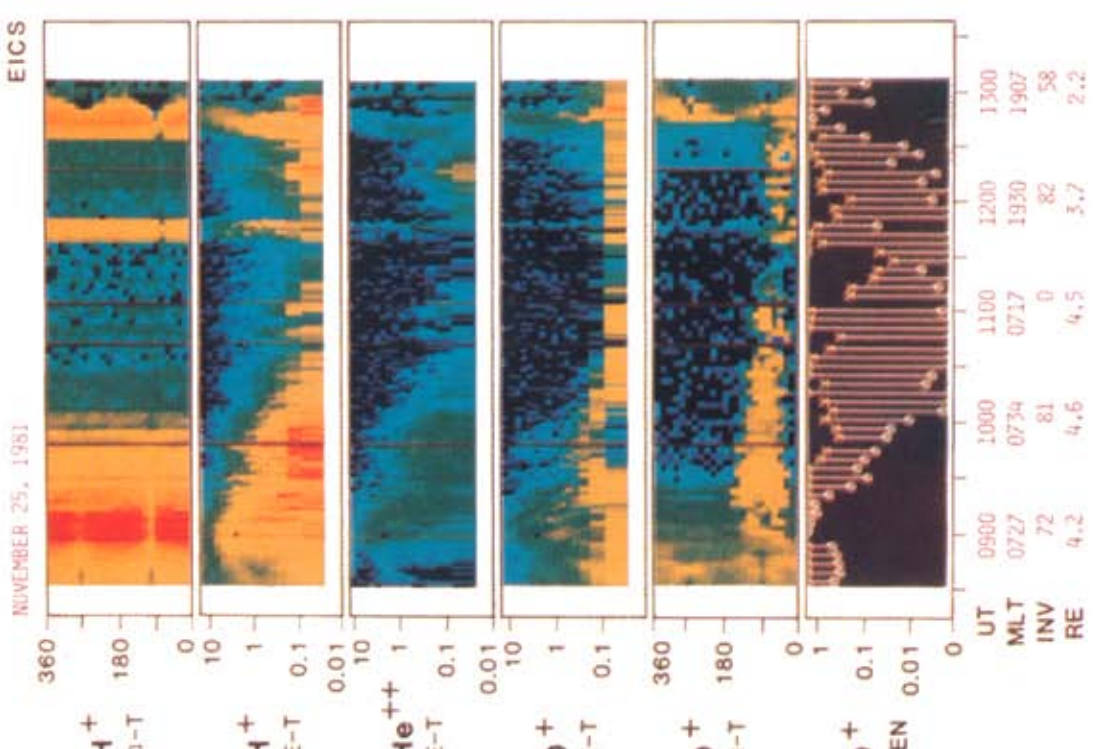

Plate 27. Continuation of Plate 25 for November 25, 1981. The signature of the transpolar arc plasmas occurs at 1142–1146 UT.

The reader probably notes two further differences in the series of ion measurements in Plate 28 relative to the three previous examples, i.e., the peak in the H^+ energy spectra at ~1–3 keV (second panel) and the lack of energetic O^+ ions (third panel) during ~1420–1530 UT. This period occurs during the traversals of plasmas associated with the morning sector of the auroral oval. These measurements might be interpreted in terms of ion acceleration above the spacecraft position. However, their quasi-isotropic angular distributions weaken arguments for a field-aligned mechanism without significant perpendicular heating. An alternative interpretation is direct entry of magnetosheath ions, with convection of the lower-energy ions away from this region before their slower motion along these field lines allows their penetration to these altitudes. No measurements of He^{++} ions are acquired during this period. This latter interpretation in terms of direct penetration of higher-energy magnetosheath ions through the throat of the polar cusp is supported by the magnetic subsatellite positions relative to the dayside auroral oval as shown in Plate 13. However, the convection pattern over the polar cap must be such that these ions are found in a zone of sunward convection (cf. Figure 16). Thus these plasmas could reasonably be associated with the magnetopause boundary layers along the magnetotail rather than the boundary of the plasma sheet. Hence energetic O^+ ions are not to be expected in this case.

In brief summary the energetic ion composition measurements show that both the absolute and relative intensities of H^+, He^{++}, and O^+ that are observed over the high-latitude auroral oval in the evening sector and over the transpolar arc are similar. On the other hand, the ratio of densities He^{++}/H^+ is found to be significantly higher over the adjacent polar cap regions. The density of hot O^+ ions is very low over the polar cap, particularly on the morningside of the transpolar arc. The ratio of densities O^+/H^+ over the cap is similar to that for the high densities over the transpolar arc and the high-latitude auroral oval in the evening sector.

6. Thermal Ion Composition at High Altitudes

The retarding ion mass spectrometer (RIMS) that is included in the instrument complement for DE 1 is a retarding potential analyzer for determining the energy spectra of thermal ions and a magnetic sector spectrometer for subsequent analysis of the composition of the ions. The instrumentation includes three sensors, one each with field of view directed parallel and antiparallel to the spacecraft spin axis, respectively, and the third sensor with its field of view directed normal to the spin axis. Angular dimensions of the field of view for the third sensor are adequate to include the direction of the local magnetic field as the spacecraft rotates about its axis for most of the spacecraft orbit. The E/Q range of the analyzer is 0 to 51 V in 50-mV integral E/Q passbands. Coverage of mass per unit charge (M/Q) ranges from 1 to 32. A grid at the entrance aperture is provided with a bias voltage that is selectable by ground command in order to obviate the effects of a spacecraft potential relative to the ambient medium. Further description of this instrument is given by *Chappell et al.* [1981].

November 8, 1981. As with most plasma instrumentation, some form of a spectrogram is required in order to provide a compact overview of the measurements. These spectrograms for the thermal ion measurements over the polar cap on November 8 are shown in Plate 29. Only observations from the sensor oriented normal to the spin axis of the spacecraft are given for this example and those that follow. The responses of the spectrometer as a function of the logarithm of the energy (electron volts) and UT to H^+ ions are given in the top panel. These responses are color coded according to the scale on the left-hand side of the spectrogram. For reference we note that the DE 1 spacecraft is located within the polar cap at the beginning of the spectrogram at 1405 UT until the exit from the polar cap into the evening sector of the auroral oval at 1640 UT (Table 2). The large ion intensities for the period later than 1652 UT are the signature of spacecraft entry into the plasmasphere. Crossing of the evening sector of the auroral oval occurs during 1640–1652 UT. Plasmas associated with the transpolar arc are sampled at 1546–1600 UT. The second panel in Plate 29 summarizes the angular distributions of the ions as the spacecraft rotates about its axis. Reference angle 0° is the direction for which the sensor is viewing into the velocity vector of the spacecraft orbital motion. The integral intensities of ions are shown and color coded according to the left-hand scale. The lines indicate the rotational angles when the axis of the spectrometer field of view is nearest the direction of the local magnetic field (dashed line, outgoing ions from the ionosphere) and furthest from this direction (dotted line, incoming ions to the ionosphere). Similar spectrograms are shown for thermal He^+ and O^+ ions in the remaining four panels of Plate 29. The orbital parameters along the abscissa of the bottom spectrogram are geocentric radial distance in units of earth radii (R_E), magnetic shell parameter (L, shown as 0.0 when not computed), magnetic local time (MLT), and magnetic latitude (MLAT).

The dominant thermal ion within the polar cap region is O^+. These low-energy ions are moving upward from the ionosphere as seen in the bottom panel of Plate 29. This observation agrees qualitatively with similar measurements at higher energies (cf. Plate 25 for the hot ion spectrometer). Over the time period 1405–1530 UT the temperature of the O^+ ions decreases as the spacecraft moves toward the transpolar arc. These temperatures are sufficiently low to be below the energy threshold of the hot ion spectrometer. Note that there is an absence of ionospheric O^+ outflow at 1535–1603 UT, which corresponds approximately to the traversal of a region of sunward convection in the vicinity of the transpolar arc (cf. Figure 13). However, there are periods such as 1535–1550 UT during which very weak intensities of heavy ions are detected with the more sensitive energetic ion spectrometer (cf. Plate 25). Cold ionospheric H^+ and He^+ ions are also observed occasionally, e.g., at 1410 UT and 1620 UT, with densities considerably less than the O^+ densities. A hot H^+ plasma is encountered at 1450 UT (Plate 29) and is also sensed by the hot ion spectrometer (Plate 25). Such comparisons of the observations with the cold and hot ion spectrometers show that these two measurements are in agreement and are complementary.

The plasmas associated with the transpolar arc at 1546–1600 UT are characterized by the presence of hot H^+, He^+, and O^+ ions. As shown in the angular distributions of Plate 29, these ions are streaming outward from the ionosphere. The composite spectra for these ions extend to energies $\gtrsim$10 keV (see Plate 25). However, the lower-energy ions are streaming upward from the ionosphere and are presumably heated by some unidentified mechanism below the spacecraft position, whereas the hot ion intensities at energies ~1–10 keV are isotropic with the exception of the minimum within the source cone. It should be further noted that there is a general absence

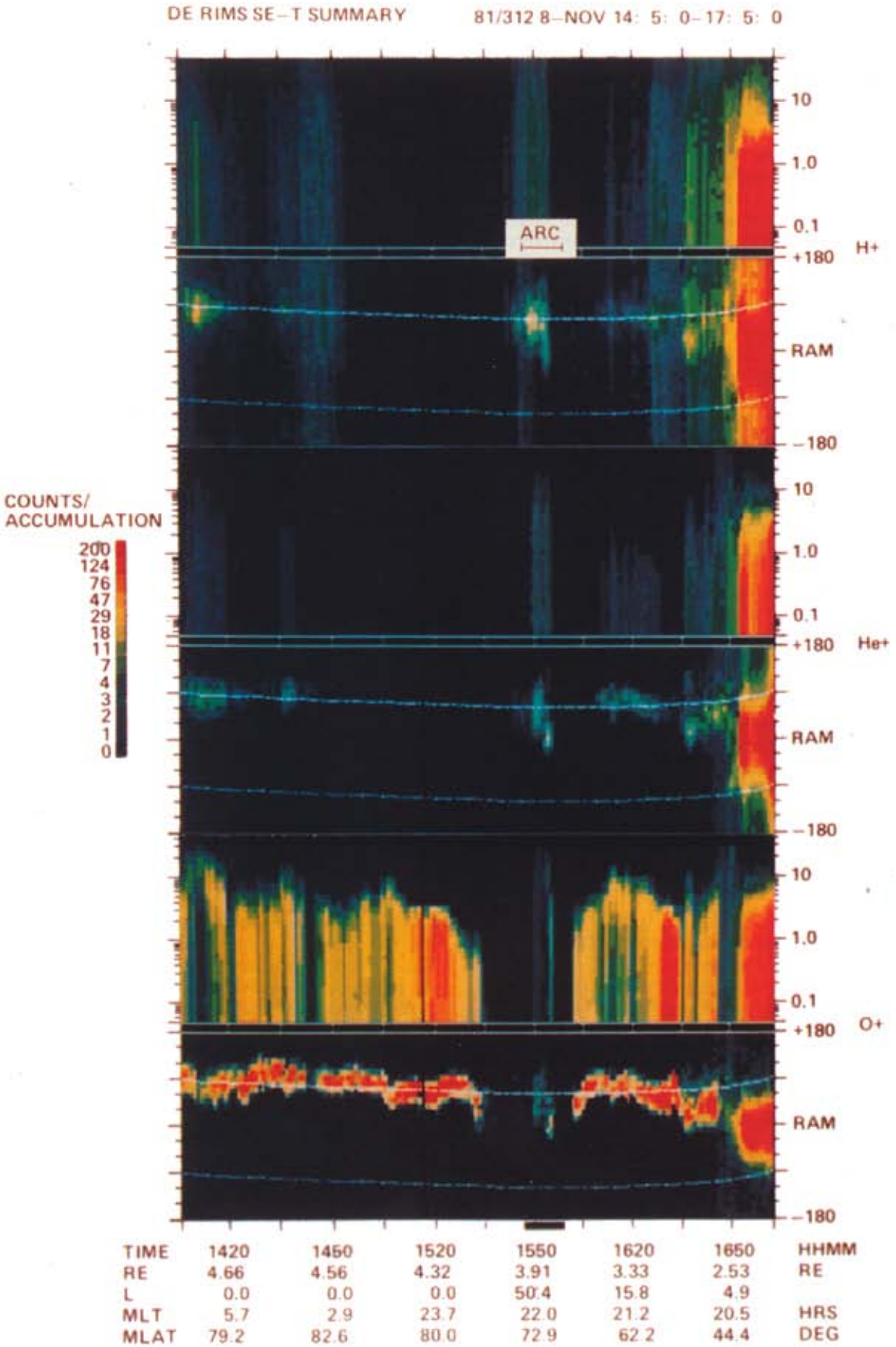

Plate 29. Surveys of the energy spectra and angular distributions of the thermal ions H^+, He^+, and O^+ at high altitudes with DE 1 on November 8, 1981. The ordinate for the energy-time spectrograms is given in electron volts. The angular distributions are taken in the plane perpendicular to the spin axis and referenced to 0° in the direction of the spacecraft velocity vector. Transpolar arc plasmas are present during 1546–1600 UT.

of cool, i.e., a few electron volts, O^+ ions in the transpolar arc region.

October 31, 1981. The thermal ion distributions within the polar cap region are displayed in Plate 30. The appearance of plasmaspheric ions at 0005 UT (November 1) is conspicuous. The period for which the spacecraft is in the polar cap is previously determined from the boundaries for higher-energy ions as 2148–2356 UT (cf. Plates 22 and 26). Relatively low fluxes of H^+ ions, with traces of He^+ and O^+ ions, are observed at 2148–2223 UT in Plate 30 in a zone just poleward of the morning sector of the auroral oval. In addition, there is a hot isotropic background of H^+ ions. These ions are also observed simultaneously with the hot ion spectrometer (Plate 26).

Large intensities of thermal ions are observed only during the period 2334–2349 UT in contrast to our previous example for November 8. The ions as shown in Plate 30 occur in a region of antisunward convection (Figure 14) and are generally interpreted as the signature of outflow of ions from a localized region near or within the polar cusp and subsequent convection across the polar cap [*Waite et al.*, 1985; *Lockwood et al.*, 1985]. Since the thermal speed of an O^+ ion with energy 1 eV is only ~3.5 km/s and the antisunward convection speed is ~2–3 km/s, this interpretation of the position of the ion source is reasonable. Such an effect, i.e., a geomagnetic spectrometer, is expected to result in a spatial dispersion of ions of different species. If ion temperatures are equilibrated at the source region in the dayside ionosphere, then lighter ions will appear at the spacecraft position earlier than heavier ions (lower thermal speed) as the spacecraft moves toward the local night sector of the pole. Such a qualitative effect can be seen in the appearances of peak intensities of He^+ at ~2130–2200 UT and of peak intensities of O^+ at ~2145–2215 UT in Plate 30.

The plasmas over the transpolar arc are traversed by the spacecraft at 2315–2327 UT. Hot thermal H^+ ions streaming outward from the ionosphere are present. Only a trace of He^+ is to be noted, and the absence of large intensities of hot thermal O^+ ions is to be contrasted with their substantial fluxes detected in this region on November 8 as noted above. As in the previous example, detectable intensities of cool O^+ ions in the energy range of a few electron volts are not present within the transpolar arc plasmas.

November 25, 1981. The thermal ion spatial distributions for this polar cap traversal that are displayed in Plate 31 exhibit similar features as the two previous examples. The spacecraft is positioned within the polar cap during 0957–1238 UT (Table 2). Within this region several zones with upward streaming ionospheric ions are observed, e.g., H^+ at 1012 UT and 1050 UT, He^+ at 1020–1105 UT, and higher densities of O^+ at 1105–1135 UT. Hot, isotropic H^+ ions are also evident at 1100 UT and 1112 UT. It is difficult to associate many of these discrete features with the hot plasma zones identified in Plate 23, for example. On the other hand, it must be remembered that the thermal speeds of many of the colder ions are similar in magnitude to the $\mathbf{E} \times \mathbf{B}$ drift speeds. Thus at these altitudes, ~3.5 R_E, magnetic field line mapping alone is insufficient to locate the source region at ionospheric altitudes.

The magnetic field lines threading the transpolar arc are traversed during 1142–1146 UT (Table 2). On the morningside of this region, thermal H^+ ions are observed to be streaming out of the ionosphere. A similar phenomenon is observed on the eveningside of the distribution of transpolar arc plasmas, but the temperatures of the H^+ ions are significantly higher. A trace of upstreaming He^+ ions is found throughout the transpolar arc zone. Again, as in the first example on November 12, 1981, there is a conspicuous absence of ionospheric O^+ thermal outflow in the region of the transpolar arc. Two possible explanations for this effect are (1) that the convection paths of plasmas in this region did not pass through the O^+-rich source region in the dayside cusp as identified by *Lockwood et al.* [1985] or (2) that the mechanism for O^+ outflow was quenched by the different plasma populations of this zone relative to those of the adjacent polar cap regions. Explanation 1 is consistent with topological projections of the transpolar arc into a different distant magnetospheric regime than that for the adjacent polar cap. The absence of thermal O^+ ions is sometimes observed in the poleward zone of the evening auroral oval, e.g., at ~2356 UT on October 31 (Plate 30). A plausible explanation is the heating and/or acceleration of O^+ ions to energies beyond the energy range of the thermal ion instrument. Such upstreaming hot O^+ ions are observed with the hot plasma composition instrument (see Plates 25 through 28).

October 17, 1981. Only H^+ and He^+ ions are measured with the instrument operating mode employed for this passage over the polar cap. These observations are shown in Plate 32. The spacecraft is within the polar cap region during ~1415–1710 UT (see plasma spectrogram of Plate 24 and Table 2). With the exception of the plasmas associated with the transpolar arc at 1641–1647 UT, the polar cap is remarkably empty of upstreaming H^+ and He^+ ions. Sporadic, low intensities of these ions are discernible, e.g., at 1606 UT and 1632 UT, and are correlated with enhanced intensities of precipitating electrons with energies in the range of 50–1000 eV (cf. Plate 24*a*).

Within the transpolar arc plasmas, hot distributions of thermal H^+ and He^+ are detected. These ions are primarily upstreaming from the ionosphere, although a low-intensity, H^+ isotropic angular distribution is superposed upon the angular distributions of the upstreaming ions.

7. Convection Electric Fields at Low Altitudes

The vector electric field instrument (VEFI) on board the low-altitude spacecraft DE 2 employs the double-floating-probe technique with cylindrical sensors separated by a distance of 21.4 m. Three orthogonal sets of these double probes are included in the spacecraft instrumentation. On this three-axis-stabilized spacecraft these three antenna pairs are mounted such that two pairs are in the orbit plane at $\pm 45°$ to the horizontal and the third antenna pair is perpendicular to the orbit plane (Z axis, east-west geographic). The Z axis antenna did not deploy after launch. Hence there are no measurements of the Z axis components of the electric fields. The other two components are rotated into components in the north-south horizontal direction (X axis) and parallel to earth nadir (Y axis), respectively. In the following presentation the $\mathbf{V} \times \mathbf{B}$ electric fields arising from the spacecraft motion are removed, and the resultant fields are transformed into a reference frame corotating with the earth. Effort is also expended in minimizing the effects of contact potentials. The resulting electric field determinations are estimated to have an accuracy of ± 4 mV/m. This instrumentation is previously discussed by *Maynard et al.* [1981].

November 8, 1981. The two components of the electric field, E_x and E_y, for this passage over a theta aurora in the northern hemisphere are shown in Figure 5 as a function of UT. The spacecraft coordinates are given along the abscissa of

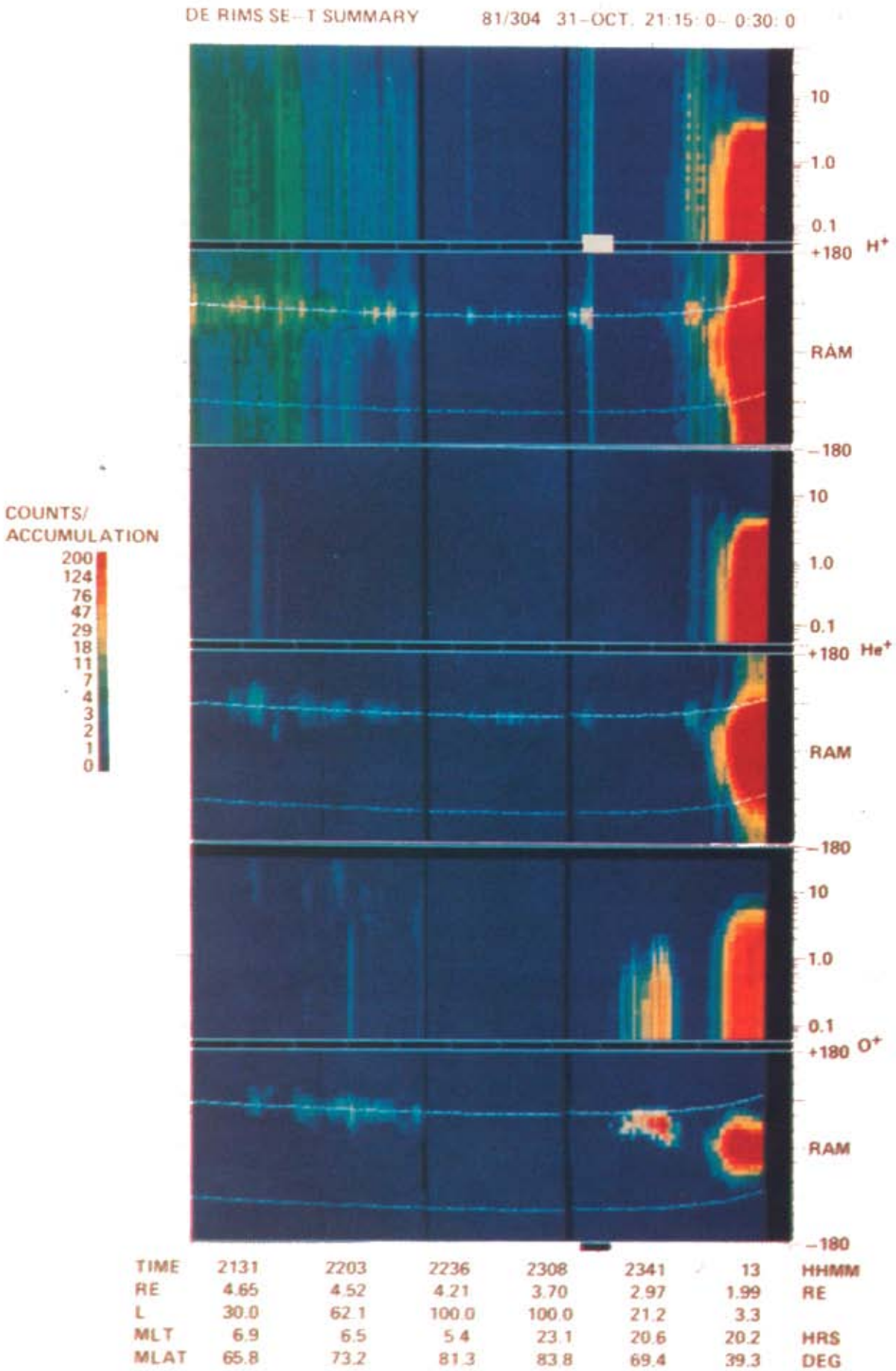

Plate 30. Continuation of Plate 29 for October 31, 1981. Transpolar arc plasmas are encountered during 2315–2327 UT.

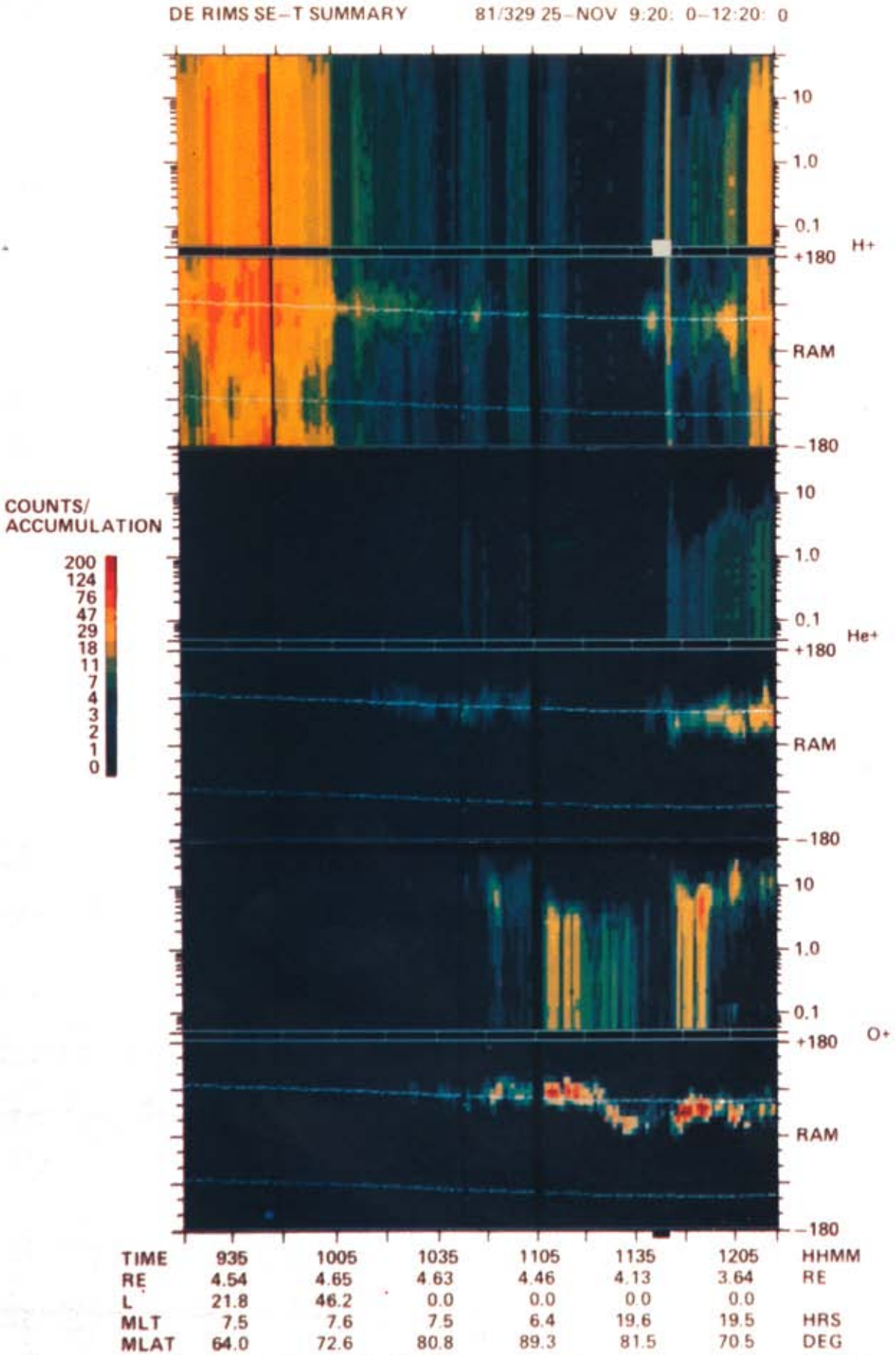

Plate 31. Continuation of Plate 29 for November 25, 1981. Transpolar arc plasmas are encountered during 1142–1146 UT.

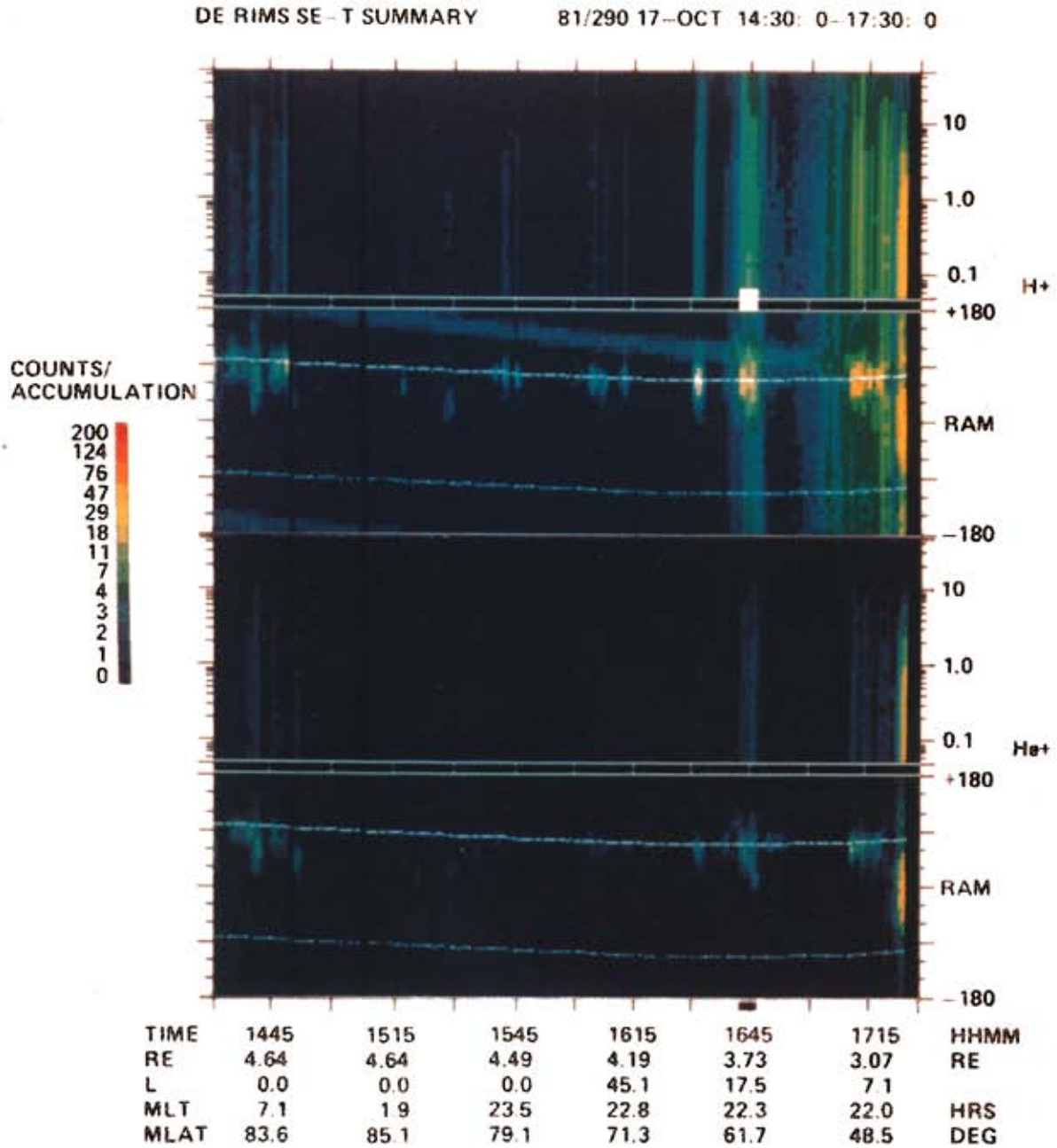

Plate 32. Continuation of Plate 29 for October 17, 1981. Transpolar arc plasmas are encountered during 1641–1647 UT.

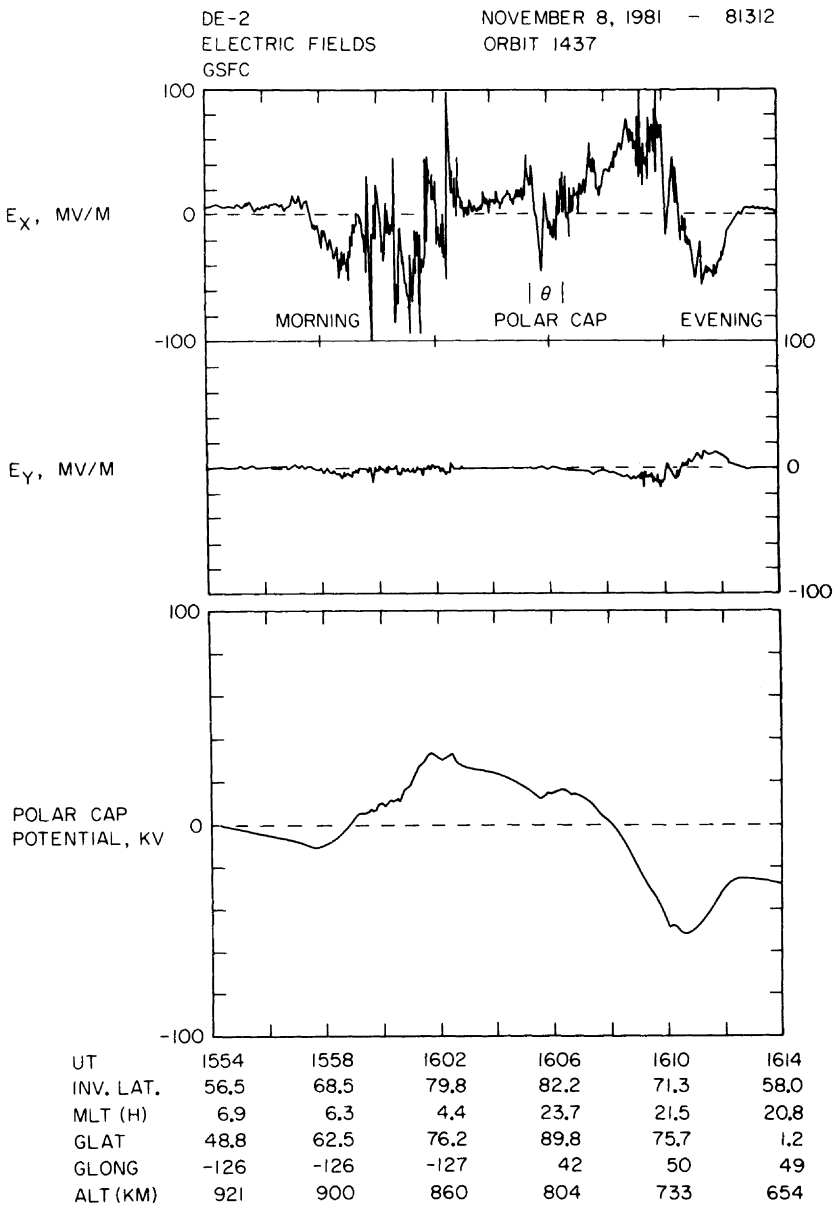

Fig. 5. Measurements of the electric fields at low altitudes over the auroral oval and polar cap in the northern hemisphere on November 8, 1981. E_x is the component of the convection electric field in the direction of the spacecraft velocity vector (top panel). The integrated potential along the spacecraft trajectory is given in the bottom panel.

this figure: invariant latitude (INV. LAT.), magnetic local time in hours (MLT), geographic latitude (GLAT) and longitude (GLONG) in degrees, and altitude (ALT) in kilometers. Our primary interest is in the horizontal component E_x shown in the top panel. Since the orbit is approximately aligned in the dawn-dusk meridional plane for these and the following examples, a positive value of E_x corresponds to antisunward flow, and negative values correspond to sunward flow. The image of Plate 4 is useful in visualizing the trajectory location relative to the auroral oval. Inspection of the hot plasma spectrograms in Plate 17 shows that the spacecraft exited the morning sector of the auroral oval at 1602:30 UT and entered the evening sector of the oval at 1610:30 UT. Thus the convection is generally sunward over both the morning and evening sectors of the auroral oval. With the exception of the zone associated with the transpolar arc at 1605:20–1606:30 UT, the convection in the polar cap is directed antisunward. The convection is sunward within the plasmas associated with the transpolar arc.

The auroral zone and polar cap potentials in units of kilovolts are shown in the bottom panel of Figure 5. The general decrease of potential with increasing UT is an artifact due to the integration of small errors in the contact potential over large distances. This effect should be ignored. An error of 2 mV/m produces a 20-kV integrated error in the 20-min time period of Figure 5, or approximately 1 kV per minute of orbital track. For the transpolar arc traversal the corresponding error in calculating the potential difference across this region is ~ 1 kV; for the morning and evening sectors of the auroral oval this error is ~ 2 or 3 kV. Inspection of Figure 5 finds that the potential differences across the morning and evening sectors of the auroral oval are ~ 45 kV and 25 kV, respectively.

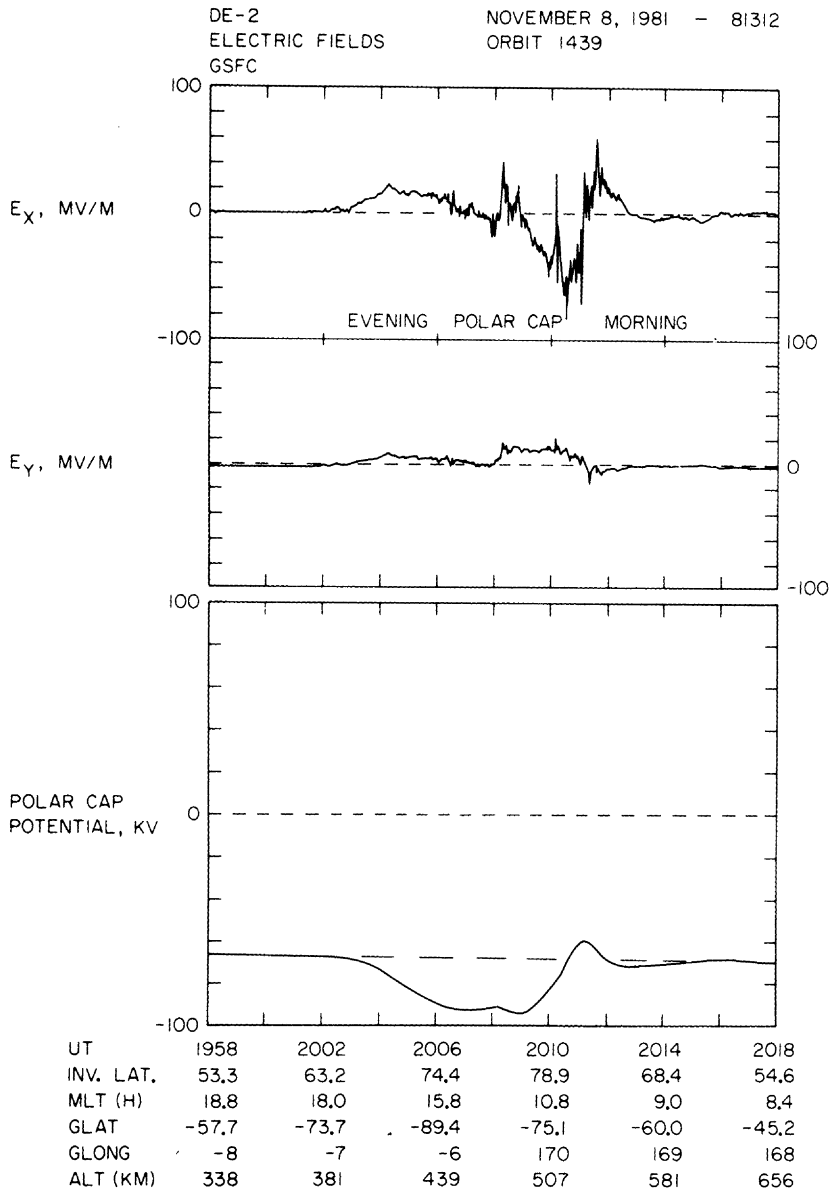

Fig. 6. Continuation of Figure 5 for the southern hemisphere ~4 hours later on November 8, 1981.

The potential difference across the entire polar cap is ~85 kV, and the corresponding potential change across the transpolar arc is ~5kV.

A detailed comparison of the position of the narrow, primary zones of electron precipitation within the transpolar arc zone in Plate 17 during 1605:20–1606:40 UT reveals a correlation with the fluctuations of the electric field component E_x shown in Figure 5. These electron precipitation zones, or arcs, occur simultaneously with electric field reversals for which the electric field vectors are directed toward the arc, i.e., $\nabla \cdot \mathbf{E} < 0$. This condition is generally found also for inverted-V events, for example over the evening sector of the auroral oval.

The convection electric fields over the polar cap in the southern hemisphere for the period ~4 hours after the above northern hemispheric observations are shown in Figure 6. For observations over the southern hemisphere, positive values of E_x correspond to flow in the solar direction, and negative values indicate antisolar flow. The magnitudes of the convection electric fields and of the potential differences are lesser than those observed 4 hours earlier over the opposite hemisphere. The sloping dashed line in the bottom panel of Figure 6 provides an estimate of the effects of contact potential on the integrated potential difference. Over the southern hemisphere the polar cap is traversed during the interval ~2007–2011 UT. A narrow zone of sunward flow is observed at 2010 UT in the overall antisolar flows of the polar cap. This convection pattern is suggestive of the occurrence of a theta aurora over the southern hemisphere. The occurrence of theta aurora over the southern hemisphere is previously reported by *Frank et al.* [1985].

October 31, 1981. This series of observations of convection electric fields over the northern hemisphere is similar to those observed for November 8. These measurements are displayed in Figure 7. The primary dissimilarities are the smaller magnitudes of the electric fields and potential differences. The potential differences across the morning and evening sectors of the auroral oval, and across the polar cap, are <5 kV. The poleward boundary of the morning auroral oval is intercepted

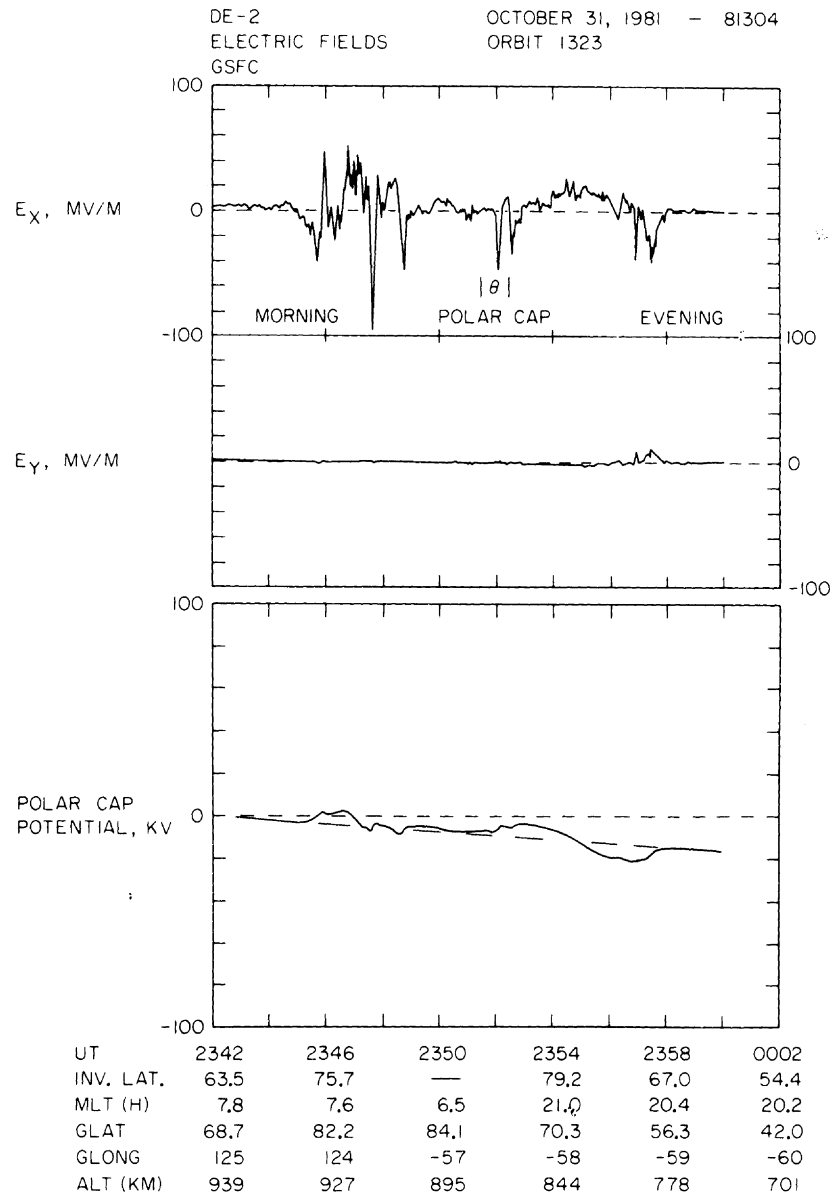

Fig. 7. Continuation of Figure 5 for October 31, 1981.

at 2348:48 UT, and that for the evening sector of the oval at 2356:50 UT (see Plate 18). Plasmas associated with the transpolar arc are traversed at 2351:30–2352:30 UT in a region characterized by sunward convection. The potential difference across the transpolar arc region is ~2 kV. Convection over the other regions of the polar cap is directed in the antisolar direction.

November 25, 1981. During this passage of DE 2 over the northern polar cap the transpolar arc of the theta aurora is very dim. The transpolar arc brightens after DE 2 completes its traversal of the auroral zones. The reader can easily see this temporal variation with a comparison of the images in Plates 11 and 12. An extremely disordered electric field pattern is present over the polar cap and auroral oval during the DE 2 polar passage as shown in Figure 8. Amplitudes of the X component (parallel to spacecraft velocity vector) of the electric fields reach 150 mV/m. As mentioned earlier, the generally downward trend of the integrated polar cap potential with increasing time is due to the effects of contact potential. Nevertheless, the polar cap potential profile is complex. The poleward boundaries of the morning and evening sectors of the auroral oval are encountered at 1131:00 UT (plasmas, Plate 19) and 1140 UT (imaging, Table 2), respectively. Inspection of the profiles of E_x in Figure 8 shows that there is no unique signature in these turbulent electric fields that is associated with these boundary crossings. Indeed, the magnetic field lines associated with the transpolar arc plasmas are traversed during 1135:00–1136:30 UT, and no unique signature is identified with this plasma feature. Thus during a period of polar arc dimming, the electric fields over the polar cap and auroral oval are observed to be highly turbulent.

October 17, 1981. The convection electric fields over the northern polar cap are turbulent in a similar manner as those observed on November 25. The measurements for October 17 are shown in Figure 9. The global auroral images show that the transpolar arc is in the initial stages of brightening and definition as DE 2 overflies the polar cap (see Plates 15 and 16 and Figure 4). Exit of the spacecraft through the poleward

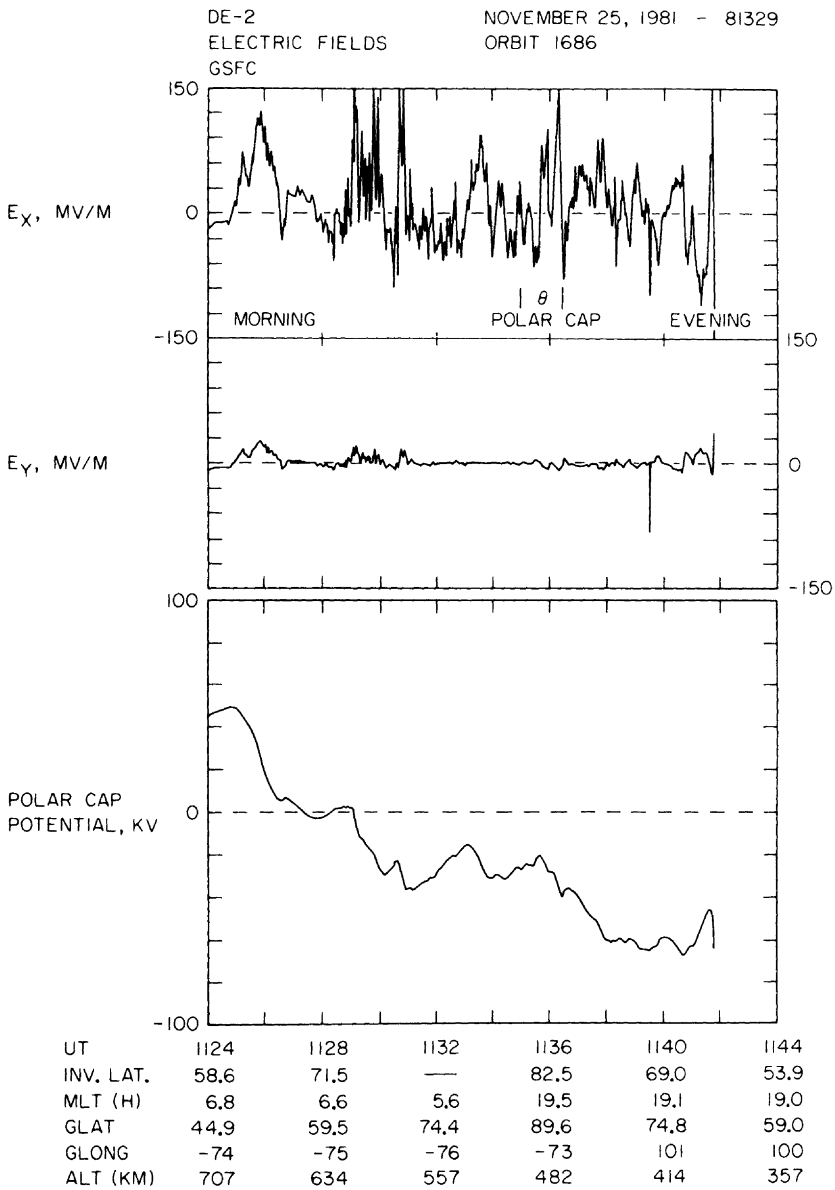

Fig. 8. Continuation of Figure 5 for November 25, 1981.

boundary of the auroral oval into the polar cap occurs at 1636:40 UT. Plasmas over the transpolar arc are traversed during 1644:30–1645:40 UT. Entry into the evening sector of the auroral oval is determined as 1647:00 UT from the simultaneous hot plasma measurements shown in Plate 20. Again, as with the observations on November 25, there is no unique signature of passages over the auroral oval or over the transpolar arc in the profiles of convection electric fields. The convection is weakly antisunward over the transpolar arc. The potential drops across the auroral oval and the polar cap are $\lesssim 5$ kV. If these low-altitude electric fields are indicative of distant magnetospheric convection, such turbulence indicates that the large-scale flow patterns, such as those suggested by *Heppner*'s [1972] survey of low-altitude convection electric fields, are not present in the distant magnetosphere and are replaced by relatively small-scale turbulent flows during these periods.

8. Ion Drift Velocities at Low Altitudes

The ion drift meter (IDM) provides a square collimator through which the ambient thermal ions are incident on a segmented planar collector. The fields of view are directed along the $+X$ axis of the DE 2 spacecraft, i.e., looking along the instantaneous velocity vector of this spacecraft. The thermal ion currents from the segments of the collectors are separately measured with logarithmic amplifiers in such a manner as to accurately determine two orthogonal components of the bulk flow of thermal ions in the plane perpendicular to the spacecraft velocity vector. The apparent velocity of the ions due to spacecraft orbital motion is subsequently subtracted from the observed velocity. The components of the ion velocity vector are measured with an accuracy of ~ 50 m/s. This instrumentation is discussed by *Heelis et al.* [1981]. The third

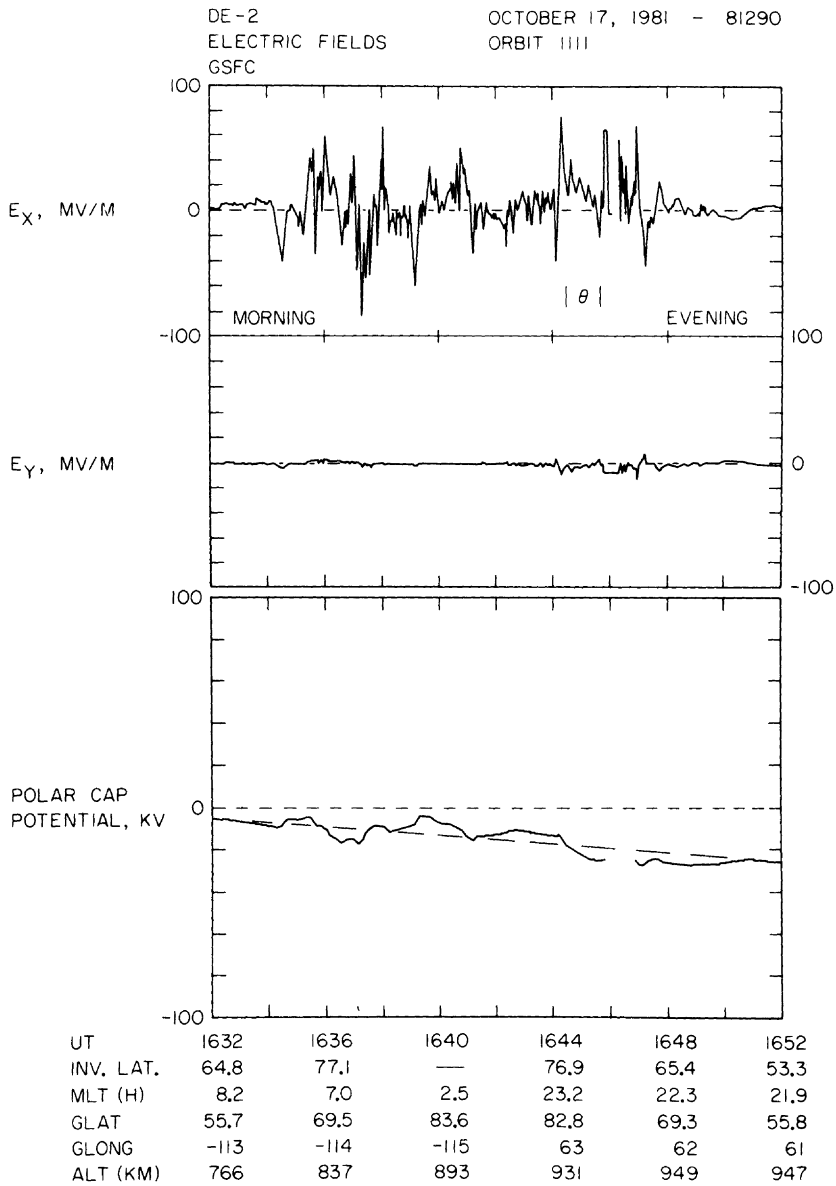

Fig. 9. Continuation of Figure 5 for October 17, 1981.

component of ion bulk velocity is determined from the thermal ion velocity distributions measured by a planar retarding potential analyzer (RPA) [see *Hanson et al.*, 1981]. Thus all three components of the ion bulk flow velocity are determined, and also the convection electric field vector can be computed via instantaneous measurement of the magnetic field.

In the following discussion we shall use the measurements of ion convection and the derived electrostatic potential distribution in order to deduce plausible polar cap convection patterns.

November 8, 1981. Observations of the ion bulk velocity perpendicular to the magnetic field are shown in the left-hand panel of Figure 10. This polar dial plot employs geographic latitude and solar local time. Local noon is directed vertically upward from the origin. The DE 2 spacecraft moves from local morning to evening with increasing time, i.e., from right to left in the plot. The contours for constant invariant latitude (solid lines) are also shown for values of 60°, 70°, and 80°. Determinations of the components of the convection electric fields are in general agreement with those determined with the direct electric field measurements discussed in the preceding section.

The polar convection pattern deduced from this single pass over the polar cap and auroral oval is shown on the right-hand side of Figure 10. The positions of luminosities associated with the evening sector of the auroral oval and with the transpolar arc as determined from the auroral images are also identified. This polar convection diagram is drawn on the same scale as the presentation of measurements in the left-hand panel. The usual sunward convection can be identified at the lower latitudes, and antisolar convection is seen over the polar cap with the exception of sunward flow associated with the transpolar arc. Four major convection cells are deduced, the evening cell (I) and a larger morning cell (II) in which two polar cap cells (III and IV) are embedded. Both luminosity regions are located at the reversal of the direction of convec-

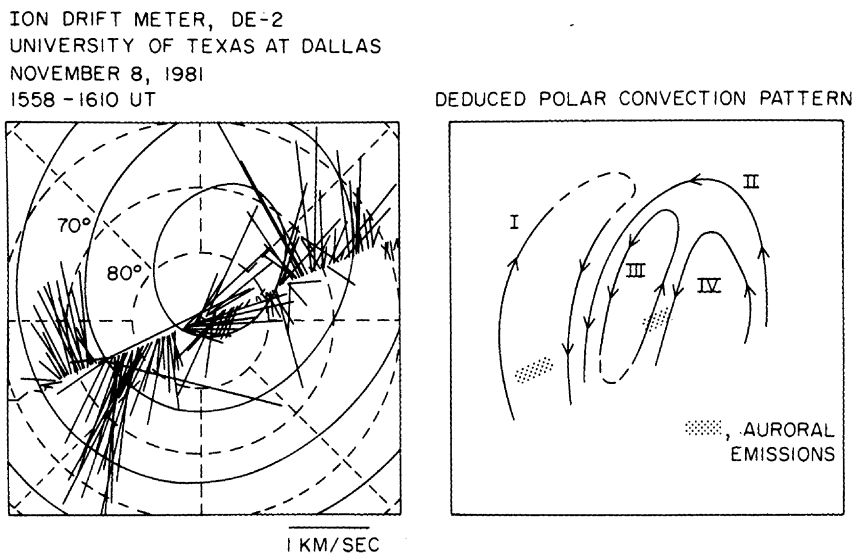

Fig. 10. Ion convection observed at low altitudes over the northern auroral oval and polar cap with DE 2 on November 8, 1981 (left-hand panel). In the right-hand panel is shown a plausible polar convection pattern for the ion convection observed during this polar passage. The positions of auroral emissions in the evening sector and in the transpolar arc are indicated by the shaded areas along the spacecraft track.

tion. The reader is reminded that these deduced patterns are not unique but provide a sensible possibility given the available observations.

October 31, 1981. As noted earlier, the convection speeds are considerably lesser than those observed on November 8. The ion bulk velocities are shown in the left-hand panel of Figure 11. The ion convection is sunward within the region associated with the transpolar arc and weakly antisunward over the polar cap. From the ion velocity measurements, only the locations of the evening convection cell I and polar cell III can be reasonably deduced. These convection cells are shown on the right-hand side of Figure 11.

November 25, 1981. No reasonable convection pattern with major cells as noted above could be matched with the ion velocities observed along the spacecraft trajectory.

October 17, 1981. Ion velocities perpendicular to the magnetic field for this polar passage over a theta aurora are shown in the left-hand panel of Figure 12. Note that there are substantial components of the ion velocities parallel to the spacecraft motion. This effect is partially due to the position of the orbit closer to the noon-midnight meridional plane in relation to the positions of the previous polar passes. A suggested polar convection pattern is shown in the right-hand panel of Figure 12. The measurements exhibit generally sunward convection associated with the transpolar arc. However, a detailed comparison of the observed ion flow vectors and the streamlines for the deduced circulation cells shows that an alternative view of the polar convection as turbulent or a collection of many small-scale cells is acceptable.

9. Convection Electric Fields at High Altitudes

The plasma wave instrument (PWI) is capable of measuring the quasi-static electric fields along the orbit of the high-altitude spacecraft DE 1. A pair of long-wire, double-probe antennas with a combined effective length of 173.1 m is used

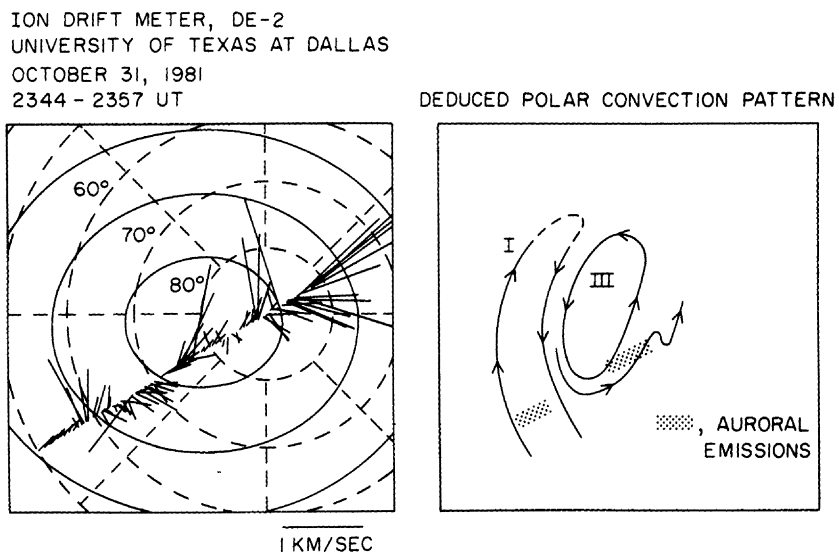

Fig. 11. Continuation of Figure 10 for October 31, 1981.

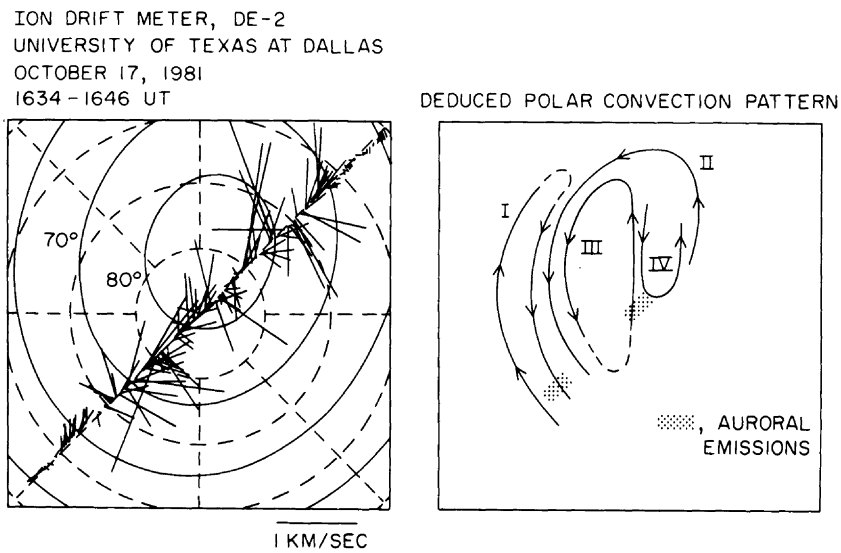

Fig. 12. Continuation of Figure 10 for October 17, 1981.

to obtain measurements of the electric field in the spacecraft orbital plane. This electric field is related to the component of plasma flow directed normal to the orbital plane. A quasi-static electric field is identified as a sinusoidal variation of the antenna voltage as a function of rotation angle for the spacecraft. The spin period is 6 s, and the sampling rate for the antennas is 16 measurements per second. A second antenna is aligned along the spin axis of the spacecraft. The effective electrical length of this tubular antenna is 8.0 m. Measurements from the second antenna are not used in this presentation. The dynamic range of this instrument is 0.5 mV/m to 2.0 V/m. Further information concerning the design and operation of this instrument is given by *Shawhan et al.* [1981].

November 8, 1981. The component of plasma flow perpendicular to the orbital plane and the corresponding electric field component parallel to this plane are shown in Figure 13 as the

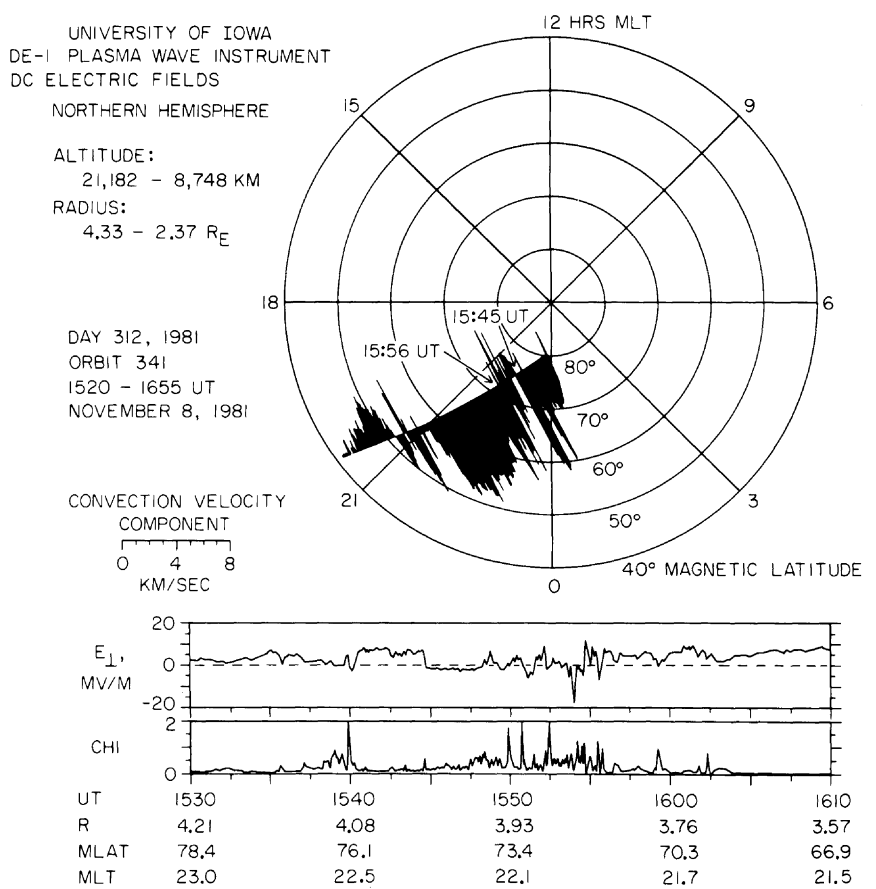

Fig. 13. Plasma convection observed at high altitudes with DE 1 on November 8, 1981 (upper panel). The component of convection directed normal to the spacecraft orbital plane is measured. The magnitudes of the corresponding electric fields in the vicinity of and within the transpolar arc are shown in the bottom panel.

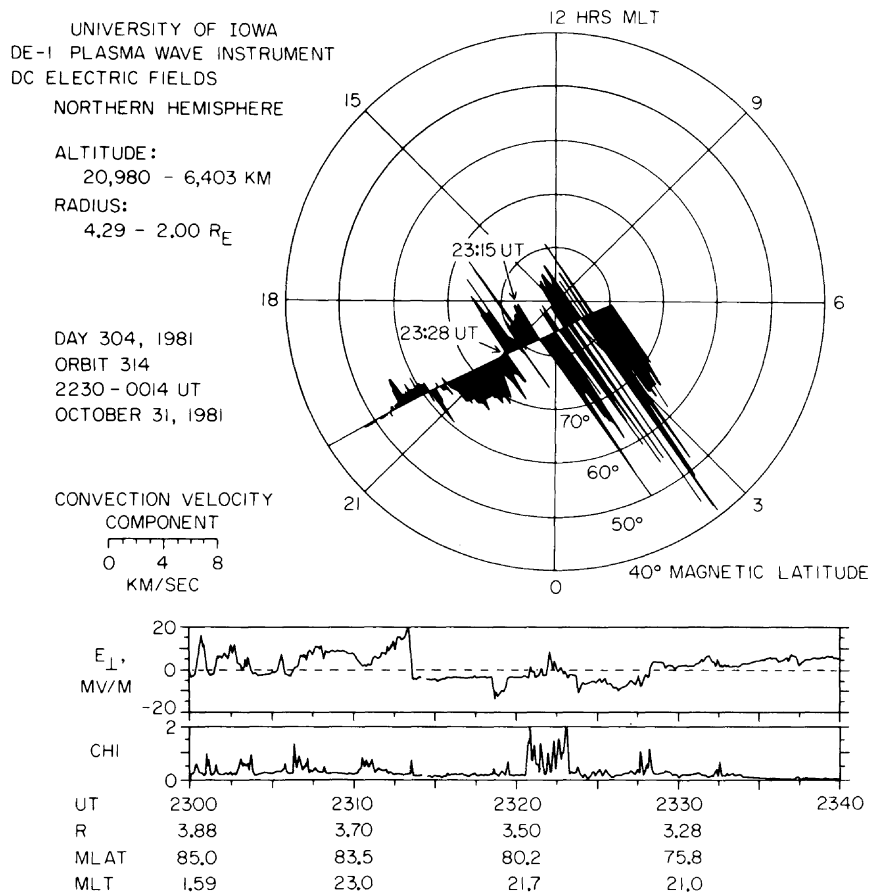

Fig. 14. Continuation of Figure 13 for October 31, 1981.

spacecraft passed over the northern hemisphere during this theta auroral event. The corresponding images as taken during crossings of plasmas associated with the morning and evening sectors of the auroral oval, and with the transpolar arc, are given in Plates 1, 3, and 2, respectively. The convection velocity components normal to the orbital plane are shown as a function of position in coordinates of magnetic local time (MLT) and magnetic latitude (MLAT). A scale for this velocity component is shown to the lower left-hand side of the polar diagram. The spacecraft orbital motion is from the right (morning) to the left (evening) in the upper panel of Figure 13. The geocentric radial distance of the spacecraft position is given as R in earth radii and appears along the abscissa of the bottom panel. At a magnetic latitude of 51° the DE 1 spacecraft exits the polar cap into the plasmas associated with the evening sector of the auroral oval where a zone of sunward convection is observed. Within the polar cap the convection is antisunward over the latitude range 58°–80° with the exception of a zone of sunward convection associated with the transpolar arc at magnetic latitudes 72°–75°. The speed of this sunward convection is in the range of several kilometers per second.

A detailed presentation of the electric fields in the orbital plane, $E_\perp$ in units of millivolts per meter, is given in the panels at the bottom of Figure 13. Negative values of $E_\perp$ indicate sunward flow; positive values correspond to antisolar flow. The global auroral images identify the time period for traversal of the transpolar arc plasmas as 1546–1600 UT, and the in situ plasma measurements show that the crossing of these plasmas occurred during 1545–1554 UT. The small difference in crossing times is within the expected inaccuracies associated with the imaging spatial resolution at auroral altitudes. Sunward convection is exhibited during the interval ~1545–1554 UT (Figure 13) and is bounded by periods characterized by antisunward convection. Hence the electric fields within the polar cap are similar in character to those observed at low altitudes (cf. Figure 5), i.e., general antisolar convection in the polar cap with a zone of sunward convection associated with the transpolar arc.

The parameter chi is an error coefficient computed in the least squares fit to the sinusoidal wave form from the antennas as a function of spacecraft rotation. Essentially, a value of ~0.25 or less for chi indicates that a good fit to the waveform is obtained. Larger values for the parameter indicate either a turbulent electric field or sheath-induced errors. The larger values of chi shown in Figure 13 for the passage through the plasmas of the transpolar arc are interpreted here as indicative of increased turbulence.

October 31, 1981. This series of electric field measurements is shown in Figure 14. The spacecraft exits the polar cap into plasmas associated with the evening sector of the auroral oval at 60° magnetic latitude. A zone of sunward convection is observed equatorward of this boundary as shown in the polar diagram of Figure 14. Passage through plasmas associated with the transpolar arc occurs during 2316–2327 UT (Table 2). This region is characterized by sunward convection and is bounded by polar cap regions with antisunward flow. The electric fields observed during the crossing of transpolar arc plasmas are shown in the bottom panel of Figure 14. For comparison the period for crossing the field lines associated

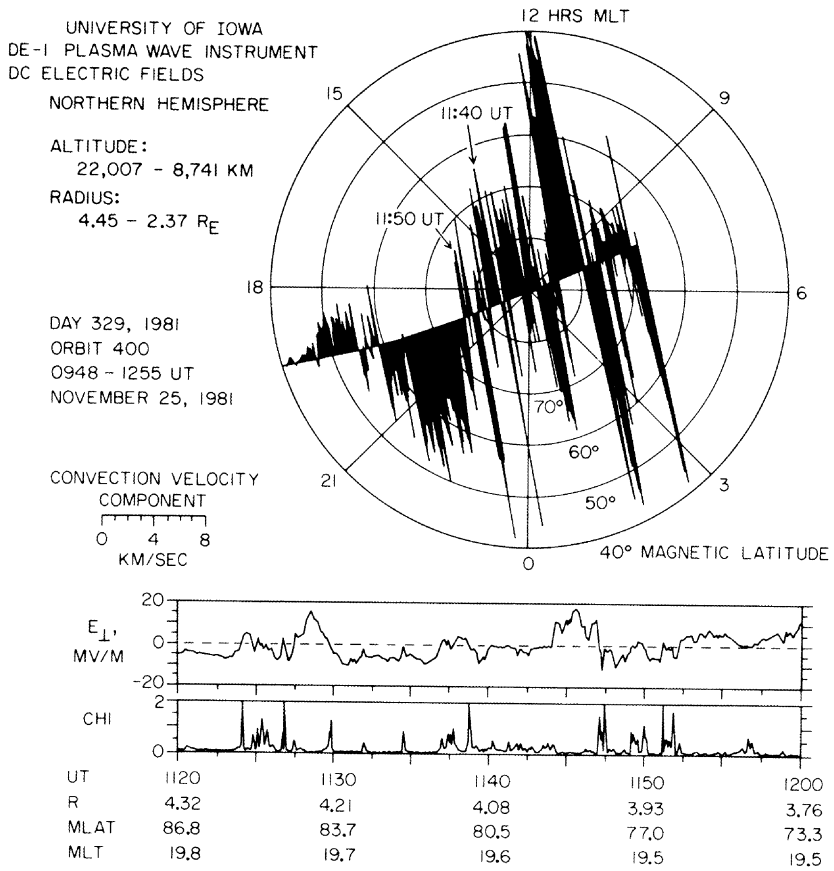

Fig. 15. Continuation of Figure 13 for November 25, 1981.

with the transpolar arc as derived from the simultaneous hot plasma observations is 2315–2327 UT (cf. Plate 26) and is coincident with the appearance of sunward plasma convection.

November 25, 1981. During the crossing of the plasma region associated with the transpolar arc, the luminosities in the arc are relatively dim as previously shown in Plates 10 and 12. By 1232 UT the transpolar arc brightens dramatically as seen in Plate 11. The onset of this brightening occurs at ~1156 UT as determined by examination of the entire sequence of images not shown here. For the summary of convection velocities in the polar plot of Figure 15, the spacecraft crosses the poleward boundary of the evening sector of the auroral oval at a latitude of 55°. Sunward flow is observed over the evening oval. At poleward latitudes the convection pattern appears to be more complex, in particular at latitudes exceeding 77° where the flow is sunward on the average and intermixed with antisunward zones of convection, i.e., turbulent. Traversal of plasmas associated with the transpolar arc occurs during the period 1142–1146 UT (Table 2) before brightening of this arc. A detailed summary of the convection electric fields within and in the vicinity of the transpolar arc plasmas is shown in the bottom panel of Figure 15. In this region the plasma convection is also to be noted as disorganized or turbulent.

Recall that the similar turbulent pattern of polar cap convection is observed at low altitudes with DE 2 (Figure 8). This spacecraft is located within the polar cap during 1131–1140 UT. During this period it is easily seen that the convection electric fields at high altitudes are also highly disorganized as shown in the upper diagram of Figure 15. The transpolar arc brightens at ~1156 UT after DE 2 passes out of the polar cap but while the high-altitude DE 1 remains in the evening sector of the polar cap. At approximately 1156 UT the plasma convection within the polar cap turns antisunward at the position of DE 1 (see Figure 15). This antisunward convection persists for approximately 1 hour until the poleward boundary of the evening oval is approached. These flows are similarly uniform with those observed on November 8. Thus during a period of substantial dimming of the transpolar arc the plasma convection over the polar cap is turbulent. With the brightening of the transpolar arc the plasma convection over the polar cap is found to be uniformly antisunward outside of the transpolar arc plasmas and poleward of the turbulent flows near the poleward boundary of the evening sector of the auroral oval.

October 17, 1981. The appearance of a well-defined transpolar arc occurs late during the series of measurements of convection velocities and electric fields shown in Figure 16. The onset of brightening and clear definition of the polar arc occurs at ~1630 UT as both the DE 1 and DE 2 spacecraft intercept the associated plasma zones (see Figure 4). Prior to this period the polar cap is characterized by a relatively complex system of polar arcs and by diffuse emissions (see Plate 13). The transpolar arc is considerably brighter by 1657 UT, as seen in the image of Plate 15. As noted in Figure 16, the DE 1 spacecraft exits the poleward boundary of plasmas associated with the morning sector of the auroral oval at ~1415 UT and magnetic latitude 81° and intercepts the poleward edge of the plasmas over the evening oval at 1710 UT and magnetic latitude 52°. Prior to brightening of the transpolar

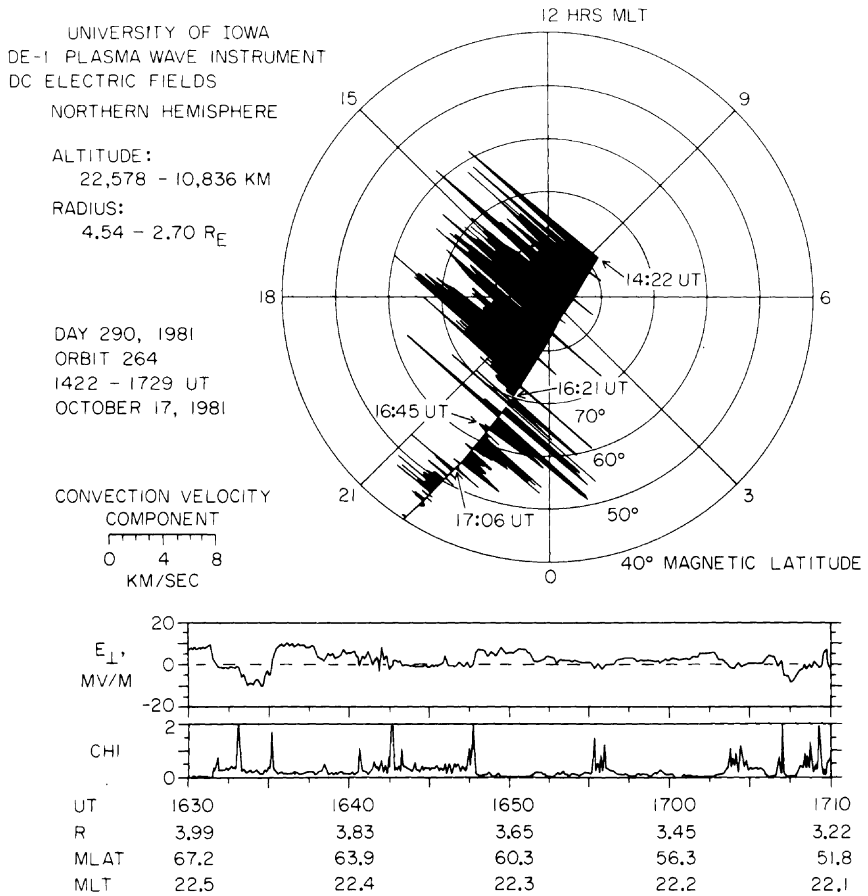

Fig. 16. Continuation of Figure 13 for October 17, 1981.

arc the plasma convection is sunward over the complex arc structure in the morning sector of the polar cap. At 1621 UT the convection is observed to turn generally toward the antisunward direction. The crossing of plasmas associated with the transpolar arc during 1641–1647 UT is characterized by very weak sunward flow, <1 km/s. Antisunward convection is observed in the evening sector of the polar cap and occurs after brightening of the transpolar arc. Thus, in a similar manner as the example for November 25, the polar cap is characterized by turbulent or sunward flows during dimming or absence of the transpolar arc with a return to antisunward flow for a well-developed, bright transpolar arc.

10. Magnetic Signatures of Field-Aligned Currents at Low and High Altitudes

DE 1 and DE 2 spacecraft are each equipped with a triaxial flux gate magnetometer (designated as MAGA and MAGB, respectively). Each of these two magnetometers provides a basic instrumental resolution of ± 1.5 nT. In addition, MAGA is capable of two operating modes with higher resolution, ± 0.25 nT and ± 20 pT. The sampling rate for both magnetometers and for any resolution mode is 16 vector measurements each second. These magnetometers are mounted on 6-m booms in order to satisfactorily reduce stray fields at their positions, which arise from magnetic materials and currents in the spacecraft main body. Detailed discussion of the magnetometer designs and operation is given by *Farthing et al.* [1981].

November 8, 1981. The residual components of the geomagnetic field for the low-altitude, DE 2 passage over earth's polar cap during a theta auroral event are shown as functions of UT in Figure 17. The corresponding auroral image is shown in Plate 4. These residual components are obtained by subtracting a computed internal magnetic field of the earth based upon a Magsat model [*Langel et al.*, 1980] from the observed values. The coordinate system is spacecraft-

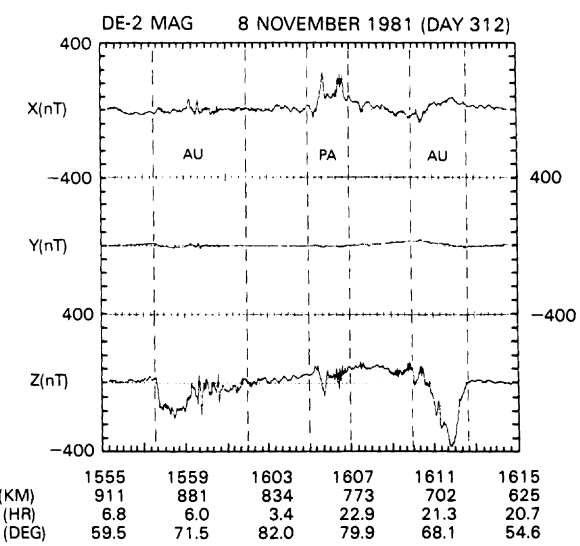

Fig. 17. The magnetic signatures of field-aligned currents over the morning and evening sectors of the auroral oval (AU) and over the transpolar arc (PA) at low altitudes on November 8, 1981.

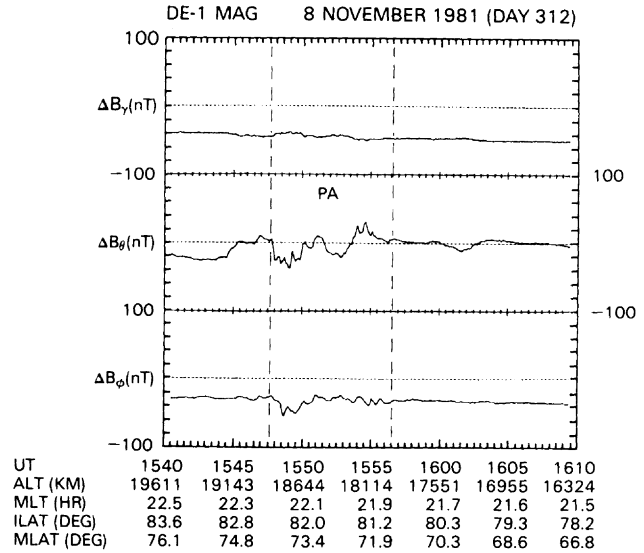

Fig. 18. The magnetic signatures of field-aligned currents at high altitudes in the transpolar arc plasmas on November 8, 1981.

referenced with X along the velocity vector of the spacecraft motion, Z normal to the orbital plane and positive eastward in geographic coordinates when the spacecraft velocity is northward, and Y chosen to obtain a right-handed coordinate system (nearly directed toward zenith). One-half-second averages of the measurements are shown in Figure 17. Coordinates along the abscissa are the usual altitude (ALT), magnetic local time (MLT), and invariant latitude (ILAT). Periods for which field-aligned currents are identified with the morning or evening sectors of the auroral oval (AU) or the transpolar arc (PA) are also identified in Figure 17. The detection of a field-aligned current system during the period 1605–1607 UT is in good agreement with the predicted encounter with transpolar arc plasmas from the simultaneous image (Table 2) and with the in situ measurements of these plasmas (see Plate 17).

The plasmas associated with the transpolar arc appear to include two distinct regions of field-aligned currents. On the morningside of the transpolar arc is a pair of current sheets each with a current sheet strength of ~0.2 A/m. The first of these sheets encountered by the spacecraft (on the morningside of the pair) carries an upward current; the second sheet carries a downward current. The upward current is probably associated with the intense flux of electrons observed with the plasma instrument (Plate 17). The second field-aligned current region is traversed at 1606:20 UT after the crossing of the first pair of current sheets and is similar in general character with the first pair, although more structured. The total integrated field-aligned current strengths are ~0.1 A/m for each of these current sheets. The orientations of these current sheets are parallel to the direction ~30° to 40° rotated clockwise looking downward as referenced to the dipole meridian.

An orthogonal pair of electric and magnetic field components associated with field-aligned currents is generally highly correlated [*Sugiura et al.*, 1982, 1984]. The east-west component of the perturbation magnetic field and the north-south component of the electric field are found to be well correlated during all four transpolar arc crossings by DE 2 reported in this paper. On the basis of the deduction by *Sugiura* [1984] that this high correlation between orthogonal magnetic and electric fields is invariant under rotation of the reference coordinate system, it is inferred that the pair comprising the north-south magnetic perturbation field and east-west electric field components is equally correlated. It is noted earlier that the east-west electric field component is not measured because of a boom deployment failure. From the above conclusion that the electric fields and magnetic fields from the field-aligned current sheets are orthogonal, it is found that the current sheets are aligned approximately parallel to the plasma convection velocity.

The magnetic field lines threading the transpolar arc are traversed during the period 1546–1600 UT at high altitudes with DE 1. The magnetic signature of the field-aligned currents is shown in Figure 18. Again, the residual field components are calculated as referenced to the aforementioned Magsat model. The coordinate system for these residual components is geomagnetic dipole spherical; positive γ, θ, and ϕ components are directed radially outward, southward, and eastward, respectively. The principal signature of the field-aligned currents occurs at 1548–1556 UT, within the region associated with the transpolar arc as identified by imaging (Table 2) and in situ plasma measurements (Plates 21 and 25). The perturbation magnetic field displays a significant B_ϕ component that indicates that the current system is not well represented by infinite sheets. Direct comparison of the high- and low-altitude measurements is obviated by the dissimilar locations of the two crossings.

October 31, 1981. The low-altitude signature of field-aligned currents associated with the transpolar arc is observed during 2351:40–2353:00 UT as shown in Figure 19. These crossing times are coincident with the observation of transpolar arc plasmas (cf. Plates 18 and 26). The value of invariant latitude ILAT in parentheses (87.0) is the dipole latitude of the magnetic subsatellite point. The small-scale fluctuations associated with field-aligned currents are of interest in this presentation. As the DE 2 spacecraft moves from the morningside to the eveningside of the transpolar arc, a pair of current sheets is observed with first upward current and then downward current densities. The current strength of each sheet is ~0.03 A/m. A second pair of current sheets is then detected on the eveningside of the transpolar arc; again the first sheet current density is directed upward, and the second sheet current density is downward. The strength of each sheet is ~0.06 A/m. A rough estimate of the alignment of these current sheets

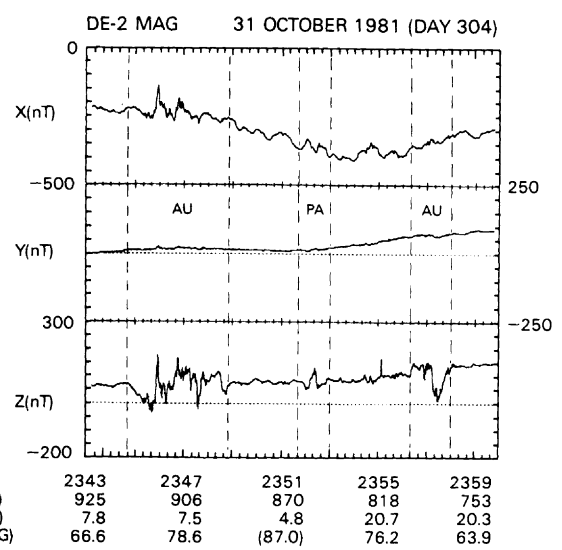

Fig. 19. Continuation of Figure 17 (low altitudes) for October 31, 1981.

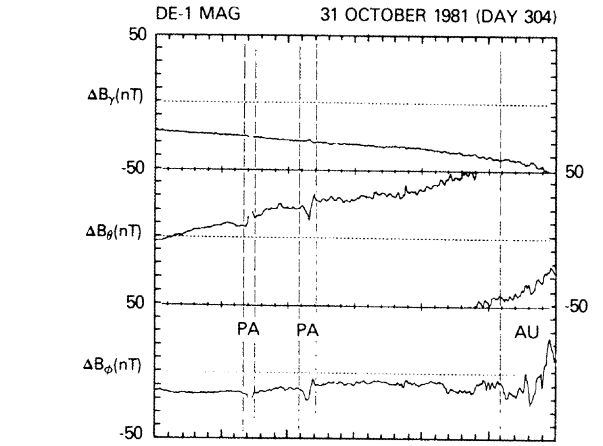

Fig. 20. Continuation of Figure 18 (high altitude) for October 31, 1981.

positions the sheets nearly parallel to the local dipole meridional plane.

The perturbation magnetic fields observed by the magnetometer on DE 1 during its traversal of the transpolar arc region and subsequent passage over the evening auroral oval are shown in Figure 20. Signatures of two distinct pairs of field-aligned current sheets are detected at 2313–2315 UT and 2322–2324 UT, and each pair is identified as PA in Figure 20. These regions are approximately coincident with areas of enhanced auroral emissions (Plate 6) and with those of transpolar arc electron precipitation. In the first of the two pairs of field-aligned current sheets, the current direction is upward in the morningside sheet and downward in the eveningside sheet. In the second pair the current directions are reversed. However, in both cases the upward currents exhibit greater current densities than those of the downward current sheets and correspond to higher-intensity electron precipitation, especially for the second pair (Plate 22*b*). The mapping from the imaging results (Table 2) predicts entry into transpolar arc plasmas at 2316 UT rather than 2313 UT as cited here. These results agree within the computational accuracy of the mapping. The DE 1 spacecraft enters the field-aligned current system of the evening auroral oval at ~2352 UT in agreement with the auroral imaging results and the in situ plasma observations (Table 2 and Plate 22*b*).

November 25, 1981. At low altitudes the field-aligned current region associated with the morning sector of the auroral oval is observed during 1125–1131 UT, as can be noted in Figure 21. Plasma measurements provide crossing times in agreement with this result (Plate 19). Auroral images show that the crossing times for the plasmas associated with the evening sector of the auroral oval are 1140–1141 UT (Table 2). The magnetic perturbations due to field-aligned currents over the evening oval can be identified in Figure 21. Crossing of the zone of plasmas associated with the transpolar arc occurs at 1135:00–1136:30 UT (Plate 19). This region is characterized by a series of multiple field-aligned current sheets oriented approximately 50° counterclockwise from the local dipole meridional plane as viewed looking downward. This direction is approximately parallel to the transpolar arc shown in Plate 12. The strengths of these sheets of upward and downward current densities are ~0.2 to 0.3 A/m. Irregular field-aligned currents are also observed in the evening sector of the polar cap and poleward of the evening sector of the auroral oval at 1136:30–1139:30 UT.

At higher altitudes with the DE 1 spacecraft the main signatures of field-aligned currents in the transpolar arc region are a broad region of predominantly downward current at 1136–1147 UT and a narrow region of upward current at 1147–1148 UT. These results are shown in Figure 22. The steep gradient at 1147:20 UT is due to an upward current sheet strength of 0.04 A/m. This current sheet is aligned along the direction obtained by rotating the dipole north-south direction counterclockwise by 55° as viewed by looking downward. This current sheet may correspond to the upward current sheet observed at low altitudes at 1136:25 UT (Figure 19) and with current strength of 0.3 A/m. The ratio of 7 in current strengths is approximately equal to the value expected for these altitudes from field-aligned sheets in a dipole magnetic field. The orientations of the current sheet at the two different altitudes are also quite similar.

October 17, 1981. The low-altitude passage over the polar cap occurs at the onset of brightening of the transpolar arc of a theta aurora (see Plate 16 and Table 2). In Figure 23 it is seen that perturbation magnetic fields in the polar region 1638:20–1647:00 UT (plasma spectrogram, Plate 20) indicate a complex system of currents in this entire region. Two primary visible polar arcs are identified in the images, one to be identified with the current sheets observed at 1641 UT and the other at 1644–1645 UT (Table 2). The latter series of current sheets is associated with the transpolar arc (see Plate 20). There are two current sheets associated with the polar arc at 1641 UT, an upward current sheet on the morningside and a downward current sheet on the eveningside. The strength of each of these sheets is ~0.08 A/m. These current sheets are aligned approximately parallel to the direction obtained by rotating the dipole north-south direction clockwise by 24° as viewed looking downward.

For the second field-aligned current system associated with the transpolar arc plasmas the directions of the currents are reversed in the pair of sheets in relation to the first current system. The field-aligned current density is directed downward in the morningside of the transpolar arc region and upward in the eveningside.

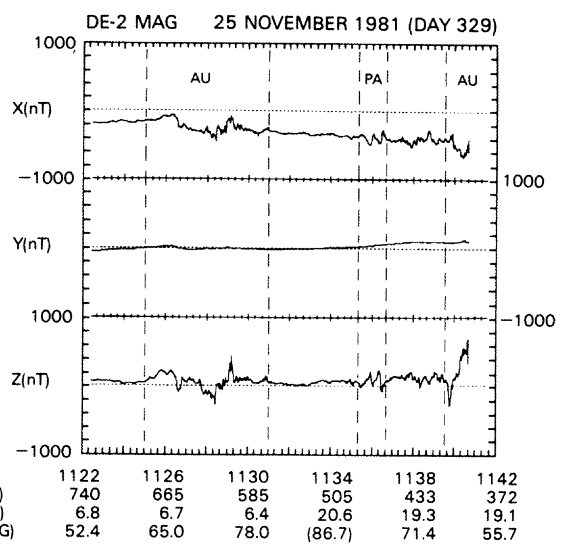

Fig. 21. Continuation of Figure 17 (low altitudes) for November 25, 1981.

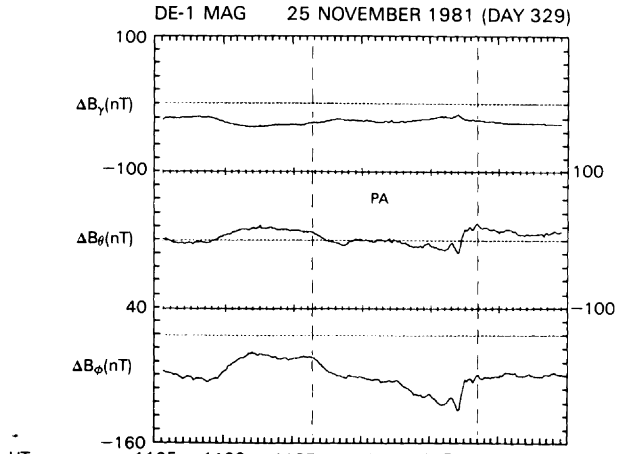

Fig. 22. Continuation of Figure 18 (high altitudes) for November 25, 1981.

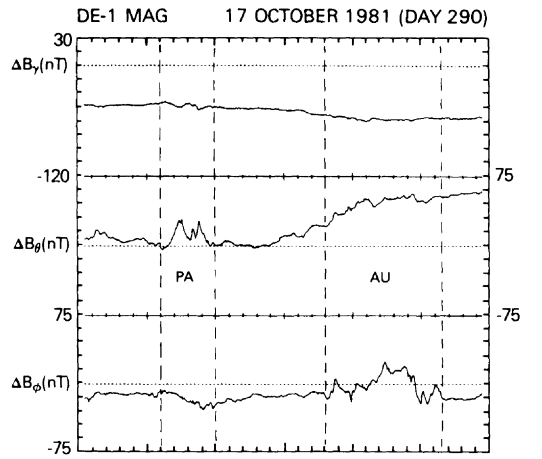

Fig. 24. Continuation of Figure 18 (high altitudes) for October 17, 1981.

The signature of these field-aligned currents in the transpolar arc region at high altitudes is evident at 1642–1650 UT in Figure 24. This traversal time agrees with those derived from images and in situ plasma measurements (Plate 14, Table 2, and Plates 24*b* and 28). Not all of the perturbations observed in the θ component can be interpreted in terms of infinite current sheets. This high-altitude crossing of the transpolar arc region occurs within several minutes of the low-altitude crossing by DE 2 during the onset of a brightening of this arc. The directions of the current densities in the sheets are reversed in relation to those observed at low altitudes; i.e., an upward current sheet is observed on the morningside of the transpolar arc region. This latter arrangement of current sheets is similar to that observed for the well-developed transpolar arcs on October 31 and November 8. This result may be due to temporal fluctuations in the field-aligned current distributions at the onset of arc brightening since the two spacecraft traversed nearly the same magnetic flux tubes.

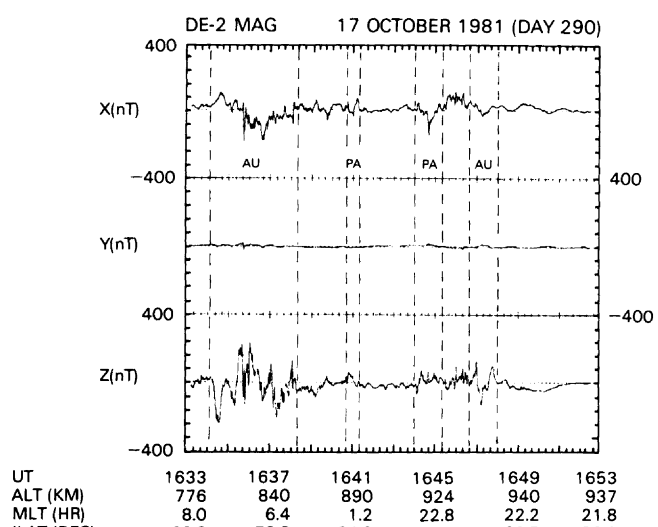

Fig. 23. Continuation of Figure 17 (low altitudes) for October 17, 1981. The transpolar arc plasmas are traversed (the period labeled PA) at ~1645 UT.

11. Plasma Waves at High Altitudes

The plasma wave instrument (PWI) on board the high-altitude DE 1 spacecraft provides measurements of plasma wave phenomena and quasi-static electric fields. The results of the observations of convection electric fields have been given previously in section 9. The instrumentation employed for comprehensive observations of plasma waves includes (1) one pair of long-wire antennas with axis perpendicular to the spacecraft spin axis, (2) one pair of shorter tubular antennas with axis directed along the spin axis, (3) one pair of wire spheres mounted on short fiberglass booms with axis parallel to that of the long-wire antennas, (4) a magnetic loop, and (5) a magnetic search coil. With this instrumentation, ac electric wave fields are measured over a frequency range of 1 Hz to 2 MHz in the amplitude range 0.03 μV/m to 100 mV/m. Magnetic wave fields are measured over the frequency range 1 Hz to 400 kHz. A detailed presentation of the instrument is given by *Shawhan et al.* [1981]. Our primary interests in the following discussion are the surveys of ac electric wave amplitudes in the frequency range 1 Hz to 400 kHz with the long-wire antenna.

November 8, 1981. These measurements of the ac electric wave amplitudes in the frequency range 1 Hz to 400 kHz are shown in the frequency-time spectrogram in Plate 33. Once each 32 s, the spectral power density is determined within 128 narrow frequency bands that are separated by logarithmically equal increments of frequency with a stepped-frequency receiver. The frequency range covered by the stepped-frequency receiver is 100 Hz to 400 kHz. The lower frequency range at 1 Hz to 100 Hz is covered in eight frequency passbands with a separate low-frequency receiver. The spectral power density, $E^2/\Delta f$ in units of $(V/m)^2/Hz$, is color coded according to the scale on the right-hand side of Plate 33. Spacecraft positional coordinates along the abscissa are geocentric radial distance (R_E), magnetic shell parameter (L), magnetic local time (MLT), and magnetic latitude (MLAT).

The spacecraft is located within the polar cap during the interval 1315–1640 UT (Table 2). Plasmas associated with the transpolar arc are encountered during the interval 1546–1600 UT. During a period approximately centered on this time interval, the spectrogram in Plate 33 exhibits a funnel-shaped auroral hiss event (~5–20 kHz) and a series of intense bursts

of broadband electrostatic noise (~5 Hz to 10 kHz). The funnel-shaped auroral hiss event is similar to those observed by this spacecraft along field lines that map into the poleward zone of the auroral oval, e.g., the region of inverted-V electron precipitation events and field-aligned currents. As discussed by *Gurnett et al.* [1983], the characteristic frequency-time pattern of these emissions is a whistler mode propagation effect. For wave normal angles near the resonance cone, whistler mode radiation from a spatially localized source is beamed into a conical emission pattern around the magnetic field. The cone angle increases with increasing frequency, which accounts for the funnel-shaped frequency-time form of the emission in the spectrogram. The vertex of the funnel is located on a magnetic field line through the source of the emission. Ray path studies by *Gurnett et al.* [1983] indicate that the radiation is being emitted from a source located well below the spacecraft, probably at an altitude of $\sim 1\ R_E$. For the event in Plate 33 this vertex is centered in the interval 1544–1554 UT, i.e., on the morningside of the transpolar arc region where the inverted-V electron precipitation is most energetic at low altitudes (plasma spectrogram, Plate 17).

Auroral hiss emission can also provide information on the electron density in the vicinity of the transpolar arc field lines. As discussed by *Persoon et al.* [1983], the upper cutoff of the whistler mode is at either the electron plasma frequency f_p or the electron cyclotron frequency f_c, whichever is smaller. When $f_p < f_c$ the electron density can be computed from the cutoff at the electron plasma frequency. In the spectrogram of Plate 33 the upper cutoff of the auroral hiss is near the electron cyclotron frequency, with the exception of the interval 1540–1547 UT. The local electron cyclotron frequency is plotted as a white line. The upper cutoff of the auroral hiss indicates that the electron density is greater than 5 cm^{-3}, except for the period around 1547 UT when the density briefly decreases to 1 cm^{-3}. Such a decrease in these densities within the auroral hiss event may indicate the existence of a density cavity of the type reported by *Calvert* [1981] along field lines associated with the poleward regions of the auroral oval.

Broadband electrostatic noise in the frequency range ~5 Hz to 10 kHz at 1545–1555 UT is closely associated with the presence of plasmas of the transpolar arc. A similar zone of broadband electrostatic noise is observed during 1638–1650 UT. This region is identified with the poleward zone of the evening auroral oval that is characterized by inverted-V events (Plate 21) and is believed to be mapped into the distant boundary layer of the plasma sheet. Broadband electrostatic noise is also detected in the boundary layer of the plasma sheet which is characterized by field-aligned ion streams and field-aligned currents carried by electrons [*Gurnett and Frank*, 1977; *Gurnett et al.*, 1976; *Frank et al.*, 1981*b*].

October 31, 1981. These plasma wave observations are shown in Plate 34 and are qualitatively similar to those for November 8. Plasmas associated with the transpolar arc are traversed during 2316–2327 UT (imaging, Table 2; plasmas, Plate 22). The spectrogram exhibits a poorly defined funnel-shaped auroral hiss event with a generally irregular upper cutoff during this period. A series of impulsive bursts of broadband electrostatic noise can also be seen from about 2315 to 2325 UT within the transpolar arc plasmas. Somewhat weaker electrostatic noise is present on the morningside of the transpolar arc region at 2242–2306 UT. Coincident impulsive appearance of low-energy electron fluxes, or "polar showers," occur with the higher-frequency electrostatic bursts during 2242–2250 UT. Several weak bursts of auroral kilometric radiation are also evident in the frequency range from about 250 to 400 kHz. These bursts of auroral kilometric radiation occur sporadically through the 2-hour interval of the spectrogram and do not show any obvious relationship to the transpolar arc.

As noted above, the upper cutoff frequency of the auroral hiss is highly structured. Within the region of the transpolar arc the upper cutoff ranges from about 3 to 30 kHz, well below the electron cyclotron frequency. This range of cutoff frequencies corresponds to electron densities ranging from ~0.1 to 10 cm^{-3}. A noticeable depression occurs in the electron density from about 2313 to 2321 UT. Evidence for a similar density depression can also be seen along magnetic field lines threading the poleward zone of the evening auroral oval at 2354–2358 UT. These two density depressions indicate that the plasma depletion mechanisms operating within the regions of the transpolar arc and the auroral oval are similar.

High-frequency broadband electrostatic noise is observed also during 2354–2359 UT with the crossing of field lines associated with the poleward zone of the evening oval (cf. Plate 22). The electrostatic noise and auroral hiss are very similar to those found to be associated with the transpolar arc.

November 25, 1981. A funnel-shaped auroral hiss event and broadband electrostatic noise are again associated with the presence of transpolar arc plasmas. These plasmas are encountered at 1142–1146 UT (Table 2). The electrostatic noise is seen to occur at 1138–1147 UT in Plate 35, and the auroral hiss is detected during 1127–1151 UT. The vertex of the funnel-shaped hiss event is centered in the interval ~1138–1146 UT, and thus along magnetic field lines threading the polar arc plasmas. The poleward boundary of the evening auroral oval corresponds to the spacecraft position at ~1238 UT (Table 2). Low intensities of broadband electrostatic noise are observed at this location. This electrostatic noise is also observed during 1050–1106 UT over the polar cap. During this period, bursts of field-aligned low-energy electrons into the atmosphere, or polar showers, are present (plasma spectrogram, Plate 23). Thus the broadband electrostatic noise is generally associated with field-aligned electron intensities within and outside the region of the transpolar arc plasmas.

October 17, 1981. The plasma wave spectrogram for this passage over earth's polar cap is displayed in Plate 36. At the time of crossing of the transpolar arc plasmas at 1641–1647 UT the transpolar arc is in the initial stages of brightening. No auroral hiss is observed during the crossing in contrast to the previous three examples. Broadband electrostatic noise is observed over a large region of the polar cap during 1540–1641 UT. Enhanced field-aligned electron intensities, or polar showers, are present at center times 1543 UT, 1613 UT, and 1635 UT, for examples. These precipitation events are to be seen in Plate 24. Thus there is a generally ubiquitous presence of broadband electrostatic noise within plasmas characterized by field-aligned electron intensities. The auroral hiss is presumably absent during this event because of the relatively low energy, hundreds of electron volts, of the electron beam at low altitudes (Plate 20), an observation which is consistent with the concurrent weak luminosities associated with the transpolar arc.

12. SUMMARY AND CONCLUSIONS

Our purpose in the foregoing presentations is to provide a comprehensive overview of the remarkable phenomenon known as a theta aurora by summarizing the imaging results for four individual examples and by relating the comprehensive in situ measurements of fields and plasmas at high and

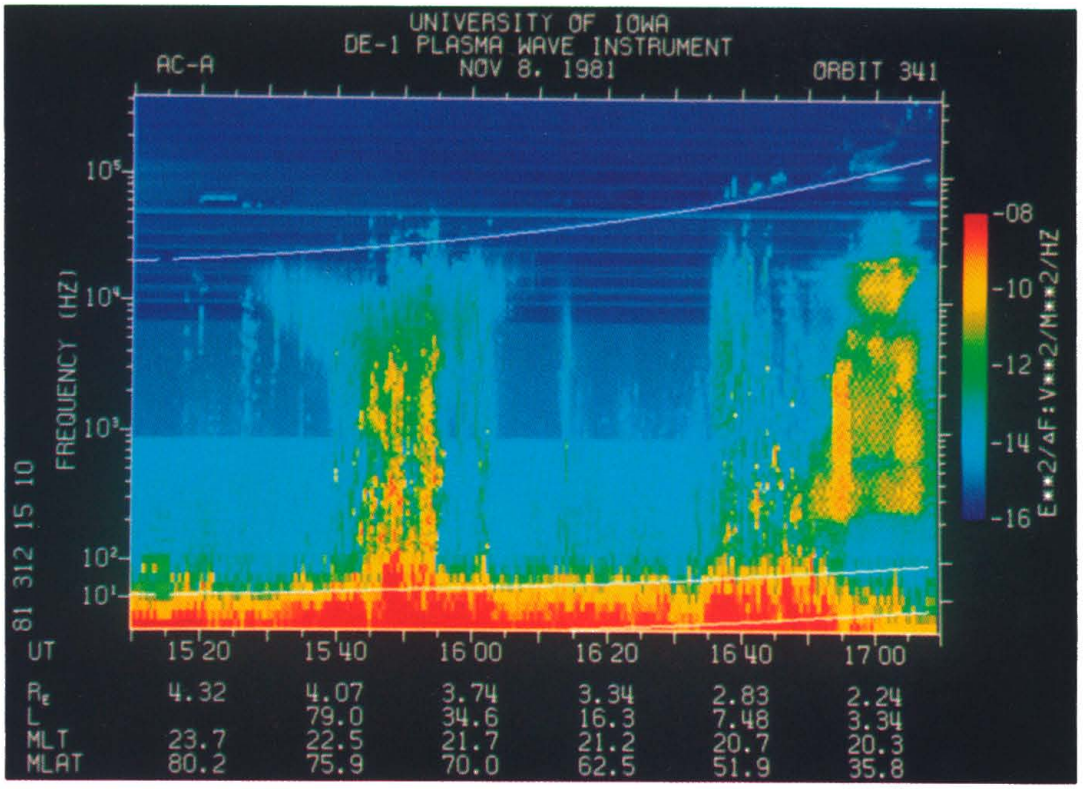

Plate 33. Frequency-time (*f-t*) spectrogram for wave electric fields during the high-altitude traversal over earth's northern auroral zones and polar cap on November 8, 1981. The spacecraft traverses magnetic field lines threading the transpolar arc during 1546–1600 UT. Broadband electrostatic noise and a funnel-shaped auroral hiss event are observed in this time period.

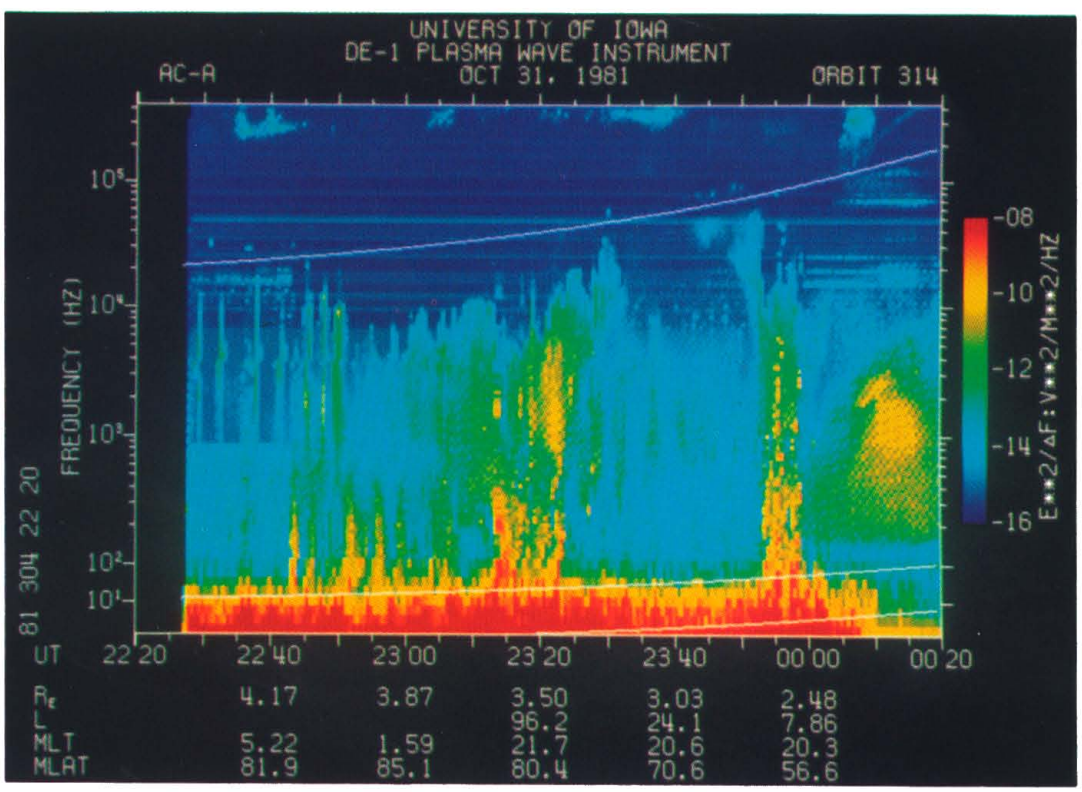

Plate 34. Continuation of Plate 33 for October 31, 1981. The spacecraft traverses magnetic field lines threading the transpolar arc during 2315–2327 UT.

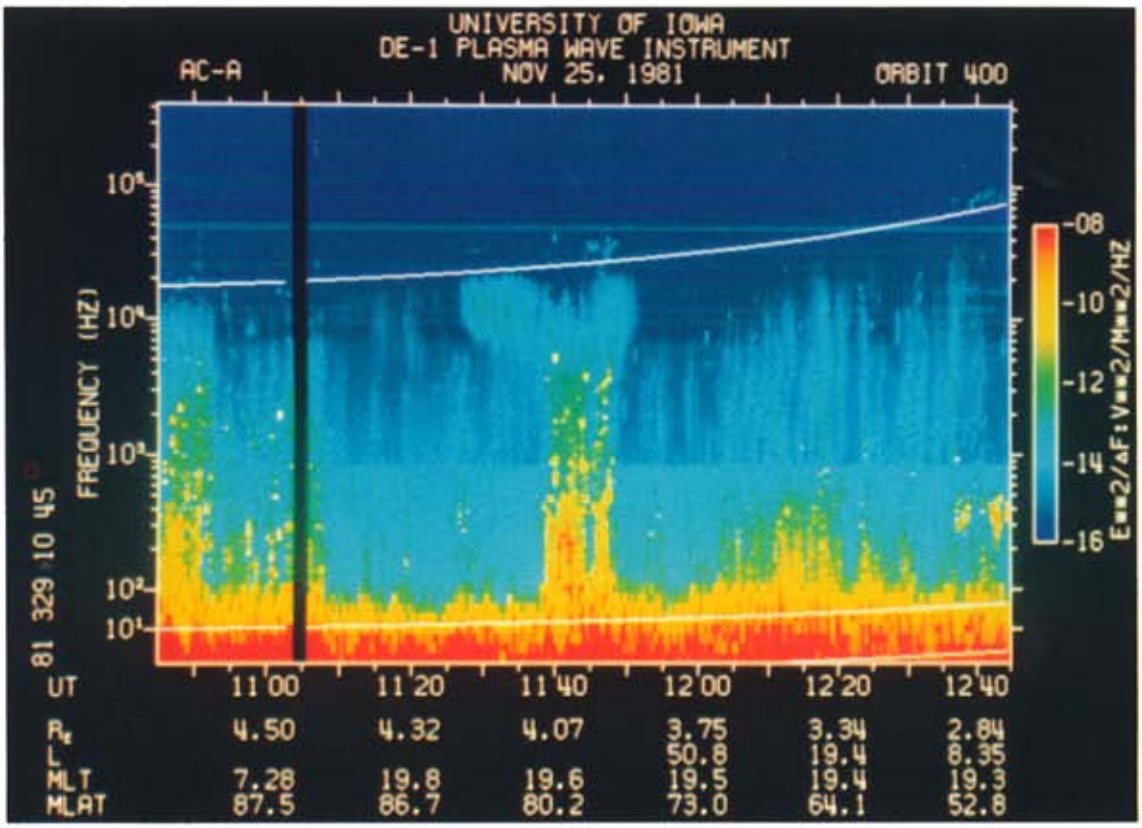

Plate 35. Continuation of Plate 33 for November 25, 1981. The spacecraft traverses magnetic field lines threading the transpolar arc during 1142–1146 UT.

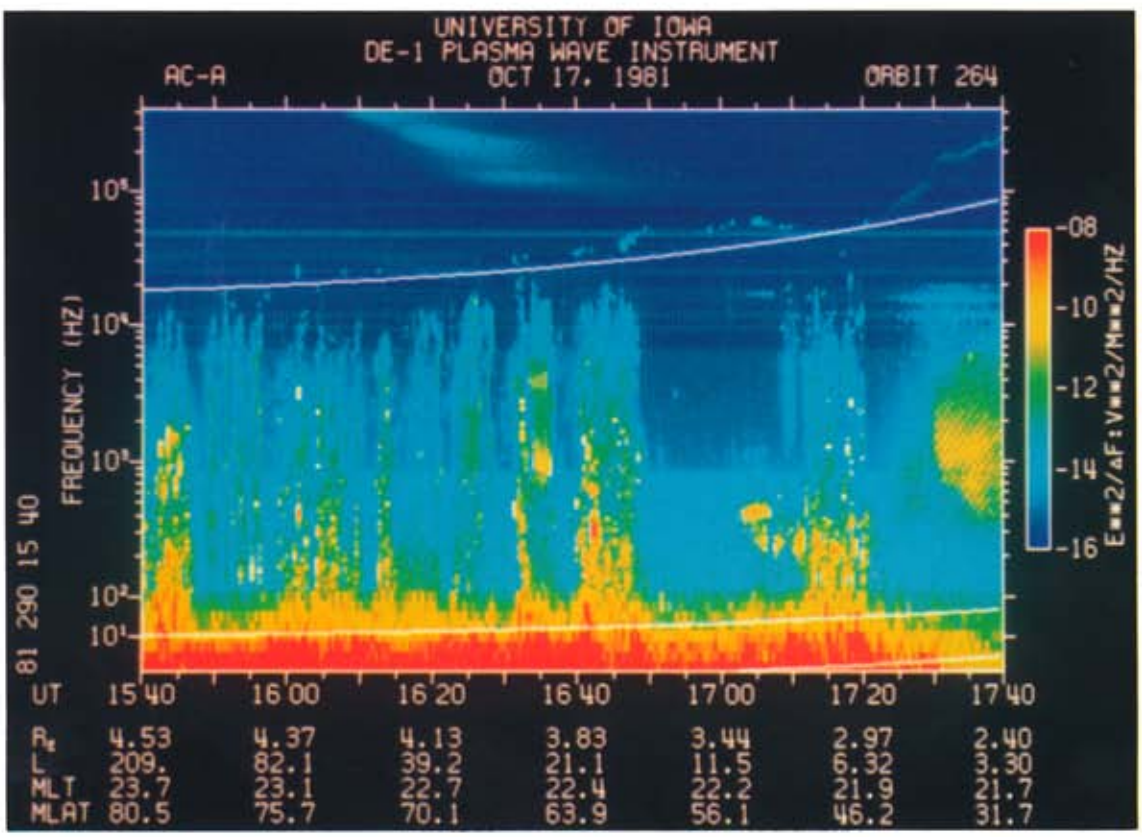

Plate 36. Continuation of Plate 33 for October 17, 1981. The spacecraft traverses magnetic field lines threading the transpolar arc during 1641–1647 UT. Auroral hiss is not observed for this crossing.

low altitudes with the DE 1 and DE 2 polar-orbiting spacecraft, respectively. We provide a narrative summary of these results in the following text.

Global imaging of the spatial distributions and temporal variations of luminosities in the polar cap and transpolar arc are vitally important in interpreting the in situ fields-and-particles observations. Alternatively, these in situ observations are crucial to establishing the relationship of the theta aurora to field-aligned current systems, polar cap and magnetospheric convection patterns, distant magnetospheric topology, and ionospheric plasma source regions. Two of the four examples discussed here are characterized by a relatively bright, well-developed transpolar arc at the times of crossings of the polar cap by both spacecraft. The dates for these more or less typical theta auroras are October 31 and November 8. The third theta auroral event on November 25 exhibited severe dimming of the transpolar arc during the traversals of the plasmas associated with the transpolar arc by these two spacecraft. Only the high-altitude spacecraft DE 1 remained within the polar cap as the arc brightened. The imaging sequence for the fourth example of October 17 shows that the polar cap is initially illuminated by a complex system of polar arcs and diffuse glows. As the two spacecraft almost simultaneously pass through plasmas associated with the transpolar arc, this arc begins to brighten and form. Thus these four cases span the range of polar cap activity ranging from that for steady state theta auroras to the complex properties observed when the transpolar arc dims or is not present.

The theta aurora occurs during periods of persistent northward directed interplanetary fields. The auroral oval contracts, and the luminosities in the oval remain relatively constant. The position of the auroral oval is relatively constant during these periods, and the major motion as observed by looking downward on the northern pole is a rotation of the oval due to the offset of the magnetic dipole from the geographic pole and the rotation of our planet. Brightenings of the oval are sometimes observed and can be described as auroral substorms. The transpolar arc which, with the auroral oval, forms the characteristic luminosity distribution known as a theta aurora displays large variations in its brightness and often rapid motions across the polar cap. The transpolar arc is distinguished from polar arcs in that it traverses the entire polar cap from the dayside sector of the auroral oval to the nighttime oval and is contiguous to the poleward zones of the oval in both local time sectors. The motion of the transpolar arc is seen to be related to the y component of the interplanetary field for simple examples of this phenomenon; i.e., the motion is generally in the direction of the y component [*Frank et al.*, 1985]. The two polar cap regions formed by the presence of the transpolar arc can exhibit detectable, lesser luminosities indicating that weak plasma precipitation is occurring in these regions [cf. *Frank et al.*, 1982].

For a well-developed transpolar arc the plasma convection is observed to be directed sunward on the magnetic field lines associated with the arc. Within the adjacent polar cap regions the plasma convection is directed antisunward. During periods of a relatively dim arc or an absence of such an arc the plasma convection over the polar cap, and often over the auroral oval, is turbulent with no unique convection signature associated with the transpolar arc region. The polar cap region is then characterized by a simultaneous appearance of complex spatial distributions of polar arcs and of field-aligned electron acceleration into the atmosphere. This state of the polar cap is similar to that reported previously with low-altitude measurements [*Burke et al.*, 1982; *Hardy et al.*, 1982].

With the brightening of the transpolar arc the plasma convection over earth's polar cap returns to an organized pattern with antisunward flows in the polar cap region. A convection pattern characteristic of the theta aurora is observed also over the southern hemisphere. The electric fields that are measured for single traverses of the polar regions are suggestive of the existence of a four-cell convection pattern spanning the auroral zones and polar cap. Two cells each with circulation in the same sense are located over the polar cap for such a pattern. The transpolar arc is positioned near the common boundary of these two cells in a region of sunward flow.

Generally, the polar cap plasmas are characterized by three principal electron distributions [*Winningham et al.*, 1973; *Winningham and Heikkila*, 1974]. The source of the first distribution is photoelectrons from earth's atmosphere with energies in the range of $\sim$1–30 eV. The second population is a low density of electrons with energies of hundreds of electron volts that are distributed over the polar cap without notable spatial structure. This phenomenon is known as "polar rain." These electrons are currently thought to be solar coronal electrons that gain entry to the polar cap on geomagnetic field lines that are open or are connected to those of the interplanetary medium [*Fairfield and Scudder*, 1985], i.e., via direct entry. Sporadic, spatially narrow zones of electron precipitation are the signatures of the third electron population. The precipitation of these electrons into the atmosphere is called "polar showers." These electron distributions exhibit often the effects of field-aligned acceleration and are associated with the major luminosity features of the polar cap.

The magnetic flux tubes threading the transpolar arc are characterized by the presence of accelerated electrons and hot ions. Often electron velocity distributions similar to those associated with inverted-V events over the poleward zones of the auroral oval are observed in the transpolar arc plasmas. Coincident with the observations of such field-aligned acceleration, the convection electric fields are directed inward toward the acceleration region, i.e., $\nabla \cdot \mathbf{E} < 0$. The acceleration region for these electrons is observed at times to extend to high altitudes, $\sim$20,000 km, although the major fraction of the energization occurs at lower altitudes of several thousand kilometers. In addition, energetic ions in the energy range $\sim$1–10 keV are present within the transpolar arc region. Such ion distributions are also observed in the poleward zones of the oval. Thus the primary characteristics of plasmas over the transpolar arc and the poleward regions of the auroral oval are similar, a situation that strengthens the concept of a close topological connection of these two regions in the distant magnetosphere. The detection of field-aligned electron acceleration into the atmosphere over the polar cap region is insufficient evidence to establish the existence of a transpolar arc since such electron distributions often occur elsewhere over the polar cap. The relatively high intensities of energetic ions in the energy range $\sim$1–10 keV are not observed in other regions of the polar cap when a bright, well-developed transpolar arc is present. This feature distinguishes the transpolar arc from other luminosity features in the polar cap.

The composition of the ions within the transpolar arc plasmas differs substantially from that of plasmas associated with other polar cap luminosity features. Energetic H^+, He^{++}, and O^+ ions in the energy range $\sim$1–10 keV are found in these plasmas. The densities and composition of these plasmas are similar to those of the plasmas associated with the poleward region of the auroral oval. This latter region is currently thought to be mapped into the boundary layers of the plasma sheet in the distant magnetosphere. Such observational evi-

dence is used by *Peterson and Shelley* [1984] to conclude that the transpolar arc plasmas are of both ionospheric and solar wind origins and that the transpolar arc is magnetically mapped into the plasma sheet or its boundary layer of streaming plasmas and field-aligned currents. These energetic O^+ ions are not generally detected at comparable intensities within the other regions of the polar cap. However, somewhat cooler H^+ and He^{++} ions with energies of less than or approximately several keV are observed generally over the polar cap. The angular distributions of these ion intensities are more or less isotropic. The ratio of ion densities, He^{++}/H^+, is significantly enhanced in relation to that found over the auroral oval. The composition of these ions and the presence of magnetosheath electrons indicate that the source of these ions is the magnetosheath via direct entry. Direct entry of magnetosheath plasmas into the polar cap has previously been suggested in order to account for extensive areas of O I 630.0-nm emissions in the polar cap during northward interplanetary magnetic fields following a large substorm [*Bunn and Shepherd*, 1979]. During one passage over the polar cap and auroral zones, energetic O^+ ions are nearly absent in the transpolar arc plasmas. On the other hand, such O^+ ions are relatively sparse over the poleward zone of the evening oval at this time, thus establishing further the association of these two regions. The region of energetic ions remains intact within the polar cap region during dimming of the polar arc and with the concurrent appearance of turbulent plasma convection over the polar cap. Thus the plasma feature associated with the transpolar arc is considerably more durable than the sunward plasma convection that accompanies the illumination of the transpolar arc.

The dominant thermal ion within the polar cap regions is O^+. Traces of H^+ and He^+ ions are also observed. These ions are flowing upward from earth's ionosphere and comprise the major fraction of ion densities within the polar cap region, including the flux tubes through the transpolar arc. Within the transpolar arc plasmas there is a dramatic disappearance of the low-energy (few electron volts) O^+ ions. This effect can be caused either by the reversal of the convective flow from antisunward to sunward, which eliminates the dayside cusp ionosphere as a source of O^+ ions, or by the heating of thermal ions by an acceleration and/or heating mechanism associated with the field-aligned electron beams in these regions.

Earth's magnetosphere is immersed within substantial intensities of solar electrons during one of the spacecraft passages through the polar region during the initial stages of development of the transpolar arc. This fortuitous situation allows a survey of the accessibility of these solar electron fluxes to various regions of the polar cap and auroral zone. These solar electrons are observed over the entire polar cap with the exception of the region associated with the transpolar arc. The access of these solar electrons to the polar cap supports the conclusion that charged particles in the magnetosheath are capable of direct access to this region, e.g., the H^+ and He^{++} ions and magnetosheath electrons previously discussed. The corresponding magnetic field lines are connected to those in the magnetosheath, i.e., open to the interplanetary medium. In contrast, the magnetic field lines threading both the transpolar arc and poleward zones of the auroral oval display an absence of comparable intensities of solar electrons. This absence of solar electrons provides substantial, but not irrefutable evidence that these magnetic field lines in these two regions are closed, thus preventing direct particle entry from the magnetosheath and interplanetary medium.

Substantial field-aligned currents are detected in the transpolar arc plasmas. For the traversals of the transpolar arcs for the examples when these arcs are relatively bright, two pairs of oppositely directed sheets are found. The arrangement of currents in each of these pairs is such that the upward current sheet is on the morningside and the downward current sheet on the eveningside. The orientations of these current sheets are approximately parallel to the transpolar arcs. Magnitudes of current sheet strengths are similar to those observed over the poleward zones of the auroral oval. The upward current is carried by electrons precipitating into the atmosphere and usually associated with the clear signature of field-aligned electron acceleration. During periods of relatively bright transpolar arcs the field-aligned currents in the polar cap region outside the arc are small or absent. With the dimming or absence of the transpolar arc, a complex field-aligned current system is observed over the polar cap and is closely related to a similar appearance of sporadic, multiple arcs.

The two principal plasma wave phenomena associated with the transpolar arcs are funnel-shaped auroral hiss and broadband electrostatic noise. The source region of the auroral hiss is located on magnetic field lines in the transpolar arc and at altitudes of $\sim 1\ R_E$. Auroral hiss is also similarly observed over the poleward zones of the auroral oval. For one of our examples at the onset of transpolar arc brightening, no auroral hiss is observed. However, the field-aligned acceleration of electrons is coincidentally weak (several hundreds of electron volts) in relation to typical values of 1 to several keV when auroral hiss is present. Broadband electrostatic noise is found in the plasmas associated with the transpolar arc as well as those plasmas over the poleward zone of the auroral oval. In the distant magnetotail this broadband noise is present in the streaming plasmas of the boundary layer of the plasma sheet [*Gurnett et al.*, 1976; *Gurnett and Frank*, 1977]. Broadband electrostatic noise is also present in the multitude of electron precipitation regions that are not associated with the transpolar arc plasmas during the periods of dimming or formation of the transpolar arc. This electrostatic noise is present coincidentally with the detection of field-aligned currents carried by electrons, regardless of the presence or absence of a hot ion population. The funnel-shaped auroral hiss appears to be observed when the electron energy reaches ~ 1 keV or greater in these field-aligned electron beams, thus indicating a threshold energy for this mechanism. Since the electron energies over the polar cap are generally lower than 1 keV in regions other than that associated with the transpolar arc, auroral hiss is not expected normally to accompany electron precipitation in these regions.

The implications of the existence of the theta aurora in terms of magnetospheric convection, magnetospheric topology, and plasma access to the polar cap region are currently being energetically debated. Nevertheless, severe restraints are placed upon our current ideas by the comprehensive survey of phenomena associated with the theta aurora as presented here. Special effort is expended here to avoid controversial interpretive comments in the presentation in order to provide a solid factual foundation for future theoretical and observational efforts. Several ideas and models for interpreting the theta aurora are already available in the literature. Attempts are made to explain the existence of the transpolar arc in terms of large asymmetries of the magnetotail relative to the earth-sun line due to the presence of z and y components of the interplanetary field [*Cowley*, 1981; *Akasofu et al.*, 1981; *Akasofu and Roederer*, 1984]. Basically, the B_y component exerts a torque on the magnetosphere about the earth-sun line. *Lyons* [1985] extends this method of adding the inter-

planetary magnetic field to that of earth's dipole field in order to explain sunward and antisunward plasma convection over the polar caps. A plasma convection system comprising viscous, merging, and magnetotail lobe cells is invoked by *Reiff and Burch* [1985] to explain the convection pattern observed over the polar cap during theta auroral events. *Frank et al.* [1982] suggest that the theta aurora is the signature of the bifurcation of magnetotail lobes by a region of upward flowing plasmas from the boundary layer of the plasma sheet in the distant magnetotail. It is already known from plasma observations at the lunar orbit that large-angle rotations of the plasma sheet do not occur [*Hardy et al.*, 1979]. Thus the transpolar arc is not the direct signature of a major reorientation of the plasma sheet relative to the ecliptic plane.

There are several major observations to be accomplished in order to resolve these questions concerning the magnetospheric convection and topology during the occurrence of theta auroras. We mention several of these unresolved issues here. The conjugacy of the transpolar arcs over the northern and southern polar caps must be established, and simultaneous determinations of their motions must be obtained. A more precise study of the details of the spatial connection of the transpolar arcs with the discrete arcs of the auroral oval is needed. Further examinations of in situ fields-and-particles measurements in the lobes of the magnetotail and distant polar magnetosphere are required in order to identify plasma regions that are associated with polar cap luminosity features.

Acknowledgments. This research was supported in part by the National Aeronautics and Space Administration (NASA) under grants NAG5-483, NAG5-310, and NGL-16-001-002 and contract NAS5-25689 and by the Office of Naval Research under grant N00014-76-C-0016 at The University of Iowa, under NASA contracts NAS5-28711 and NAS5-28712 and by the Air Force Geophysics Laboratory under contract AFGL 7121840006 at Southwest Research Institute, under NASA grants NAG5-306 and NAG5-305 at The University of Texas at Dallas, and under NASA contract NAS5-28710 at the Lockheed Palo Alto Research Laboratory.

The Editor thanks the two referees for their assistance in evaluating this paper.

REFERENCES

Akasofu, S.-I., The dynamical morphology of the aurora polaris, *J. Geophys. Res.*, *68*, 1667–1673, 1963.

Akasofu, S.-I., Recent progress in studies of DMSP auroral photographs, *Space Sci. Rev.*, *19*, 169–215, 1976.

Akasofu, S.-I., and M. Roederer, Dependence of the polar cap geometry on the IMF, *Planet. Space Sci.*, *32*, 111–118, 1984.

Akasofu, S.-I., D. N. Covey, and C.-I. Meng, Dependence of the geometry of the region of open field lines on the interplanetary magnetic field, *Planet. Space Sci.*, *29*, 803–807, 1981.

Anger, C. D., A. T. Y. Lui, and S.-I. Akasofu, Observations of the auroral oval and a westward traveling surge from the ISIS 2 satellite and the Alaskan meridian all-sky cameras, *J. Geophys. Res.*, *78*, 3020–3026, 1973.

Anger, C. D., W. Sawchuk, and G. G. Shepherd, Polar cap optical aurora seen from ISIS-2, in *Magnetospheric Physics*, edited by B. M. McCormac, D. Reidel, Hingham, Mass., 1974.

Bunn, F. E., and G. G. Shepherd, The solar terrestrial event of 14–21 December 1971: The pattern of 6300 Å emission over the polar cap, *Planet. Space Sci.*, *27*, 973–996, 1979.

Burch, J. L., S. A. Fields, and R. A. Heelis, Polar cap electron acceleration regions, *J. Geophys. Res.*, *84*, 5863–5874, 1979.

Burch, J. L., J. D. Winningham, V. A. Blevins, N. Eaker, W. C. Gibson, and R. A. Hoffman, High-altitude plasma instrument for Dynamics Explorer-A, *Space Sci. Instrum.*, *5*, 455–463, 1981.

Burke, W. J., M. C. Kelley, R. C. Sagalyn, M. Smiddy, and S. T. Lai, Polar cap electric field structures with a northward interplanetary magnetic field, *Geophys. Res. Lett.*, *6*, 21–24, 1979.

Burke, W. J., M. S. Gussenhoven, M. C. Kelley, D. A. Hardy, and F. J. Rich, Electric and magnetic field characteristics of discrete arcs in the polar cap, *J. Geophys. Res.*, *87*, 2431–2443, 1982.

Calvert, W., The auroral plasma cavity, *Geophys. Res. Lett.*, *8*, 919–921, 1981.

Chappell, C. R., S. A. Fields, C. R. Baugher, J. H. Hoffman, W. B. Hanson, W. W. Right, H. D. Hammack, G. R. Carignan, and A. F. Nagy, The retarding ion mass spectrometer on Dynamics Explorer-A, *Space Sci. Instrum.*, *5*, 477–491, 1981.

Cowley, S. W. H., Magnetospheric asymmetries associated with the *y*-component of the IMF, *Planet. Space Sci.*, *29*, 79–96, 1981.

Davis, T. N., The morphology of the polar aurora, *J. Geophys. Res.*, *65*, 3497–3500, 1960.

Eather, R. H., and S.-I. Akasofu, Characteristics of polar cap arcs, *J. Geophys. Res.*, *74*, 4794–4798, 1969.

Fairfield, D. H., and J. D. Scudder, Polar rain: Solar coronal electrons in the earth's magnetosphere, *J. Geophys. Res.*, *90*, 4055–4068, 1985.

Farthing, W. H., M. Sugiura, B. G. Ledley, and L. J. Cahill, Jr., Magnetic field observations on DE-A and -B, *Space Sci. Instrum.*, *5*, 551–560, 1981.

Frank, L. A., and K. L. Ackerson, Local-time survey of plasma at low altitudes over the auroral zones, *J. Geophys. Res.*, *77*, 4116–4127, 1972.

Frank, L. A., J. D. Craven, K. L. Ackerson, M. R. English, R. H. Eather, and R. L. Carovillano, Global auroral imaging instrumentation for the Dynamics Explorer Mission, *Space Sci. Instrum.*, *5*, 369–393, 1981*a*.

Frank, L. A., R. L. McPherron, R. J. DeCoster, B. G. Burek, K. L. Ackerson, and C. T. Russell, Field-aligned currents in the earth's magnetotail, *J. Geophys. Res.*, *86*, 687–700, 1981*b*.

Frank, L. A., J. D. Craven, J. L. Burch, and J. D. Winningham, Polar views of the earth's aurora with Dynamics Explorer, *Geophys. Res. Lett.*, *9*, 1001–1004, 1982.

Frank, L. A., J. D. Craven, and R. L. Rairden, Images of the earth's aurora and geocorona from the Dynamics Explorer Mission, *Adv. Space Res.*, *5*(4), 53–68, 1985.

Gurnett, D. A., and L. A. Frank, A region of intense plasma wave turbulence on auroral field lines, *J. Geophys. Res.*, *82*, 1031–1050, 1977.

Gurnett, D. A., L. A. Frank, and R. P. Lepping, Plasma waves in the distant magnetotail, *J. Geophys. Res.*, *81*, 6059–6071, 1976.

Gurnett, D. A., S. D. Shawhan, and R. R. Shaw, Auroral hiss, *Z* mode radiation, and auroral kilometric radiation in the polar magnetosphere: DE 1 observations, *J. Geophys. Res.*, *88*, 329–340, 1983.

Gussenhoven, M. S., Extremely high latitude auroras, *J. Geophys. Res.*, *87*, 2401–2412, 1982.

Hanson, W. B., R. A. Heelis, R. A. Power, C. R. Lippincott, D. R. Zuccaro, B. J. Holt, L. H. Harmon, and S. Sanatani, The retarding potential analyzer for Dynamics Explorer-B, *Space Sci. Instrum.*, *5*, 503–510, 1981.

Hardy, D. A., P. H. Reiff, and W. J. Burke, Response of magnetotail plasma at lunar distance to changes in the interplanetary magnetic field, *J. Geophys. Res.*, *84*, 1382–1390, 1979.

Hardy, D. A., W. J. Burke, and M. S. Gussenhoven, DMSP optical and electron measurements in the vicinity of polar cap arcs, *J. Geophys. Res.*, *87*, 2413–2430, 1982.

Heelis, R. A., W. B. Hanson, C. R. Lippincott, D. R. Zuccaro, L. H. Harmon, B. J. Holt, J. E. Doherty, and R. A. Power, The ion drift meter for Dynamics Explorer-B, *Space Sci. Instrum.*, *5*, 511–521, 1981.

Heppner, J. P., Polar-cap electric field distributions related to the interplanetary magnetic field direction, *J. Geophys. Res.*, *77*, 4877–4887, 1972.

Iijima, T., Field-aligned currents during northward IMF, in *Magnetospheric Currents, Geophys. Monogr. Ser.*, vol. 28, edited by T. A. Potemra, pp. 115–122, AGU, Washington, D. C., 1984.

Iijima, T., T. A. Potemra, L. J. Zanetti, and P. F. Bythrow, Large-scale Birkeland currents in the dayside polar region during strongly northward IMF: A new Birkeland current system, *J. Geophys. Res.*, *89*, 7441–7452, 1984.

Ismail, S., and C.-I. Meng, A classification of polar cap auroral arcs, *Planet. Space Sci.*, *30*, 319–330, 1982.

Ismail, S., D. D. Wallis, and L. L. Cogger, Characteristics of polar cap sun-aligned arcs, *J. Geophys. Res.*, *82*, 4741–4749, 1977.

Langel, R. A., R. H. Estes, G. D. Mead, E. B. Fabiano, and E. R. Lancaster, Initial geomagnetic field model from Magsat vector data, *Geophys. Res. Lett.*, *7*, 793–796, 1980.

Lassen, K., The quiet-time pattern of auroral arcs as a consequence of magnetospheric convection, *Geophys. Res. Lett.*, *6*, 777–780, 1979.

Lassen, K., and C. Danielsen, Quiet time pattern of auroral arcs for different directions of the interplanetary magnetic field in the *y-z* plane, *J. Geophys. Res.*, *83*, 5277–5284, 1978.

Lockwood, M., J. H. Waite, Jr., T. E. Moore, J. F. E. Johnson, and C. R. Chappell, A new source of suprathermal O^+ ions near the dayside polar cap boundary, *J. Geophys. Res.*, *90*, 4099–4116, 1985.

Lyons, L. R., A simple model for polar cap convection patterns and generation of θ auroras, *J. Geophys. Res.*, *90*, 1561–1567, 1985.

Maezawa, K., Magnetospheric convection induced by the positive and negative *z* components of the interplanetary magnetic field: Quantitative analysis using polar cap magnetic records, *J. Geophys. Res.*, *81*, 2289–2303, 1976.

Maynard, N. C., E. A. Bielecki, and H. F. Burdick, Instrumentation for vector electric field measurements from DE-B, *Space Sci. Instrum.*, *5*, 523–534, 1981.

Meng, C.-I., and S.-I. Akasofu, The relation between the polar cap auroral arc and the auroral oval arc, *J. Geophys. Res.*, *81*, 4004–4006, 1976.

Persoon, A. M., D. A. Gurnett, and S. D. Shawhan, Polar cap electron densities from DE 1 plasma wave observations, *J. Geophys. Res.*, *88*, 10,123–10,136, 1983.

Peterson, W. K., and E. G. Shelley, Origin of the plasma in a cross-polar cap auroral feature (theta aurora), *J. Geophys. Res.*, *89*, 6729–6736, 1984.

Potemra, T. A., L. J. Zanetti, P. F. Bythrow, A. T. Y. Lui, and T. Iijima, B_y-dependent convection patterns during northward interplanetary magnetic field, *J. Geophys. Res.*, *89*, 9753–9760, 1984.

Rairden, R. L., L. A. Frank, and J. D. Craven, Geocoronal imaging with Dynamics Explorer: A first look, *Geophys. Res. Lett.*, *10*, 533–536, 1983.

Reiff, P. H., and J. L. Burch, IMF B_y-dependent plasma flow and Birkeland currents in the dayside magnetosphere, 2, A global model for northward and southward IMF, *J. Geophys. Res.*, *90*, 1595–1609, 1985.

Shawhan, S. D., D. A. Gurnett, D. L. Odem, R. A. Helliwell, and C. G. Park, The plasma wave and quasi-static electric field instrument (PWI) for Dynamics Explorer-A, *Space Sci. Instrum.*, *5*, 535–550, 1981.

Shelley, E. G., D. A. Simpson, T. C. Sanders, E. Hertzberg, H. Balsiger, and A. Ghielmetti, The energetic ion composition spectrometer (EICS) for the Dynamics Explorer-A, *Space Sci. Instrum.*, *5*, 443–454, 1981.

Shelley, E. G., W. K. Peterson, A. G. Ghielmetti, and J. Geiss, The polar ionosphere as a source of energetic magnetospheric plasma, *Geophys. Res. Lett.*, *9*, 941–944, 1982.

Sugiura, M., A fundamental magnetosphere-ionosphere coupling mode involving field-aligned currents as deduced from DE-2 observations, *Geophys. Res. Lett.*, *11*, 877–880, 1984.

Sugiura, M., N. C. Maynard, W. H. Farthing, J. P. Heppner, and B. G. Ledley, Initial results on the correlation between the magnetic and electric fields observed from the DE-2 satellite in the field-aligned current regions, *Geophys. Res. Lett.*, *9*, 985–988, 1982.

Sugiura, M., T. Iyemori, R. A. Hoffman, N. C. Maynard, J. L. Burch, and J. D. Winningham, Relationships between field-aligned currents, electric fields, and particle precipitation as observed by Dynamics Explorer-2, in *Magnetospheric Currents*, *Geophys. Monogr. Ser.*, vol. 28, edited by T. A. Potemra, p. 96, AGU, Washington, D. C., 1984.

Waite, J. H., Jr., T. Nagai, J. F. E. Johnson, C. R. Chappell, J. L Burch, T. L. Killeen, P. B. Hays, G. R. Carignan, W. K. Peterson, and E. G. Shelley, Escape of suprathermal O^+ ions in the polar cap, *J. Geophys. Res.*, *90*, 1619–1630, 1985.

Winningham, J. D., and W. J. Heikkila, Polar cap auroral electron fluxes observed with ISIS 1, *J. Geophys. Res.*, *79*, 949–957, 1974.

Winningham, J. D., S.-I. Akasofu, F. Yasuhara, and W. J. Heikkila, Simultaneous observations of auroras from the South Pole station and of precipitating electrons by ISIS 1, *J. Geophys. Res.*, *78*, 6579–6594, 1973.

Winningham, J. D., F. Yasuhara, S.-I. Akasofu, and W. J. Heikkila, The latitudinal morphology of 10-eV to 10-keV electron fluxes during magnetically quiet and disturbed times in the 2100–0300 MLT sector, *J. Geophys. Res.*, *80*, 3148–3171, 1975.

Winningham, J. D., J. L. Burch, N. Eaker, V. A. Blevins, and R. A. Hoffman, The low altitude plasma instrument (LAPI), *Space Sci. Instrum.*, *5*, 465–475, 1981.

Zanetti, L. J., W. Baumjohann, and T. A. Potemra, Ionospheric and Birkeland current distributions inferred from the Magsat magnetometer data, *J. Geophys. Res.*, *88*, 4875–4884, 1983.

J. L. Burch and J. D. Winningham, Southwest Research Institute, 6220 Culebra Road, P. O. Drawer 28510, San Antonio, TX 78284.

C. R. Chappell and J. H. Waite, Marshall Space Flight Center, Huntsville, AL 35812.

J. D. Craven, L. A. Frank, D. A. Gurnett, and S. D. Shawhan, Department of Physics and Astronomy, University of Iowa, Iowa City, IA 52242.

R. A. Heelis, University of Texas at Dallas, P. O. Box 688, Richardson, TX 75080.

N. C. Maynard, Space Physics Division, Air Force Geophysics Laboratory, Hanscom Air Force Base, MA 01731.

W. K. Peterson and E. G. Shelley, Lockheed Palo Alto Research Laboratory, 3251 Hanover Street, Building 255, Department 52/12, Palo Alto, CA 94304.

M. Sugiura, Goddard Space Flight Center, Greenbelt, MD 20771.

D. R. Weimer, Research Center, Regis College, 235 Wellesley Street, Weston, MA 02193.

(Received May 24, 1985;
revised August 26, 1985;
accepted August 27, 1985.)